Institute of Hydrology
Albert-Ludwigs-University of Freiburg, Germany

Bastian Pöschl

Streamflow change of glacierized basins in Canada, Norway, and the European Alps

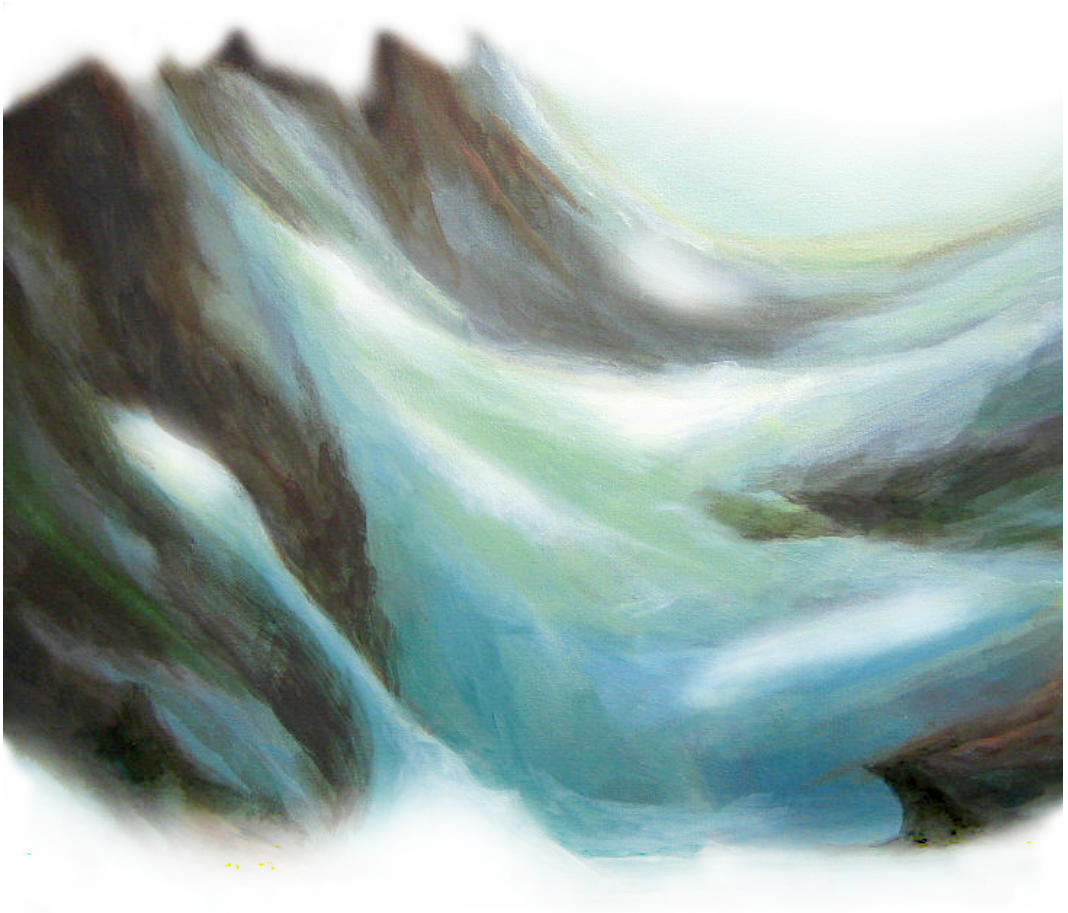

Supervisor: Prof. Dr. Markus Weiler

Co-Supervisor: Dr. Kerstin Stahl

Freiburg im Breisgau, July 2009

Institut für Hydrologie
der Albert-Ludwigs-Universität Freiburg im Breisgau

Bastian Pöschl

Abflussänderung vergletscherter Einzugsgebiete in Kanada, Norwegen und den Europäischen Alpen

Referent: Prof. Dr. Markus Weiler
Koreferent: Dr. Kerstin Stahl

Diplomarbeit unter der Leitung von
Prof. Dr. Markus Weiler

Freiburg im Breisgau, Juli 2009

Acknowledgements

I would like to thank Prof. Dr. Markus Weiler for making this work possible as well as Dr. Kerstin Stahl for supervising this study and spending so much time in discussions.

A comparing analysis, based on data of two continents and five countries, is impossible without the help of many people. I especially want to thank Helmut Spiss and Martin Neuner from 'Hydrographischer Dienst in Österreich', Prof. Michael Kuhn from the University of Innsbruck, Heidi Escher-Vetter from the 'Comission for Glaciology' of the Bavarian Academy of Sciences and Humanities, Edith Oosenbrug at the Swiss Hydrological Survey 'BAFU', Hege Hisdal and Trine Fjeldstad from the University of Oslo, Emmanuel Paquet at EDF-DTG and David Hutchinson at Environment Canada.

Thanks also go to Klemens Ronin for the many questions answered and for his helpful hints how to handle *R* as well as my fellow students who encouraged me with controversial debates. Especially without the diploma students of "Rheinstraße" Olivier Faber, Manuela Nied, and Fabian Ries this work would not be what it is. Thank you all! Further thanks go to Anja Walter, who helped me so kindly with my english phrases.

I want to dedicate this work to my little family, Stefanie and Timon Pöschl. You are my motivation and the most important thing to me.
Last but not least I am very thankful to my and Stefanie's parents who have supported us such a long time.

Contents

List of Figures

List of Tables

List of Abbreviations

BC	British Columbia
BCD	British Columbian Data Set
CA	Cluster Analysis
Cl	Cluster
COD	Correlation Data Set
ELA	Equilibrium Line Altitude
EU	European Alps
EUD	European Alps Data Set
GMD	Geomorphologic Data Set
HTC	High Air Temperature Correlation Data Set
LTS	Long Time Series (1960-2004)
MK	Mann-Kendall Trend Test
NAO	North Atlantic Oscillation
NCM	Northern Coast Mountains
NO	Norway
NOD	Norwegian Data Set
PC	Principal Component
PCA	Principle Component Analysis
PDO	Pacific Decadal Oscillation
RM	Rocky Mountains
SCM	Southern Coast Mountains
STS	Short time series (1979-2004)

Summary

In this thesis streamflow time series from glacierized basins in Canada, Norway and the European Alps has been analysed. Based on the work of *Stahl & Moore* (2006) the question aroused if glacial fed streamflow shows a comparable reaction to climate change in different regions and if the results derived from a certain region are adaptable to another. As a first step I selected adequate catchments. For Canada and Norway the meta data like *catchment size*, *mean altitude*, *glacierized catchment fraction* were available from former studies. However, for the European Alps basins I had to create the database by hand, using data sheets and tables in publications. With runoff data requests the several responsible water surveys had to be contacted and the obtained time series must be formatted consistently. Only in a few cases meteorological measurement could be found nearby the hydrometrical station. Thus I used the next available station. For the European Alps basins no freely available meteorological time series could be found. Alternatively I used reanalysis data for this region and the Norwegian basins. I arranged the derived data sets by glacierized proportion of the catchment and rejected single time series if either duration was too short, anthropogenic influences were detected, or lake area seemed to be too big. Statistical analysis for every single basin was now performed using the programming language *R*. To automate the workflow I created a Linux *Shell*-script and exported the results in a file as well as in a report paper that was generated by LaTeX via *Sweave*. *Sweave* is a programming language creating a dynamic connection between *R* and LaTeX.

The first results showed that the distribution of catchment sizes between Canada and the European data sets made a comparison impossible. The Canadian data set contained many large area catchments with a small glacierized proportion, whereas the majority of the European catchments is of medium size. Thus a subset with a comparable distribution was build and used in the analysis.

Large scale atmospheric fluctuations can play an important roll on runoff behaviour. The comparison of runoff, air temperature and precipitation anomalies with indexes of the Pacific Decadal Oscillation and the North Atlantic Oscillation showed that there are connections between these pattern and streamflow in the glacier fed rivers of the study regions. In Norway summer air temperature was lower than the long time mean value in a period from 1970 until 1993. In the same time the North Atlantic Oscillation index had a negative phase and the entire weather promoted the accumulation of snow. Thus mass balances of the most of the Norwegian glaciers had been positive in this period. In Canada the change of the Pacific Decadal Oscillation in 1976 resulted in an increase of variation of runoff from glacierized catchments.

The analysis of runoff correlation showed that the basins of the European Alps are the most influenced region in terms of air temperature while the basins of Norway are the most influenced region in terms of precipitation. To detect general differences I applied a principal component analysis on the regional data sets. Whereas the results for the European Alps and Norway are very similar, the Canada data set shows regional differences what might result in different streamflow behaviour. The correlation values were used for a cluster analysis and showed that the glacierized fraction of a catchment is the most important parameter to characterise streamflow change from glacierized catchments.

The glacierized fraction of a catchment is also found to be correlated with the strength of the trend in streamflow. Highly glacierized catchments show, responding to an increasing air temperature and with absence of increasing precipitation rates, a strong positive trend. With decreasing grade of glacierization this trend slope weakens. The threshold from which an influence of glacierization can be expected is dependent of the mass throughput. The value of the Norwegian data set (10 %) is much lower than for the European Alps data set (20 %). For Canada no such threshold could be identified as the data were too sparse.

Differences in streamflow from glacierized basins are mainly caused by the variability in precipitation. The reaction of runoff on accumulated snow, rain and summer snowfall can be positive ore negative, depending in the point of time. Basins with a strong correlation of runoff with precipitation, either during the accumulation period or during the ablation period show no uniform behaviour in terms of streamflow change. However, those basins with a high correlation of runoff with temperature allowed to interpret the general differences between the regions Norway and the European Alps. The Norwegian data have a stronger reaction to climate change in comparison to the European Alps data. The linear relations, derived of both data sets, have similar gradients but are located offset.

Results derived out of regional data can therefore only be adapted to other regions, having regard to the local climatic circumstances. For Canadian data it is recommended to differentiate between the individual glacierized regions. Furthermore the base data has to be sufficiently comparable.

Zusammenfassung

In dieser Diplomarbeit wurde das Abflussverhalten vergletscherter Einzugsgebiete in Kanada, Norwegen und den Alpen untersucht. Auf Grundlage der Arbeit von *Stahl & Moore* (2006) sollte die Frage geklärt werden ob die Gletscherschmelze in den Einzugsgebieten der verschiedenen Regionen ähnlich auf den Klimawandel reagiert, oder ob man generelle Unterschiede feststellen kann. Dazu musste ich zunächst geeignete Einzugsgebiete auswählen. Für die vergletscherten Regionen in Kanada und Norwegen lagen bereits umfangreiche Datensätze inklusive beschreibender Einzugsgebietsattribute wie *Einzugsgebietsgröße*, *mittlere Einzugsgebietshöhe*, *vergletscherter Anteil* und weitere vor. Für die Einzugsgebiete der Alpen hingegen stellte ich diese erst aus einzelnen Datenblättern und Publikationen zusammen. Da die Daten aus verschiedenen Staaten stammen, musste bei jeder zuständigen Behörde eine separate Datenanfrage erfolgen. Die erhaltenen Abflusszeitreihen lagen ebenfalls in unterschiedlichen Formaten vor und wurden vor der Verwendung in eine einheitliche Form gebracht. Letztendlich konnte ich alle Metadaten zu einer gemeinsamen Tabelle mit einheitlichen Einzugsgebietsattributen vereinigen. In dieser Tabelle wies ich den Einzugsgebieten eine eindeutige Kennung für die statistische Analyse zu. Sie erfolgte durch eine Zahl, entsprechend ihrem Rang in Bezug auf den vergletscherten Flächenanteil des Einzugsgebietes, und durch einen vorangestellten Buchstaben, der die Region kennzeichnet. Bei den zugehörigen Zeitreihen von Lufttemperatur und Niederschlag gab es in Zentral-Europa keine frei verfügbaren Zeitreihen für die entsprechenden Gebiete. Daher nutzte ich im Datensatz der Alpen und Norwegen Reanalyisisdaten. Für Kanada verwendete ich die Zeitreihen der nächstgelegenen meteorologischen Messstationen. Um keine beeinflussten Abfluss Zeitreihen zu verwenden wurden alle Einzugsgebiete mit großen Seen und bekannter starker anthropogener Überprägung ausgeschlossen. Für jedes einzelne Einzugsgebiet konnte nun eine komplette statistische Analyse in *R* durchgeführt werden. Um den Umgang mit solch großen Datenmengen zu vereinfachen, automatisierte ich diesen Vorgang mittels eines *Shell*-Skripts und ließ die Ergebnisse sowohl in eine Ergebnisdatei schreiben, als auch einen automatischen Bericht über *Sweave* erstellen. *Sweave* ist eine Programmiersprache, die eine dynamische Verbindung zwischen *R* und dem Textsatz-Programm LaTeX herstellt.

In den ersten Ergebnissen zeigte sich ein sehr starker Unterschied in der Verteilung der Einzugsgebietsgrößen. Während in Europa eine Vielzahl an kleinen Einzugsgebieten mit einer relativ hohen Vergletscherung bemessen wird, stammen die meisten Zeitreihen aus Kanada von sehr großen Einzugsgebieten mit vergleichbar geringem vergletscherten Anteil. Aus diesem Grund wurde der Kanadische Datensatz an die Verteilung der beiden anderen Regionen angepasst. Auf dieser Datengrund-

lage erfolgten nun die vergleichende statistische Analyse. Diese wurde wiederum in *R* durchgeführt.

Einen wichtigen Aspekt stellen die großräumigen Atmosphärenschwankungen dar, deren Index Werte Aufschluss über vorherrschende Wetterlagen geben können. So lagen beispielsweise die Sommertemperaturen zwischen 1970 und 1993 in den Norwegischen Untersuchungsgebieten unter dem Mittelwert der Untersuchungsperiode. Zur selben Zeit befand sich auch der Nordatlantische Oszillationsindex in einer negativen Phase. Die Gesamtheit der dadurch begünstigten Wetterlagen führte zu einer Zunahme der Gletschereismasse in ganz Norwegen. Erst seit dem Anfang der 90er Jahre wechselte der Trend auch in Norwegen hin zu negativen Massenbilanzen. In Kanada verursachte der Wechsel der Pacific Decadal Oscillation 1976 von einer negativen in eine positive Phase vor allem eine Steigerung der Variation des Gletscher Abflusses.

Die Untersuchungen der Korrelation des Abflusses mit der Lufttemperatur zeigte, dass die Einzugsgebiete in den Alpen in jedem Abschnitt der Ablationsperiode über den Werten der anderen beiden Regionen lagen. Bei der Korrelation des Abflusses mit dem Niederschlag hingegen waren die Norwegischen Einzugsgebiete herausragend. Hier konnte nicht nur der stärkste mittlere Zusammenhang festgestellt werden, auch die Spanne zwischen den Einzugsgebieten ist hier am größten.

Um generelle Zusammenhänge und Unterschiede innerhalb der Regionen aufzudecken unterzog ich die regionalen Datensätze einer Hauptkomponentenanalyse. Die Datensätze der Alpen und Norwegens ergaben ein relativ homogenes Bild im Gegensatz zum Datensatz aus Kanada. Dort konnte man deutliche Unterschiede zwischen den einzelnen Vergletscherungsgebieten erkennen und es gibt Grund zu der Annahme, dass diese ebenfalls im Verhalten der Gletscherschmelze wiederzufinden sind. Bei der nachfolgenden Clusteranalyse ist trotz der Anpassung der Datensätze eine Abgrenzung der Kanadischen Einzugsgebiete erkennbar. Betrachtet man die Korrelation zwischen den Abflusssummen während der Schmelzsaison (Ablationsperiode) und den vermeintlichen Einflussfaktoren, so zeigt sich ein wesentlich durchmischteres Bild. Es ist dadurch einfach ersichtlich, dass die Einzugsgebietsgröße nicht die entscheidende Variable bei der Charakterisierung vergletscherter Einzugsgebiete darstellt, sondern vielmehr der Grad der Vergletscherung.

In Bezug auf die Trends, die man in den Abflusszeitreihen feststellen kann lässt sich ebenfalls eine Abhängigkeit vom vergletscherten Anteil des Einzugsgebietes feststellen. Hoch vergletscherte Einzugsgebiete weisen bei gleichbleibenden Niederschlägen und steigender Lufttemperatur einen starken positiven Trend auf. Dieser Einfluss geht mit sich verringerndem Gletscheranteil im Einzugsgebiet zurück. Der Grenzwert, ab dem noch ein Einfluss des vergletscherten Anteils zu erwarten ist hängt vom Massenumsatz der Gletscher ab und ist in Norwegen mit 10 % niedriger als in den Europäischen Alpen (20 %). Für die Kanadischen Daten konnte aufgrund der Datenlage keine eindeutige lineare Beziehung aufgestellt werden.

Durch multivariate Analysenmethoden konnten im folgenden gezeigt werden, dass Unterschiede im Abflussverhalten vor allem durch die Variation in den Niederschlags-

mengen gesteuert werden. Die komplexen Zusammenhänge zwischen Akkumulation von Schnee im Winter, sowie Regen und Schneefall im Sommer können sich sowohl positiv, als auch negativ auf den Abfluss auswirken. Stark vom Niederschlag oder Schneespeicher abhängige Einzugsgebiete zeigten daher keine einheitliche Abflussänderung. Aus den Gletscher-dominierten Einzugsgebieten konnten generelle Unterschiede zwischen den Untersuchungsgebieten festgestellt werden. Die Norwegischen Daten zeigten eine stärkere Reaktion auf die Klimaänderung als die Untersuchungsgebiete in den Alpen. Der lineare Zusammenhang in beiden Datensätzen weist eine ähnliche Steigung auf. Diese kann beispielsweise durch den höheren Massenumsatz hervorgerufen werden.

Eine übertragung von Ergebnissen zwischen den Untersuchungsgebieten ist also nur möglich, wenn man die klimatischen Einflussfaktoren berücksichtigt. Im Falle Kanadas sollte allerdings bereits im Vorhinein zwischen den einzelnen vergletscherten Regionen unterschieden werden. Außerdem muss eine ausreichend vergeichbare Datenlage vorherrschen.

1 Introduction

1.1 General introduction

Glacier ice contains 75 % of all available freshwater on earth. Whereas 99.5 % of the ice masses are located in the Greenland and Antarctic ice sheets (*IPCC*, 1996), the remaining 0.5 % of the ice masses are spread as glaciers over high mountainous areas. In semi-arid regions like the prairies of Canada, Central Asia, the Himalaya, and much of South America's Andes Mountains, glacier meltwaters are the dominant component of the water balance (*Cogley*, 2005; *Barnett et al.*, 2005). The glaciers provide a big storage for drinking water and have a balancing influence on stream flow variation as they produce melt water and thus rise summer water levels when most basins are in low flow conditions (e.g. *Willis*, 2006; *Fountain & Tangborn*, 1985). During wet years big amounts of snow are accumulated on the glacier. In the following summer they appear as a reflection shield because of the high albedo as well as a storage for liquid precipitation (*Weber*, 2004). Furthermore, glaciers can be seen as indicators for climate change (*Oerlemans*, 2005, e.g.). Their sensitive reaction to the altering of air temperature and of precipitation rates nowadays results in a retreat of the glacier tongues as well as in a reduction of ice thickness, which is highly visible (*Meier et al.*, 2003). Projected increases in surface air temperature over the next century will deplete seasonal and longer-term storage in these basins as snowpacks melt earlier and glaciers continue to retreat. The earlier onset of the spring freshet and the reduction of streamflow during summer is of particular concern, because human demand for this important resource is maximal at this point of time (*Barnett et al.*, 2005).

1.2 Glacier hydrology

1.2.1 Glaciers

The mountainous cryosphere is a complex storage of water with resident times between a few hours and hundreds of years (*Fountain & Tangborn*, 1985; *Jansson et al.*, 2003).

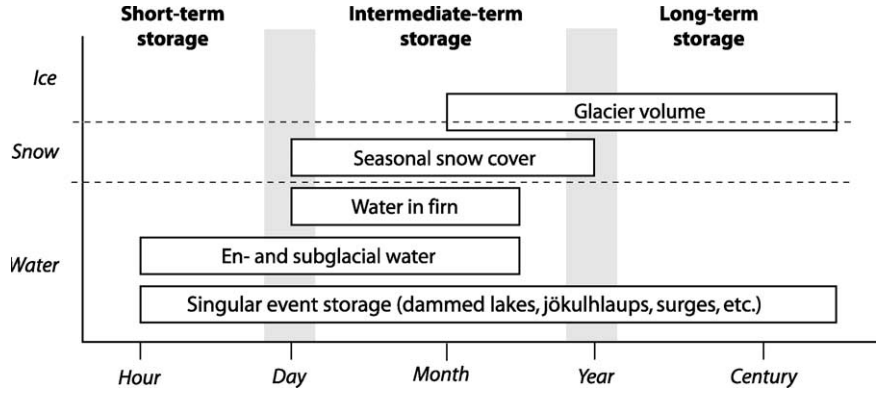

Figure 1.1: Time-scales in storage of liquid water, snow, firn, and glacier ice (*Jansson et al.*, 2003)

Depending on air temperature and thus elevation as well as topography, precipitation accumulates as snow. Due to self-weight and melt processes the snow pack alters and compresses to firn and later ice. Following the gradient this ice moves downward by several flow mechanisms (e.g. plastic flow, basal gliding and surging (see *Paterson*, 1998; *Van der Veen*, 1999; *Hooke*, 2005, and others for details.)). At a certain altitude the ice flow crosses the so called equilibrium line where the glacier is divided in the accumulation zone, where a gain of ice mass takes place, and ablation zone, with a netto loss of ice mass. The altitude of this equilibrium line (ELA) depends on the throughput of ice, on the melting rate and the glacier's surface albedo (e.g. *Collins*, 1982). Snow with its high albedo values protects the glacier surface from melting while dark debris on bare ice highly absorbs the energy of solar radiation and leads to higher melting rates (*Siegert*, 2005; *Cogley*, 2005). Downward from the ELA ablation rate increases evenly until the glacier terminus is reached. This is the place where meltwater typically leaves through the glacier mouth and ice calving takes place.

1.2.2 Runoff generation

Runoff generation in glacierized catchments can be divided into the area without glaciers and the ice covered area. The ice free sites are dominated by precipitation and snow melt water. Depending on the structure of the underground and the local gradient there is also a dependency on groundwater, contributed by precipitation

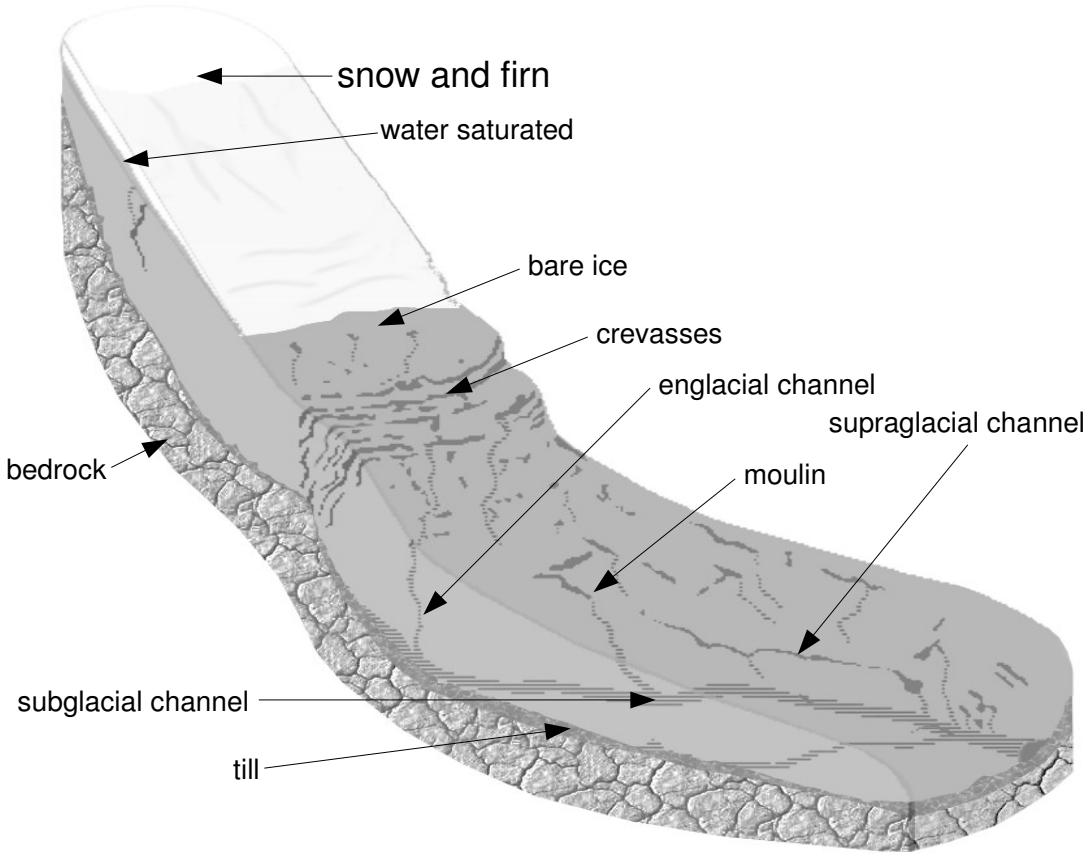

Figure 1.2: Idealized block figure of a temperate alpine glacier with the main hydrological components

and snowmelt possible. At the glacierized areas the runoff generation is rather complex. Figure 1.2 visualizes an idealized alpine glacier with the diversity of sections and flowpaths. In first order there are the supraglacial processes. Adjoining the atmosphere this is the place where melt water is produced and precipitation might infiltrate. During ablation period the energy budged at the surface is dominated by short and longwave radiation. Fluxes of turbulent and latent heat are further energy sources and sinks. They are linked to the atmospheric moisture and the temperature gradients in the boundary layer, as well as to local glacier wind systems that are responsible for the sustainment of characteristic convective and advective processes (*Hagg*, 2003; *Hock*, 2005). Snow and firn layers store the infiltrating water and thus smooth out diurnal variations of meltwater (*Fountain & Walder*, 1998). Percolation rates are controlled by gravity and the local degree of water saturation, leading to a delay in runoff (see figure 1.1). Once melt water reaches the glacier ice or the glacier builds the boundary to the atmosphere itself, runoff follows the gradient on the ice surface, concentrates in supraglaciel channels and enters the englacial via crevasses

or moulins (*Nienow & Hubbard*, 2006; *Collins*, 1982). The velocity and temporary storage of melt waters may lead to a lag of several days between the melting process and the arrival at the glacier snout. Due to the evolution of pathways this delay declines spatially from accumulation to ablation zone and temporally within the ablation period (*Lang*, 1973; *Lang et al.*, 1979; *Behrens et al.*, 1982; *Collins*, 1982; *Fountain & Walder*, 1998). Englacial conduits route the water to the subglacial drainage system. The pathways are dependent of the energy from meltwater throughflow and thus generally widen with big meltwater rates and close, driven by the inward creep of ice, after ablation period (*Collins*, 1982; *Fountain & Walder*, 1998). This "R" channels, called after *Röthlisberger* (1972), who was first to describe the hydraulics and thermodynamics that lead to dynamic ice conduits, have a relatively low surface-to-volume ratio. Hence they behave as fast flow paths in contrast to slow flow paths consisting of the water film on the ice-rock interface, connected cavities and other flow paths, that are affected by the properties of bedrock and glacial till (*Fountain & Walder*, 1998).

1.2.3 Hydrology of glacierized catchments

Glacierized catchments differ in their behaviour from non glacierized ones. They have an additional storage capacity in the form of ice. The bigger the proportion of this storage gets, the more runoff concentrates on the summer months and the smaller is the influence of rain on the runoff building processes in the basin (*Röthlisberger & Lang*, 1987; *Chen & Ohmura*, 1990; *Fountain & Tangborn*, 1985; *Jansson et al.*, 2003). The hydrograph of glacierized catchments shows a distinctive annual run, involving marked melt-induced diurnal cyclicity and a concentration of annual flow during the melt season as figure 1.3 shows.

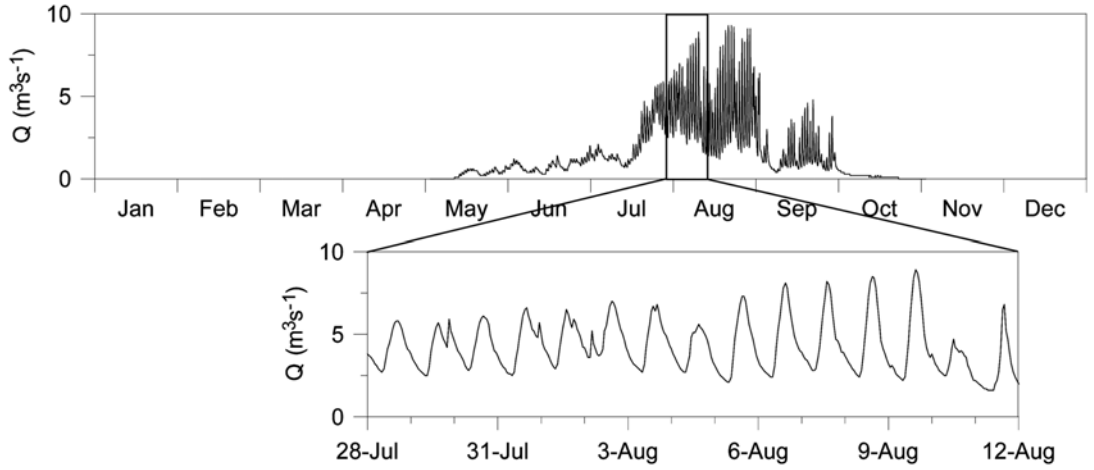

Figure 1.3: Hourly discharge at Vernagtferner, Austria, 1990, showing typical seasonal and diurnal variations (*Hock*, 2005)

With rising air temperature snow melt starts usually in May and passes into glacier melt during July. This change is fuzzy and can not be clearly confined. The growing

bare rock areas around the ice lead to an increase in sensible heat exchange with the glacier surface. During September the runoff decreases again and reaches low flow condition with the first snowfall events. (*Lang*, 1973). *Konovalov* (1994) found that the months from August to September are the most influenced runoff period by glacial melt waters. With a higher snow accumulation during the winter months, or snowfall during the ablation period, it is likely that the snow cover lasts longer and ablation is dimmed by the increased albedo (*Collins*, 1987; *Escher-Vetter & Siebers*, 2007; *Hock*, 2005). The temporal variations in snow melt are illustrated in figure 1.4, whereas figure 1.5 gives an example for the distinct influence of exposition and altitude on glacial runoff. Annual meltwater yield is directly proportional to summer energy input, whereas the relationship with precipitation is rather complex (*Collins*, 1987; *Singh et al.*, 2000). For European glacierized catchments evaporation can generally be considered small in contrast to the amount of precipitation and runoff (*Gurtz et al.*, 2002; *Verbunt et al.*, 2003; *Braun et al.*, 2007). The value is affected by sublimation and condensation over snow and ice as well as by wind-induced laterally transport of snow. *Aizen & Aizen* (1993) proved evaporation to be an important factor affecting runoff in the north slopes of the Himalayas where it leads to a net loss of up to 57 % of heat, whereas the area of Southeast Tibet receives 20 % of heat due to condensation (see table 1.2). Snow cover varies inter and intra annually and can thus not be assumed to be stationary. The influence of glacier ice instead can be assumed to be constant over short time periods (*Fountain & Tangborn*, 1985). This leads to the fact that the inter annual runoff variability depends on the percentage of the catchment that is covered by glacier ice . Catchments covered 10 % to 40 % by glacier ice show a minimum in seasonal or annual runoff variability (*Tvede*, 1983; *Fountain & Tangborn*, 1985; *Ferguson*, 1985; *Chen & Ohmura*, 1990), the so called *glacier compensation effect* after *Lang* (1986).

1.2.4 Climate change and glaciers

The effect of climate change on streamflow of glacierized catchments has been discussed in several publications (see e.g. *Kaser et al.*, 2003). On the one hand, solar radiation is the main source for melt energy, on the other hand glacier retreat is mainly influenced by changes in air temperature and precipitation (*Oerlemans*, 2005). With increasing air temperatures the sensible heat flux increases as well as the longwave radiation balance and only rising albedo values due to precipitation, falling as snow, can compensate this effects (see *Weber*, 2004, for details). Thus climate change results in a change of the forcing variables causing alteration in either accumulation, ablation or both of it (*Jansson et al.*, 2003). $1\,^{\circ}C$ warming is generally compensated by a 25 % increase in precipitation, showing that the weight is far more on the temperature side (*Oerlemans*, 2005). While a glacier grows, less runoff is generated than expected out of precipitation values and vice versa for periods of glacial retreat (*Jansson et al.*, 2003). It is obvious, that the recession of a glacier leads to a release of stored water and thus to an additional amount of discharge. On the other hand, a smaller glacier must release smaller amounts of melting water. This opposed effects lead to a preliminary increase in glacier runoff

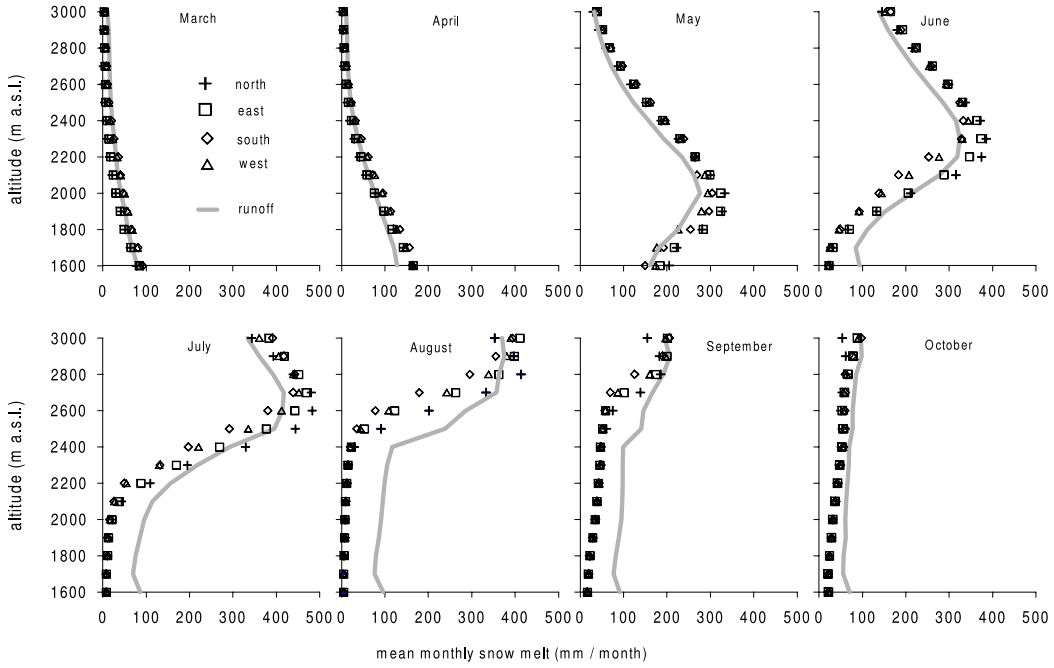

Figure 1.4: Mean monthly temporal variation of snowmelt-altitude distribution and exposition in the Dischmabach catchment, March until October in the period 1981-2000 (*Gurtz et al.*, 2002)

(excess runoff) before the melting rates retreat and the glacier finally disappears (*Kaser et al.*, 2003; *Jansson et al.*, 2003; *Collins*, 1987). Depending on the glacier size and mean accumulation rate each glacier has a certain response time (*static mass balance sensitivity*, see *Adalgeirsdóttir et al.*, 2006, e.g.) on the climate change signal (*Meier et al.*, 2003; *Kuhn et al.*, 1985). *Kuhn et al.* (1985) pointed out the coherence between area-altitude distribution and response time as the main influence beneath topography that is affecting ablation. Beneath general climate, the slope and the balance gradient play another remarkable roll on the sensitivity of glaciers to climate change. In wetter climate and with shallow surface slopes glaciers react more sensitive (*Oerlemans & Fortuin*, 1992; *Oerlemans*, 1994). Although there is general agreement that negative glacier mass balances will intensify (*Oerlemans et al.*, 1998, e.g.), the strong inter annual variability of climate has an unpredictable effect on projections concerning glacier extend (*Huss et al.*, 2008). Additionally unknown feedback mechanisms are expected to occur when changing glacier dynamics affect ice divides as well as subglacial watersheds and water courses (*Flowers et al.*, 2005; *Jóhannesson et al.*, 2006). *Lambrecht & Kuhn* (2007) showed that the degree of glacier retreat in Austria is more uniform over high glacierized areas, than over scarcely glacierized areas where special local conditions leads to high variations in glacier loss area. A further influence on glacier behaviour is their teleconnection to large-scale atmospheric circulation processes (e.g. *Meier et al.*, 2003). *McCabe et al.* (2000) found out that winter mass balance mechanisms in the North American glaciers are different to those in Scandinavia and Central Europe, where this

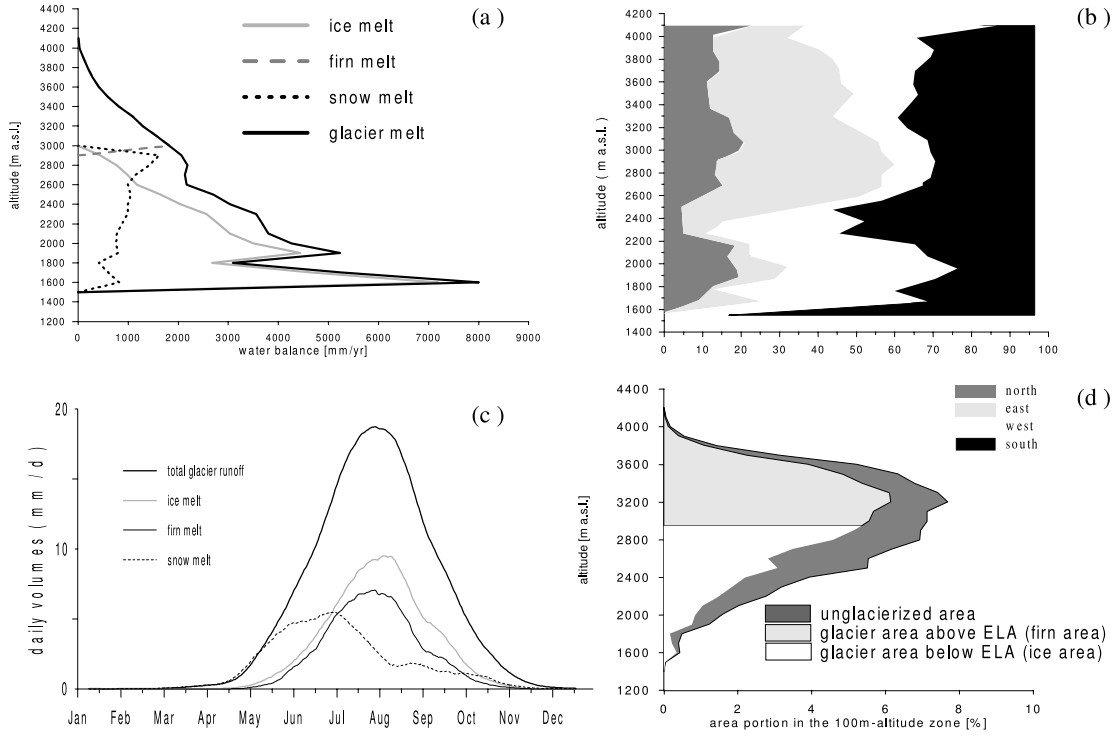

Figure 1.5: Mean altitudinal (a) and temporal (c) distribution of runoff from Massa catchment including the portions of the main expositions (b) and of the glacierized/unglacierized areas in the altitudinal zones (d) (*Gurtz et al.*, 2002)

mechanisms seem to be rather equal. Overall, glacier fluctuations, as a reaction to climate signals, can be characterized as a function of height (*Oerlemans*, 2005).

1.3 Review

In hydrology the relation between runoff and the meteorological variables is crucial. In contrary glaciological science is commonly based on measurements of ice mass and terminus length instead of runoff, what is reflected by the literature in the common journals. The majority of the studies concern either mass-balance measurement, energy modelling or both. Unfortunately they apply this methods just on one, or in a few cases on a small amount of glaciers (see *Klok et al.*, 2001; *Kaser et al.*, 2003; *Schaefli et al.*, 2005; *Rees & Collins*, 2006; *Koboltschnig et al.*, 2007, e.g.). Within mass-balance measurement the glacier volume is determined by a balance between the state after accumulation (winter period with snow fall and wind drift) and ablation, occuring during summer, primarily driven by the surface energy balance (*Jansson et al.*, 2003). Most common in modeling approaches is the method that uses air temperature as a proxy for the main factors, controlling glacier melt (*Verbunt et al.*, 2003). The following paragraphs overview selected research publications, in regard to streamflow analysis in glacierized basins. The publications are ordered chronologically.

One of the first publications about time series analysis with glacier runoff, temperature and precipitation was presented by *Lang* (1973). He used two time series of four years and analysed how much the relation between discharge and meteorological elements is modified by specific seasonal terms. To ensure more or less steady state condition he subdivided the ablation period into four sub periods. The abbreviations and descriptions shown in table 1.1 are used in the following parts of this thesis.

Table 1.1: Ablation sub-periods after *Lang* (1973)

Label	Period	Description
$L1$	Beginning of May to mid-June	Start of snow melt, high snow cover percentage, high albedo
$L2$	Mid-June to the end of July	Snow melt and glacier melt, generally reduced albedo, improved drainage
$L3$	End of July to mid-September	Minimum of snow cover, low albedo, well-developed drainage system
$L4$	Mid-September to mid-October	Upper parts of catchment generally with new snow cover

In each sub period *Lang* (1973) used a sample size of $n > 170$ to compute correlation and performed regression analysis for the two test sites. The geomorphological difference of those sites caused significant differences in the results. The Massa catchment on the one hand is highly glacierized (67 % which equals 130.5 km^2) whereas the Rosegbach catchment on the other hand is just one third in catchment

size and with 22 km^2 glacier cover the ice covered area reaches 33 %. The influence of precipitation on runoff was found to be more positive in the Rosegbach than in the Massa catchment, where precipitation showed predominantly a negative correlation. Only the days with lag 0 in $L2$ and $L3$ indicate a positive influence of precipitation on runoff. For the prediction of runoff *Lang* (1973) applied a regression in form of equation 1.1.

$$q = c + b \left(\frac{t_0 + t_{-1} + ... + t_{-5}}{6} \right) \tag{1.1}$$

The author showed that besides temperature, precipitation and sunshine duration the influence of snow cover and its spatial distribution is essential in the runoff behaviour of a basin. Further the glacier altitude distribution and vapour pressure have been detected as main factors. A decline in delay time during the ablation period was verified.

With the intention to relate runoff directly to climate variables without reference to glacier mass balance *Collins* (1987) analysed runoff data from glacierized catchments in the upper Rhone valley. Melt water yield is directly related to summer energy input. Thus he analysed summer air temperature as well as mean annual precipitation for the period May, 1st until September, 30th. High glacierized catchments showed a good correlation with temperature whereas this correlation decreased with decreasing glacierized area. *Collins* (1987) used multiple regression analysis and proofed an additional amount of explanation by introducing precipitation additional to temperature. The use of winter precipitation in regression analysis lead to the highest gain in explanation. The author continued this study in 2005 with updated time series. *Collins* (2006) assumed that if the proportion of glacierized area has an influence on runoff variability it might also affect runoff responses due to warming climate.

Chen & Ohmura (1990) discussed the influence of glaciers on runoff changes in 39 catchments of the Swiss and Austrian Alps. These basins had a glacierized proportion from 83 % at the Vernagtbach basin down to 0.02 % at the Adda basin. The authors divide annual runoff Q_a from partly glacierized basins into the glacierized part Q_{ag} and the non glacierized part Q_{an}. As the basin area can be divided similarly, specific annual discharge q_a might thus be written as shown in equation 1.2, with α representing the glacierized part of the basin.

$$q_a = (1 - \alpha)\, q_{an} + \alpha\, q_{ag} \tag{1.2}$$

Chen & Ohmura (1990) computed the inter annual variation of their runoff time series and developed an empirical equation (1.4) to predict long-term runoff change Δq_a out of the physical equation 1.3 using only α, air temperature during the summer period T_s and annual precipitation P_a.

$$\Delta q_a = \frac{\partial q_a}{\partial \alpha}(\Delta \alpha) + \frac{\partial q_a}{\partial T_s}(\Delta T_s) + \frac{\partial q_a}{\partial P_a}(\Delta P_a) \tag{1.3}$$

$$\Delta q_a = \tilde{q_a}\,\Delta\alpha + \alpha\, a_1\,\Delta T_s + (1-\alpha)\,\tilde{a_1}\,\Delta P_a \tag{1.4}$$

While $\tilde{q_a}$ is the runoff difference factor between the specific runoff from ice-covered and ice-free parts, a_1 and $\tilde{a_1}$ represent the linear regression factors of T_s and P_a on q_a. Analysing the influence of the three main factors, shown in equation 1.3 the authors found the change in basin ice-cover to be the most important one.

For the Himalayan glaciers in North Tien Shan, Central Tien Shan *Aizen & Aizen* (1993) showed that temperature is not always a suitable predictor for glacial runoff. Depending on the proportion that turbulent heat exchange (H) obtains in the local heat balance they suggested to include further parameters like solar radiation balance (R), humidity and wind speed. Where no solar radiation data can be derived they commended a calculation via air temperature, considering general circulation characteristics. Results derived during field studies are presented in table 1.2, where additionally the flux of latent heat (LE) and the soil heat flux (S) are presented. The differences between the several regions are obvious. *Aizen & Aizen* (1993) presented locally adjusted regression methods that account for these main atmospheric influences and were able to compute a general integrated curve of runoff with altitude.

Table 1.2: Average heat balance components during melting period corresponding to field expeditions after *Aizen & Aizen* (1993)

Region	R (%)	H (%)	LE (%)	S (%)	Year of observation (month)
Central Tien Shan 4100 m	8.5 (96)	0.4 (4)	-0.6 (7)	-8.3 (93)	1989-90 (07-08)
North Tien Shan 3400 m	9.3 (85)	1.6 (15)	-0.8 (7)	-10.1 (93)	1985-92 (05-09)
Southeast Tibet 3400 m	3.6 (45)	2.8 (35)	+1.6 (20)	-8.0 (100)	1990 (09-10)
North Himalayas 5700 m	2.4 (86)	0.4 (14)	-1.6 (57)	-1.2 (43)	1991 (08-09)

Four years later, the authors came up with another study about the Tien Shan area in which they analysed and described the climatic and hydrologic changes over a period of 52 years. *Aizen et al.* (1997) found an increase in temperature and precipitation over the whole area, whereas snowpack declined. The ongoing glacier recession led to an increase in runoff from highly glacierized basins. Overall, the runoff in the region decreased with significant changes in the western and central parts of the study area. However, runoff is expected to increase with rising precipitation sums. The authors explain this by an increase in evaporation and percolation into the dominating sedimentary rock which is permeable for a longer period through the year. Further, the declining snow cover is compensated by glacial runoff in the high catchment areas.

Barbet et al. (1993) worked on the data set of Sarennes glacier basin which had a fraction of 41 %, covered by glacier ice. For June 1992 they developed a multilinear regression (equation 1.5) to fill their gaps in the runoff time series including the air temperature T_{a1} and precipitation P_1 of the previous day ($lagtime - 1$) as well as $lagtime - 4$ air temperature T_{a4} and a residual error term ϕ.

$$Q_0 = 136.9 + 22.6\,T_{a1} + 0.189\,P_1 + 9.49\,T_{a4} + \phi \tag{1.5}$$

Thus, they accounted for the delay in time of concentration, that is about 24 hours in the Sarennes glacier. Beneath the strong correlation of runoff with temperature, *Barbet et al.* (1993) found the glacial discharge being strongly autocorrelated and precipitation having a small negative influence on runoff. The start- and end period of ablation had high correlation coefficients in contrary to the high melt season, that behaved not as predictable. This is suspected to arise from the different melt processes of snow and ice (*Barbet et al.*, 1993).

With the focus on Himalayan basins in India, several studies have been carried out (*Singh & Kumar*, 1997; *Singh et al.*, 2000; *Singh & Jain*, 2002; *Singh & Bengtsson*, 2005; *Singh et al.*, 2006). While most of the studies followed a modelling approach with semi distributed, lumped hydrological models like the UBC-Watershed model (*Quick & Pipes*, 1977), *Singh et al.* (2000) applied the statistical approach and analysed autocorrelation and correlation of runoff, air temperature and precipitation at the Dokriani Glacier basin. With a drainage area of 16.13 km^2, and a glacierized proportion of 60 % this catchment is unique, as hydrological and meteorological data over a contiguous period of two years (1995-1997) are not available for any other high glacierized basin in the Himalayan region. The authors chose July-August as a representative glacier melt period and subdivided the ablation period by months (June, July, August and September). Autocorrelation with runoff from previous days was found to be very high, whereas correlation with temperature during June showed an important influence on runoff. Precipitation had its main influence during July and August, when the drainage network within the glacier is well developed and the periglacial can be expected to be free of snow and able to contribute runoff during rainfall events.

To determine the interactions between climate change, climate variability and the resulting glacier response, *Moore & Demuth* (2001) analysed streamflow, climate, and glacier data of Place Glacier in British Columbia, Canada. To explain relations between mass balance and climatic variability they applied a multiple regression analysis to model summer ablation (b_s) by the predictors winter mass balance (b_w) and summer air temperature (T_s) , shown in equation 1.6. These were strongest correlated predictors. Winter accumulation is influencing summer ablation by snow and thus water equivalent heights, and the end of the snowmelt period when bare ice lies open.

$$b_s = 6296 - 599\,T_s + 0.490\,b_w \tag{1.6}$$

The only significant negative trend occured in the August runoff data. This might be caused by the rather small sample size and the strong variability in the data. Slope and magnitude of the trend excluded the possibilities of measurement errors and led to the assumption that lower parts of the glacier contribute higher proportions of melt water. With the recession of Place Glacier large parts of the former ablation area have disappeared and thus melt rates decreased. Another possible explanation is the shifting of the drainage divide, causing the melt water from higher elevations to route down the southern Joffre Glacier rather than the northern Place Glacier.

Stream flow time series from various stations in Switzerland have been analysed by *Birsan et al.* (2005). One of the results was the extraction of main factors controlling stream flow trends. Besides altitude and soil depth of a catchment they found the glacierized part to be one of the key factors. While most of the catchments had decreasing trends during the summer months, those with more than 10 % glacier covered area behave oppositional.

With a data set of 169 glacier length time series *Oerlemans* (2005) developed a method to extract the climate signal. As air temperature and precipitation are the main influences on glacier mass balance and thus affect indirectly glacier length, the mean annual temperature perturbation (T') can be described as shown in equation 1.7 , with c being the climate sensibility ("decrease in equilibrium glacier length per degree temperature increase"), τ being the response time and L' representing the glacier length.

$$T'(t) = -\frac{1}{c}\left[L'(t) + \tau\,\frac{dL'(t)}{dt}\right] \tag{1.7}$$

The time series have been smoothed to get rid of annual noise (*Oerlemans*, 2008). τ and c were derived out of glacier length, mean slope and characteristic annual precipitation. The resulting reconstructed T' for the regions concerning this thesis are shown in figure 1.6 .

Applying a detailed multiple regression *Shea et al.* (2005) analysed the hydrological and meteorological relationships on the Haig Glacier in Alberta, Canada. Using mean daily discharge, daily average temperature, total daily incoming solar radiation, average daily detrended temperature, and standardised discharge range. The strongest seasonal correlation was observed with previous day's discharge, detrended temperature and accumulation-area-ratio as an indirect measure of average glacier albedo. Autocorrelation in regression analysis has been decreased by using detrended temperature values.

Stahl & Moore (2006) focused on the analysis of August streamflow, which is mainly glacier influenced in the region of British Columbia, Canada. Using Spearmans rank correlation coefficient (r_s) they found negative trends dominating the streamflow of glacierized catchments, whereas no uniform behaviour could be detected within the unglacierized basins (see figure 1.7). For additional information on glacier-influenced effects, rather than climate influence, *Stahl & Moore* (2006) applied a multiple re-

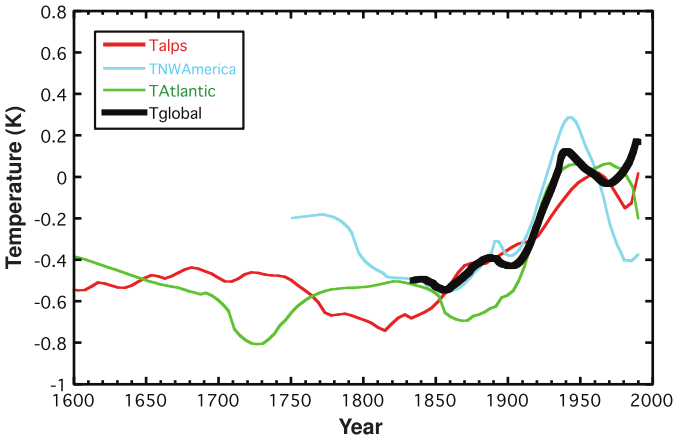

Figure 1.6: Reconstructed temperature in three glacierized regions (European Alps, North West America and Atlantic region). The black curve shows an estimated global mean value derived from the complete data set. After *Oerlemans* (2005)

gression shown in equation 1.8. They computed August runoff Q_{Aug} with the fluctuation in July runoff Q_{Jul} (as a term for carry-over storage), August air temperature T_{Aug} and precipitation P_{Aug}. While $\beta_0, \beta_1, \beta_2, \beta_3$ are estimated coefficients, e is the residual (observed minus predicted).

$$Q_{Aug}(t) = \beta_0 + \beta_1 Q_{Jul}(t) + \beta_2 T_{Aug}(t) + \beta_3 P_{Aug}(t) + e(t) \tag{1.8}$$

Changes in the residuals were only visible in the glacierized subset and showed that the trends are not only related to the interannual variations in climate but do also express changes in glacier conditions, what is consistent with an observed declining glacier area.

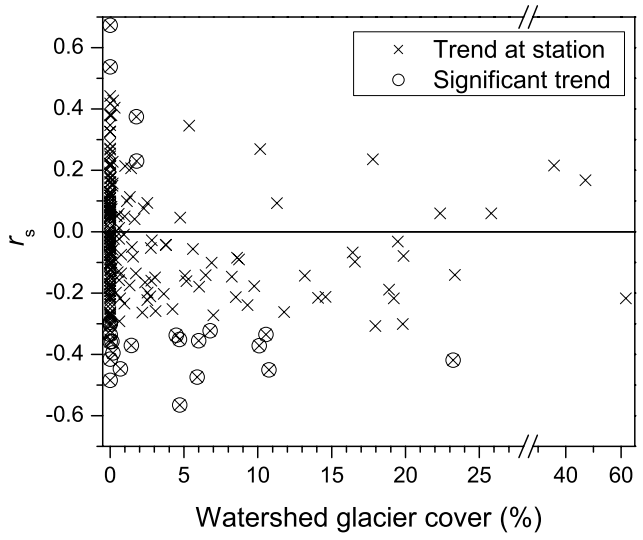

Figure 1.7: Annual August streamflow trends in relation to glacierized part of the basins (*Stahl & Moore*, 2006)

Lin et al. (2008) analysed the variations of the Lhasa river basin in Tibet, that is glacierized by 2.6 % and has a size of 26225 km^2. Time series of monthly mean runoff, precipitation, and air temperature data were derived from two hydrological and three meteorological stations. They found an increasing trend in annual as well as in summer runoff. After applying the non-parametric Pettitt test (*Pettitt*, 1979) the main change points have been detected. The strongest abrupt change occured around 1970. Precipitation has been found to have the strongest influence on the runoff variability in the Lhasa catchment.

Bhutiyani et al. (2008) divided their time series from four glacierized catchments in the North Western Himalaya into three sub-periods per year. Winter discharge lasted from November to February and persisted of base flow from sub-glacial melting and storage as well as of groundwater contribution. Spring discharge was dominated by seasonal snow melt and ended in May, followed by the monsoon discharge. This was the glacier melt season which lasted from June until October. It was also strongly affected by the monsoon rainfall. *Bhutiyani et al.* (2008) detected significant differences between the higher glacierized basins of Chenab and Satluj river and the lower glacierized ones of Ravi and Beas river. Whereas decreasing averages in runoff have been detected for the latter, the glaciers of the Chenab and Satluj basin compensated these effects until 1990. From that point of time the Satluj river also showed decreasing flows.

1.4 Goals of the thesis

During the last century the mean air temperature rose approximately 0.6 $^{\circ}C$. Nowadays there is common sense that this increase will enhance in the near future and is anthropogenically-caused (*Pachauri & Reisinger*, 2008). This will result in an ongoing or even amplified glacier decline, leading to a modification in streamflow pattern from high mountainous glacierized catchments (*Hock et al.*, 2005). The aim of this thesis was to analyse latest trends in streamflow, especially during the peak icemelt season in summer, and to compare recent developments in different glacierized mountain regions (particularly Western Canada, Norway, and the European Alps). The assignability of similar analysis of Canadian data by *Stahl & Moore* (2006) was put into question by scientists with a focus on glaciers in the European Alps and offered therefore an interesting study field. Mass balance comparisons carried out by *Dyurgerov & Meier* (2005) and *Kaser* (2006) indicated regional differences in glacier retreat. It was not intended to model and explain all modes of variability in detail, but as a regional comparative study, the aim was to elucidate first-order controls on recent streamflow changes, focusing on the role of glacier retreat in particular. Large data sets require the use of well structured and automated analysis methods. To accommodate these requirements the study is sectioned as follows:

- As a first step, I selected appropriate catchments and requested the data. Further I collected additional information and generated a data base of all high glacierized basins in the study regions.
- As a second step, I analysed the time series of runoff, air temperature and precipitation for each basin in the same period.
- The results have been taken into account in the third step, where I adjusted the distribution of the regional data sets.
- Within the last step, I analysed the similarities and differences between the study regions.

2 Study areas

2.1 Canada

British Columbia (BC) is the most western and third largest province in Canada. Its mountainous geography is dominated by two major mountain systems that are part of the Western Cordillera (see figure 2.1). The so called Pacific Coast Ranges rise directly out of the ocean followed by the Interior Plateau and the Rocky Mountains (RM). Both systems are about a 100 km wide and formed in a shape more or less parallel to the coastline of BC (*McGillivray*, 2000). From the Canada-United States border they extend to the boundary between BC and Yukon Territory with a distance of approximately 1500 km (*Clarke & Holdsworth*, 2002).

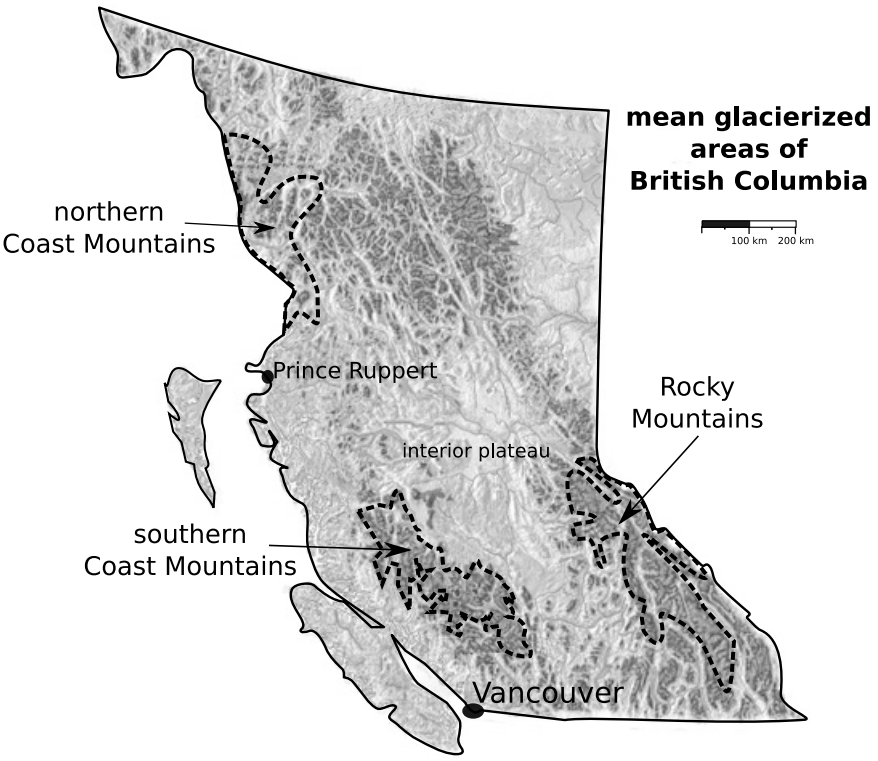

Figure 2.1: Relief map of British columbia containing the three major glacierized areas

2.1.1 Glaciers

Most of the Canadian glaciers can be found in BC. The three predominantly regions with huge plateau glaciers feeding several valley glaciers are shown in figure 2.1. The glacierized area between Vancouver and Prince Rupert is called Southern Coast Mountains (SCM). The average altitude of these glaciers is given by *Schiefer & Wheate* (2008) with 2023 m a.s.l., which lies between the region of Northern Coast Mountains (NCM) with approximately 1666 m a.s.l. and the more central RM with an average glacier height of 2397 m a.s.l. There are also glacierized areas at St. Elias, the Central Coast Mountains, and on the islands (*Schiefer & Wheate*, 2008). Many of these glaciers are characterized by high rates of mass turnover (*Arendt et al.*, 2002). The glaciers in Canada can be described as *winter accumulation glacier type* (*Hagg*, 2003). An general overview is given in table 2.1.

Table 2.1: Summary of the glacier area in British Columbia after *Schiefer & Wheate* (2008)

region	number of glaciers	total area [km^2]	numbers of glaciers larger than 10 km^2
SCM	3183	7145	88
NCM	2983	8549	124
RM	1623	1998	19
total BC	12031	25008	298

2.1.2 Climate

The climate of BC's mountains is dominated by dry summers and wet winters. To westerly mid-latitude cyclons they form a barrier, leading to high amounts of precipitation due to orographic uplift and advective moisture transport. Most of these low level flows are held off by the SCM and NCM. The RM obtain their precipitation mostly by mid-tropospheric lows that continue eastward with sufficient moisture (*Shea et al.*, 2004). Mean annual values for the high mountain regions vary between 400 mm/a and 4000 mm/a (*AtlasOfCanada*, 2009). The significant differences in local climate parameters derive from the complex topography. Air temperature is rather mild nearby the coast and gets a more pronounced seasonality with increasing distance to the coast and with raising hight. During the last century average annual temperature has warmed by 0.6 $^{\circ}C$ in the SCM, 1.1 $^{\circ}C$ in the RM and up to 1.7 $^{\circ}C$ in the NCM. Although the detailed view on air temperature trends give a more versatile perspective. The NCM have a strong increase in air temperature during spring but no significant change in summer and autumn. The SCM and the RM show also trends in mean and maximum air temperatures during the summer months. Precipitation increased slightly over whole BC and the timing of snowmelt and peak flow in major rivers shifted to earlier point of time. (*Fraser*, 2002; *Shea et al.*, 2004; *Déry et al.*, 2009). Climate in BC is linked to the Pacific Decadal

Oscillation (PDO) (*Moore & Demuth*, 2001; *Pelto*, 2004) that generally persists for 20 to 30 years. The cool PDO phase brings cooler temperatures and moister weather whereas the warm phase is responsible for warm ocean temperatures and drier weather (*Pelto*, 2004). Glacier mass balance has been strongly negative until the early 1990's when it stabilised somewhat. However *Evans* (2008) pointed out that this behaviour is not uniform. Even small glaciers in the Bridge River District did not share the recent acceleration of the wastage that is reported for most small glaciers in the European Alps.

2.2 Norway

The Norwegian mountains build the coastline to the Atlantic ocean, intermixing with the sea in a complex maze of fjords. The relief of the mountains is by far more even than the Canadian and central European mountain terrain. The peaks have been eroded by glaciers and wide plateaus (fjells) dominate the landscape. The highest mountain peak is the Galdehøpiggen (2469 m a.s.l.)

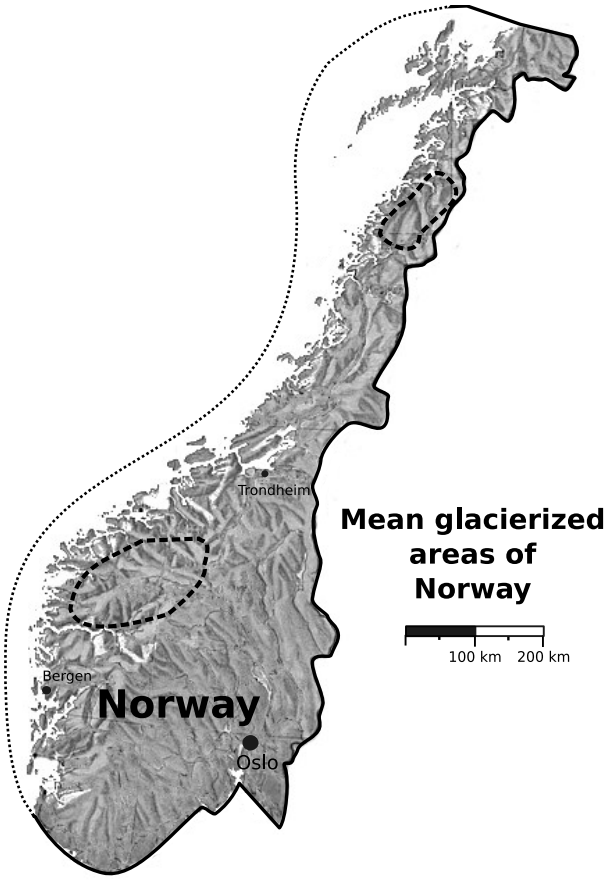

Figure 2.2: Relief map of Norway containing the major glacierized areas

2.2.1 Glaciers

Scandinavian glaciers are predominantly plateau glaciers in form of ice caps that build outlet glaciers draining into several valleys. The majority is larger and thicker than alpine glaciers. The maritime climate makes them more sensitive to winter precipitation than to summer temperatures (*Kuhn*, 2007). Although most glaciers in Norway (NO) experience maritime influence, there is a considerable gradient from west to east due to increasing continentality. A high proportion (15 %) of runoff in NO comes from glacierized areas and most of the electricity is generated by hydropower production (*Zemp et al.*, 2009). Figure 2.2 shows the main glacierized areas of NO with the Folgefonna, Hardangerjøkulen, Breeheimen, Jotunheimen, and Jostedalen in the Southwestern part and the Okstindan and Svartisen ice caps as well as further glaciers in Lyngen and Skjomen in the Northern area (*Zemp et al.*, 2009). Table 2.2 gives a summary of the number and total area of the Norwegian glaciers.

Table 2.2: Summary of the glacier area in Norway after *Østrem & Haakensen* (1993)

region	number of glaciers	total area [km^2]	numbers of glaciers larger than 10 km^2
Norway	1627	2595	33

2.2.2 Climate

The climate of the Norwegian mountains can be described as maritime mountain climate and equals the climate of the Canadian coast mountains (*Beniston*, 2005). However summers are much moister in NO than in BC. Annual precipitation is given by *Chinn et al.* (2005) with a range from 3500 mm/a at the foot of the coastal mountain regions, up to 5000 mm/a in the mountains. While there is agreement about an ongoing increase in air temperature, the prediction of precipitation is rather uncertain. Mass balance measurements show a positive trend for the last century, but changed their leading sign over the last decades (*Dyurgerov & Meier*, 2005). Nowadays, the retreat of the Norwegian glaciers is highly visible (*Kjollmoen et al.*, 2007).

2.3 European Alps

The mountain ranges of the European Alps (EU) stretch about 1200 km in a crescent shape along Slovenia, Italy, Austria, Switzerland, Germany, and France (*Rott et al.*, 1993). Tectonic processes are responsible that the Western Alps developed higher peaks than the Eastern Alps. Nevertheless, the general behaviour of glaciers can be

assumed to be of similar type (*Hagg*, 2003). The highest peak is the Mont Blanc with 4808 m a.s.l.

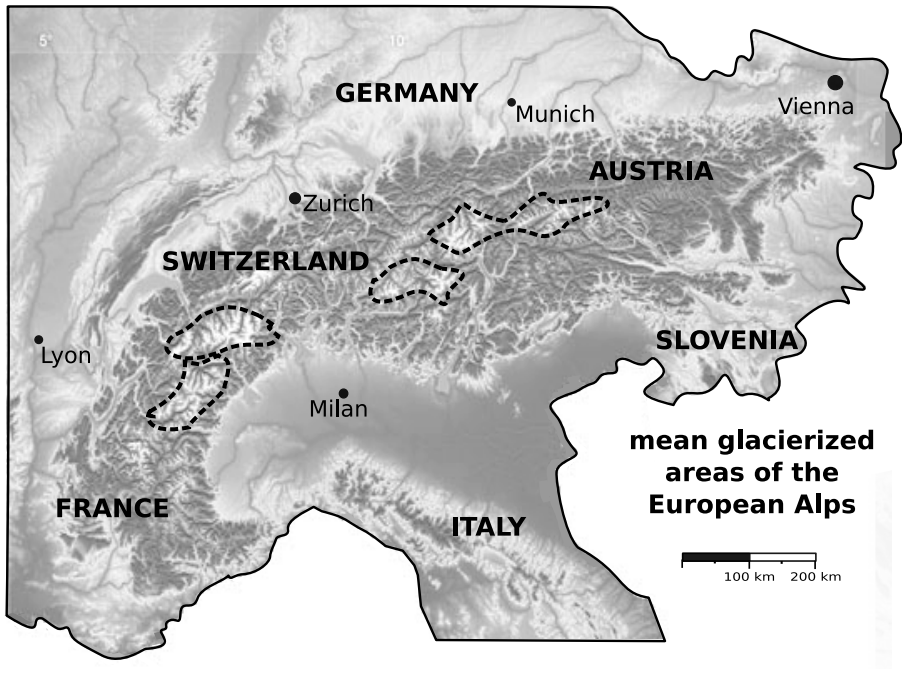

Figure 2.3: Relief map of central Europe containing the three major glacierized areas of the Alps

2.3.1 Glaciers

The major glacierized areas are arranged along the crest of the Alps. Large glaciers are mostly located at the highest elevations, combined with comparatively big areas above the snowline. Various smaller glaciers, however, can be found scattered throughout the Alps. Northern slopes have a higher degree of glacierization than Southern because of the lower energy inputs (*Rott et al.*, 1993). The ELA can be assumed to be higher than 2600m. Valley- and cirque glaciers are the most frequent form. Case studies have pointed out that alpine glaciers react more sensitive to temperature than to changes in precipitation (*Steiner*, 2008). A summary of the number and total area is presented in table 2.3. A good overview in terms of aspects, glaciersize, and gradients was presented by *Evans* (2006).

Various languages and dialects spoken throughout the EU led to many different terms for the word *glacier*. *Gletscher*, *Ferner*, *Kees* and the French *Glacier* are the most common in this work.

Table 2.3: Summary of the glacierized area within the European Alps

country	number of glaciers	total area [km^2]	numbers of glaciers larger than 10 km^2
Austria	925	542	5
Switzerland	1828	1342	17
France	640	350	6

2.3.2 Climate

The vertical extend of up to 4800 m a.s.l. forms a high barrier to the atmospheric circulation. Due to lifting processes and convective patterns, the precipitation amounts are usually bigger than in the surrounding plains. The versatile relief leads to an uneven distribution. The valleys in the inner Alps, Wallis and Tirol e.g., get just a fraction of the amount of precipitation which can be measured in Tessin, Vorarlberg or South-Tirol (*Braun & Weber*, 2001). The amount of precipitation varies between 600 mm/a and 1500 mm/a. *Escher-Vetter & Siebers* (2007) found an increase in air temperature over the highly glacierized catchment of Vernagtbach, Austria of 1.5 $^{\circ}C$ from 1986 to 2005. On the contrary snowfall decreased in the first part period and increased in the last, showing a high year to year variation. In the last 50 years, summer air temperature increased stronger compared to winter air temperature. Climate modeling prooved this ongoing trend and predict air temperature to increased by 3 $^{\circ}C$ until 2050 compared to 1990 (*North et al.*, 2007). Precipitation does not show an uniform behaviour. However, summer snow fall events decrease. More because of athmospheric conditions than due to higher temperatures (*Kuhn*, 2005). For Switzerland, *Birsan et al.* (2005) found winter precipitation to increase. The resulting mass balance for the European glaciers is negative during the last century, dominated by a strong ongoing decrease beginning in the early 80's (*Dyurgerov & Meier*, 2005). An outstanding year in glacial retreat was 2003, when previous ice volume losses where exceeded by nearly 60 % . This happened as a result of long lasting high air temperatures, sparse precipitation, and an unusual low albedo, that was caused by Sahara dust deposits (*Lemke et al.*, 2007). *Paul et al.* (2004) did not only confirm the general decline of glaciers in the EU but found even increasing rates of retreatment.

3 Data

Table 3.1: Data sources

Country	Runoff data	Climate data
Austria	Hydrographischer-Dienst-Tirol / Bayerische Akademie der Wissenschaften	Hydrographischer-Dienst-Tirol / Bayerische Akademie der Wissenschaften / poor man's reanalysis
Canada	Water survey, BC Ministry of Environment	Climate survey, BC Ministry of Environment
France	EDF-DTG	Reanalysis EDF-DTG / poor man's reanalysis
Norway	Norges vassdrags- og energidirektorat	poor man's reanalysis
Switzerland	BAFU, section hydrology	poor man's reanalysis

Data are derived from the sources given in table 3.1, were quality-controlled and formatted in different ways. In a first step they had to be converted. In a second step, additional information was collected to set applicable limits to the data set. Some meta data could be queried directly as they did arise of other research studies (*Stahl & Moore*, 2006). However, in many cases this data had to be assembled by hand using maps, atlases, world wide web-sources, and tables in journal publications. I arranged the derived data sets by glacierized proportion of the catchment and rejected single time series if either duration was too short, anthropogenic influences were detected, or lake area seemed to be too big. Only in a few cases meteorological measurement could be found nearby the hydrometrical station. I used the next available station. being aware of the uncertainties within assigning meteorological data this was the only possibility for the Canadian data to derive long lasting time series. In Europe it was even impossible to get the necessary meteorological data without payment. Thus we decided to use freely available Reanalysis data (*Berg & Christensen*, 2008). This data can be chosen from a 0.12 degree grid and thus should be highly representative. Unfortunately precipitation from the reanalysis set is first mostly biased, second seldom represents annual cycles, and third shows a tendency to an overestimated occurrence. For data management, the files where renamed to an identification number (ID) with a leading letter, assigned to the glacierized proportion of the catchment and to the region. Further, the data sets where subdivided into a long period data set (*LTS*), lasting from 1960 to 2004, and a

short period data set (*STS*), starting in 1979 and lasting until 2004. Unfortunately additional data about the glaciers like hypsometry, exposition, and ablation area were scarcely available. The data provided at the *World Glacier Monitoring* website (`http://nsidc.org/data/glacier_inventory/index.html`) and the *Global Land Ice Measurements from Space* website (`http://www.glims.org/`) do not offer the required time series of data for this case. They rather integrate special case studies like *Haeberli et al.* (1991) or *Paul et al.* (2004) e.g., and provide online access to volumes of mass balance bulletins. Table 3.2 gives the total numbers of time available series for each country.

Table 3.2: summary of the data set

Country	number of time series
Austria	5
Canada	74
France	3
Norway	15
Switzerland	14

3.1 Errors

The biggest errors can be found in precipitation values. Uncertainties in the extrapolation and the usage of constant annual altitudinal dependence together with strong spatial variability of precipitation might lead to an overestimation of values (*Verbunt et al.*, 2003). In contrast, single raingauge measurements systematically underestimate precipitation amounts and have to be corrected (*Klok et al.*, 2001). It is uncertain which amount of precipitation falls as rain or as snow. One possibility is the development of empirical equations in dependence of air temperature (*Aizen & Aizen*, 1993) but they would have to be determined separately for every single glacier which exceeds the possibilities of this study. To compare data within the reanalysis data set, single stations have been selected where precipitation and temperature are available over a long period. Reanalysis precipitation values tend towards high values and frequency. Air temperature data represent the measured values in an adequate way. Several reasons are responsible for the errors in runoff data. Beneath systematical errors in methods and stochastical errors in high mountainous basins there are problems due to ice, high bed load and log jams. Another error may arise out of the status and the change in glacierized area over the study time period. In this work I used one value. It can not be expected that this value represent the status of 2008 in all catchments, neither it will represent the average of the study time period. Being aware of these errors, the study will focus more on the general behaviour of the catchments than on certain values.

3.2 Scales

The different regions vary not only within the latitude and longitude but rather in their land use form, population density, and history. All of these aspects govern the size and locations of hydrological measured basins. While the Canadian data set contains many low glacierized catchments with a large area, the data set of the EU is dominated by very small basins that have a high glacierized proportion. The glacierized basins of the Norwegian data set instead are also highly glacierized but the size of the glacier area of the European basins is rather small in contrast to the Canadian basins. To make the data sets comparable a sub set of the Canadian data set has been selected. Figure 3.1 and figure 3.2 show the difference between the original data set and the sub set. It is obvious that the majority of the Canadian data set consisted of very large catchments, where precipitation, groundwater and evapotranspiration might be of overriding importance. The selection was done randomly by an algorithm that accounted for the catchment size, the glacierized proportion and the number of catchments in a glacierization class.

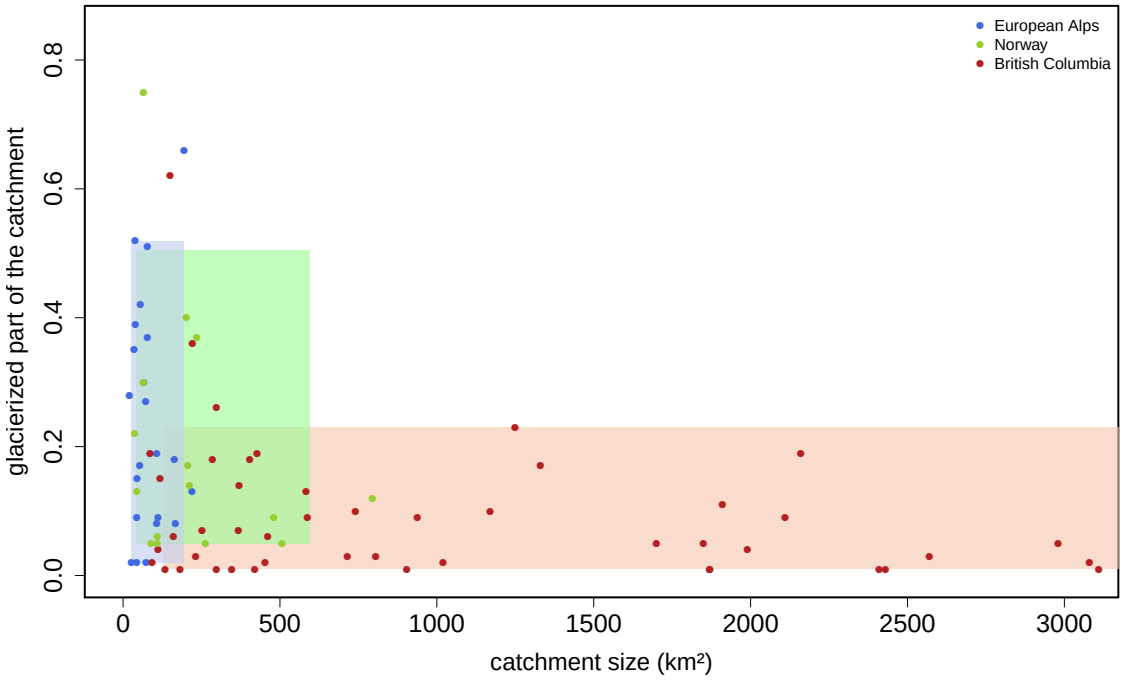

Figure 3.1: Catchment sizes (smaller than 3000 km^2) and glacierization of the Canada, Norway, and the European Alps data set. The boxes represent the 5 % to 95 % quantiles

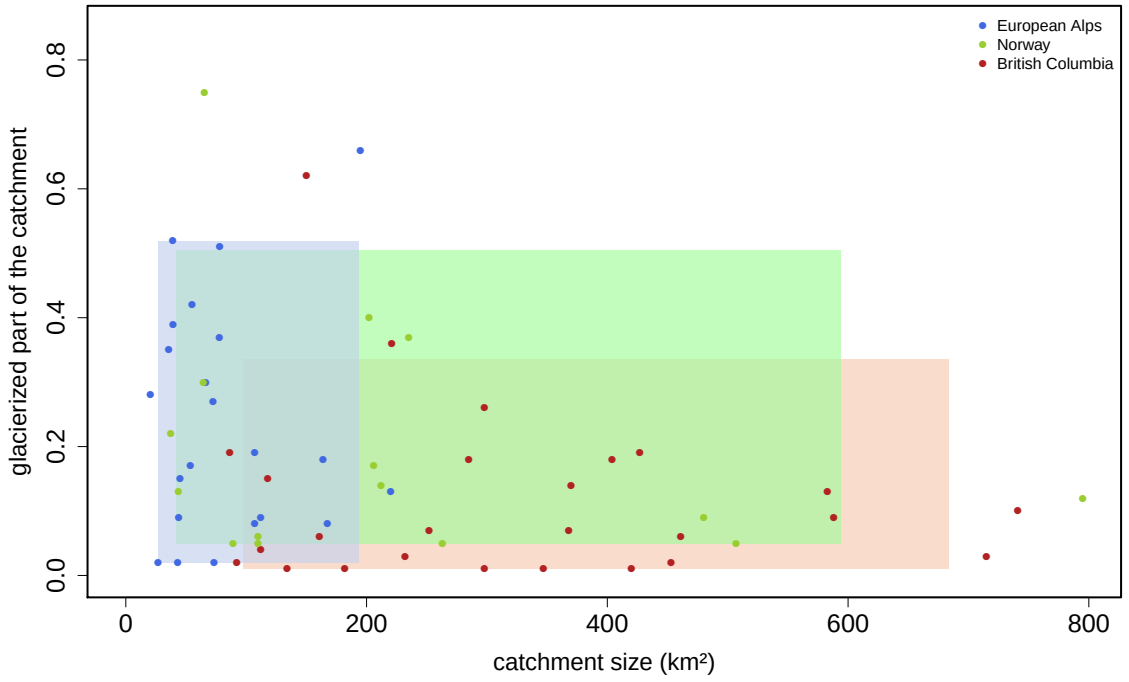

Figure 3.2: Catchment sizes and glacierization of the Canada, Norway, and the European Alps data set, used in analysis. The boxes represent the 5 % to 95 % quantiles

3.3 Dams and hydropower

In Switzerland nowadays about 40 % of the electricity is produced by hydropower driven by storage reservoirs (*Schaefli et al.*, 2007). Figure 3.3 shows the history of dam construction for the particular regions. The efforts of Switzerland during the 60's represent the general development in Central Europe and show, that the number of rivers with natural flow decreased dramatically in this time. Even in high mountainous regions and close to the termini of the glaciers outtakes were built that lead the meltwater through maintains, crossing several catchments into big storage reservoirs. In the EU, today only a hand full of basin outlets can be considered to represent natural flow conditions from glacierized basins. The development of hydropower in NO had its peak ten to fifteen years later. The affluence on rivers with high flow rates and steep gradients made it possible that NO increased the installed output by 10730 MW, setting NO to first position in European hydropower (*Andersen*, 2006). Canada is the world leading country in hydropower (*Andersen*, 2006). 40 % of the electricity consumed in the Pacific North West is generated by federal dams in the Columbia River Basin (*Hamlet et al.*, 2002). Canada produces 70000 MW with over 475 hydroelectric plants. Formally, the government invested into major projects where large storage reservoirs have been flooded. Nowadays, the capacities and the acceptance for such programs are missing. Nevertheless, the

engagement in hydropower is unbroken. Rivers in every region and especially in BC, get more and more used to produce electricity in so called small hydro power plants. This development makes it very difficult to gather data, that represent streamflow from glacierized basins.

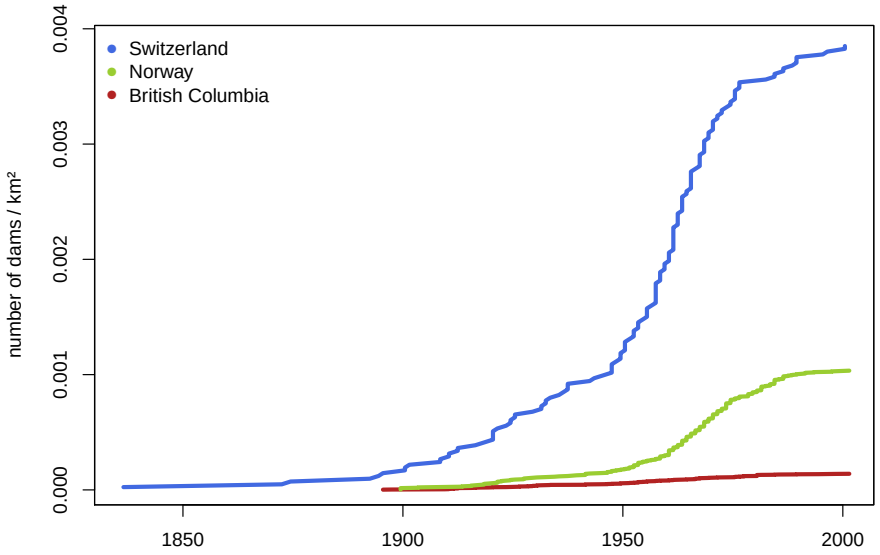

Figure 3.3: Construction of dams in Switzerland, Norway, and British Columbia

4 Methodology

4.1 Statistical methods

In this study I used various statistical methods. Table 4.1 overviews the applicated methods and the data used. The following subsections summarise the essentials of these applied methods.

Table 4.1: Statistical methods, their use and the kind of data

Analysis	Method	Data
Detection of gaps or jumps	Exploratory data analysis	five day moving average time series data
Correlation	Correlation analysis	annual sums and sums of sub-periods
Trends	Trend analysis	sums of sub-periods
Residual analysis	Regression	sums of sub-periods
Moving correlation and regression	Correlation and regression analysis	daily values of sub-period carried foreward
Detection of intra-regional similarities and differences	Principal component analysis	standardized geomorphologic parameters, sums and correlation values
Detection of inter-regional similarities and differences	Cluster analysis	standardized geomorphologic parameters, sums and correlation values

4.1.1 Exploratory data analysis

Runoff, air temperature, and precipitation time series of each catchment have been plotted (figure 4.1 e.g.) and visually controlled, to detect data gaps and implausible values. If longer data gaps or step changes were present, the concerning time series were excluded. During the next steps quantiles, sums and correlation coefficients were computed to summarize the crucial characteristics of the time series. To include all possible influences the winter accumulation was considered beneath mean precipitation, mean ablation, and mean temperatures in several sub-periods (yearly, monthly, and partitioned into certain ablation periods, see section 1.3). To determine the influence of large scale atmospheric patterns mean standardised time series

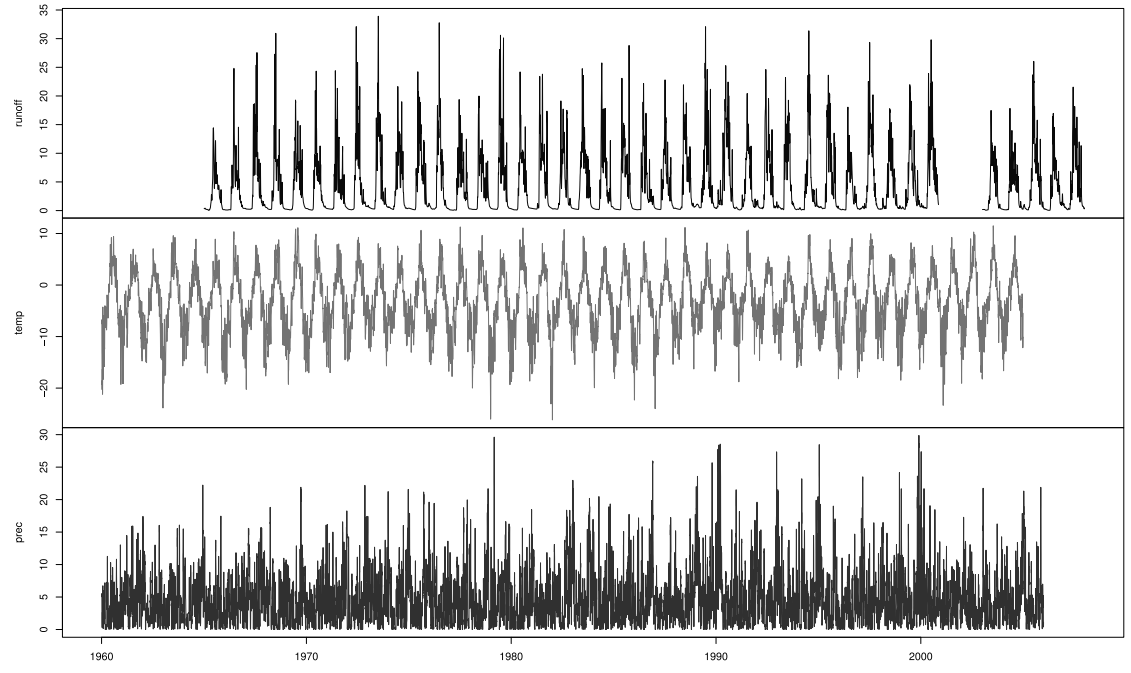

Figure 4.1: Time series plot of Liavatn, Norway exposing limits and a gap

where computed and the mean value of the time series was subtracted. A special case is the Pardé coefficient, that is computed by monthly and annual mean values, as shown in equation 4.1.

$$Pk_i = \frac{12}{n} \sum_{j=1}^{n} \left(\frac{Q_{ij}}{\sum_{i=1}^{12} Q_{ij}} \right) \tag{4.1}$$

4.1.2 Correlation

Correlation analysis estimates the extent of the relationship between a pair of variables. The most common methods are the Pearson-, Spearman- and Kendall correlation. The derived correlation coefficients range between -1, expressing totally negative influence, and $+1$, representing a perfect positive influence. A good visual correlation test is the scatterplot (figure 4.2). All variables are plotted against each other what makes special relationships easily visible. In this thesis the Spearman correlation was computed because it is independent of a certain distribution and is more robust against outliers. The only condition to apply this method is a monotonic relation between the two variables. The data are ranked in a first step and Pearson correlation is applied to the ranks in a second step. So the coefficient explains the relationship between the ranks more than between the real values (see *Reimann et al.*, 2008, e.g).

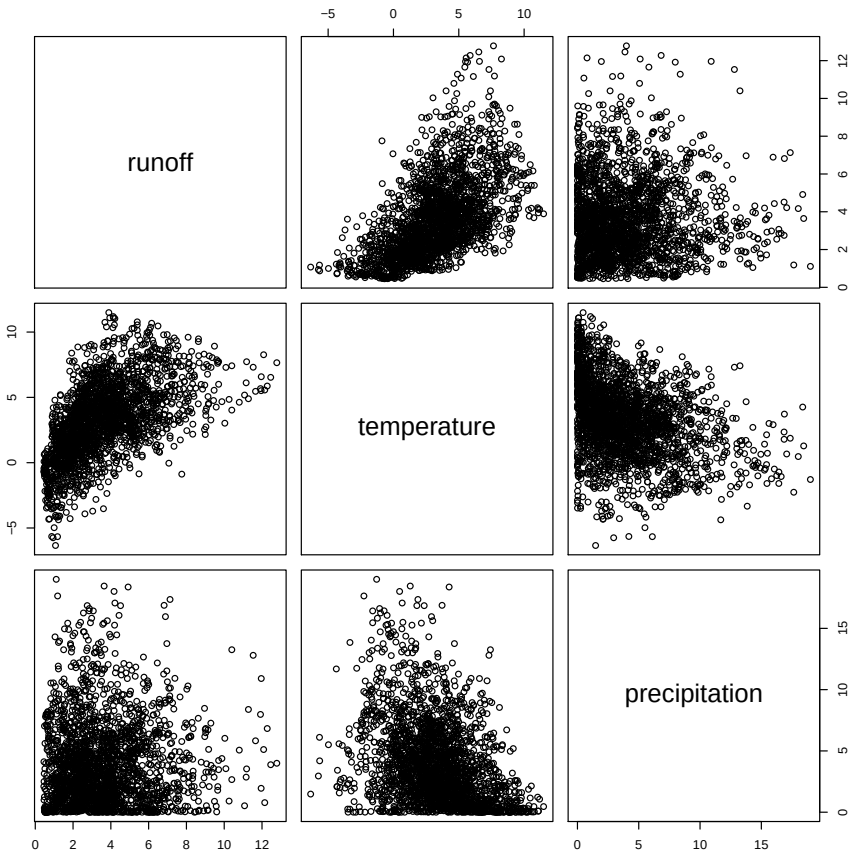

Figure 4.2: Scatter plot, showing the relation between runoff (m^3/s), air temperature ($°C$), and precipitation (mm) at Liavatn, Norway.

4.1.3 Regression

The aim of regression analysis is to predict the response of a dependent variable x_t by one or more independent variables $z_{t1}, z_{t2}, ..., z_{tq}$. In this thesis time series of climatic data are used. Precipitation and air temperature are assumed to be independent and an empirical equation is developed to predict runoff. The influence of the predicting variables were generally understood and tested by correlation analysis. Equation 4.2 shows a simple linear regression model with unknown $\beta_1, \beta_2, ..., \beta_q$ fixed regression coefficients and ω_t expressing the random error or noise term. The coefficients are estimated by minimizing the residual sum of squares (*Shumway & Stoffer*, 2000).

$$x_t = \beta_1 z_{t1} + \beta_2 z_{t2} + ... + \beta_q z_{tq} + \omega_t \tag{4.2}$$

4.1.4 Trend analysis

Trend analysis is a recently strongly discussed field. Formally often used to account for changes in runoff (*Hisdal et al.*, 2001; *Burn & Hag Elnur*, 2002; *Kundzewicz & Robson*, 2004; *Déry & Wood*, 2005; *Li et al.*, 2007, e.g.) nowadays there are concerns in applying these techniques. The main problem is that hydrological time series are expected to underlay long-range persistence (see *Bhutiyani et al.*, 2008, e.g.). This makes the concept of trend analysis unfeasible (*Koutsoyiannis & Montanari*, 2007). In contrary this study uses trend tests only to show similarities or differences in changing stream flow pattern instead of focusing on statistical significance.

4.1.4.1 Mann-Kendall trend test

The Mann-Kendall trend test (MK) is a non-parametric test for trend detection in time series and has been widely applied in environmental sciences (recently in *Bhutiyani et al.*, 2008; *Lin et al.*, 2008; *Déry et al.*, 2009). It was developed by *Kendall* (1938, 1970) and *Mann* (1945) and is based entirely on ranks. Therefore it is robust against non-normality and censoring (*Hirsch & Slack*, 1984). The rank correlation τ compares the actual score of the dataset with the maximum possible score that would be reached if the dataset was ordered by ranks (*Kendall*, 1938).

Null and alternative hypothesis of the MK test for a trend in a random variable x is presented in equation 4.3 and 4.4.

$$H_0 : Pr\left(x_j > x_i\right) = 0.5, j > i \tag{4.3}$$

$$H_A : Pr\left(x_j > x_i\right) \neq 0.5, (\text{twosided test}) \tag{4.4}$$

$$S = \sum_{k=1}^{n-1} \sum_{j=k+1}^{n} sgn(X_j - X_k) \tag{4.5}$$

In equation 4.5 the MK statistik test is calculated, where X_k and X_j represent sequential data values while n is the length of the data set and $sgn(\Theta)$ is the signum function explained in equation 4.6.

$$sgn(\Theta) = \begin{cases} +1, & \Theta > 0 \\ 0, & \text{if } \Theta = 0 \\ -1, & \Theta < 0 \end{cases} \tag{4.6}$$

Within the MK test there are two important parameters for trend detection. One is the level of significance, indicating the strength of the trend, the other is the slope magnitude explaining the direction and magnitude of the trend. The obvious

missing term was a value for this slope, that could be used to show the trend line in graphics. The work of *Theil* (1950) (in *Déry & Wood*, 2005) and *Sen* (1968) led to a linear equation that represents this magnitude and slope of a trend in the dataset. A good overview is given by *Helsel & Hirsch* (1993) and *Granato* (2006).

4.1.5 Multivariate statistical methods

With high dimensional data sets a graphic representation is difficult. Even three dimensional plots are often not helpful in terms of understanding. Thus multivariate statistical methods try to reduce the information of a high dimensional data set to a complexity that can be visualised.

4.1.5.1 Principle component analysis

The aim of the principle component analysis (PCA) is to reduce the dimensions of a data set by creating new, independent components (PC). Few of these PCs are expected to describe the majority of the variability in the data set (*Reimann et al.*, 2008). The method can be characterised as an orthogonal, linear transform on a number of possibly correlated variables into a smaller number of uncorrelated variables called principal components. The aim is to interpret the linear combinations in some natural context. If the first few principal components account for the majority of the observed variation and the following components describe only small amounts of variance, the multivariate data set can be displayed and interpreted easily. The statistical procedure contains the subtraction of the mean as a first step. Then the correlation matrix R is built for the case of p x-variables in a second step. Equation 4.7 shows the coefficients $a_{n\,i}$ of the x-variables in a linear transform. Corresponding to the i^{th} principal component Y_i, these coefficients are the elements of the eigenvector, corresponding to the i^{th} largest eigenvalue (α_i) of R (*Backhaus et al.*, 1996). The sum of all squared coefficients has to be one (equation 4.8). The proportion of the variation in the data, explained by the i^{th} principal component is explained in equation 4.9.

$$Y_i = a_{1\,i}\,X_1 + a_{2\,i}\,X_2 + ... + a_{n\,i}\,X_n \tag{4.7}$$

$$\sum\nolimits_{i=1}^{n} {a_i}^2 = 1 \tag{4.8}$$

$$\alpha_i = \sum\nolimits_{j=1}^{p} \alpha_j \tag{4.9}$$

A good overview about PCA and Factor Analysis is given by *Backhaus et al.* (1996) and *Reimann et al.* (2008).

4.1.5.2 Cluster analysis

Various cluster analysis methods exist. The general aim of the method is to discover structures in a data set by building groups with related unities. In this thesis the hierarchical tree clustering was applied. This method joins the most similar unities and creates stepwise new clusters. As a distance measure the Euclidean distance (equation 4.10) was chosen. The rule for the linkage between clusters was computed by the Ward method, that attempts to minimise the sum of squares for all pairs of clusters that can be formed at each step (*Reimann et al.*, 2008; *Backhaus et al.*, 1996). The advantage of cluster analysis over PCA is that even large data sets can be displayed in a clear way. However, the interpretation of the scatterplot is often much easier than the interpretation of a large dendrogram, that is strongly affected by the cluster method and the distance measure. Thus, the regions have been analysed by PCA first and compared by cluster analysis later.

$$distance(x, y) = \sum\nolimits_i (x_i - y_i)^2 \tag{4.10}$$

4.2 Software

All statistical methods have been applied by using the statistical programming and data analysis language *R*. The packages used within *R* are named *dynlm*-package for time series regression, *zyp*-package for Theil-Sen Robust line and MK statistic. The code has been implemented into a *Sweave* document, where LaTeX reports containing results, figures and even tables (computed within the *R* code by the *xtable*-package) are produced automatically. The initialization and recursive processing of all time series is controlled by a *Linux Shell* script. The complete workflow is presented in figure 4.3.

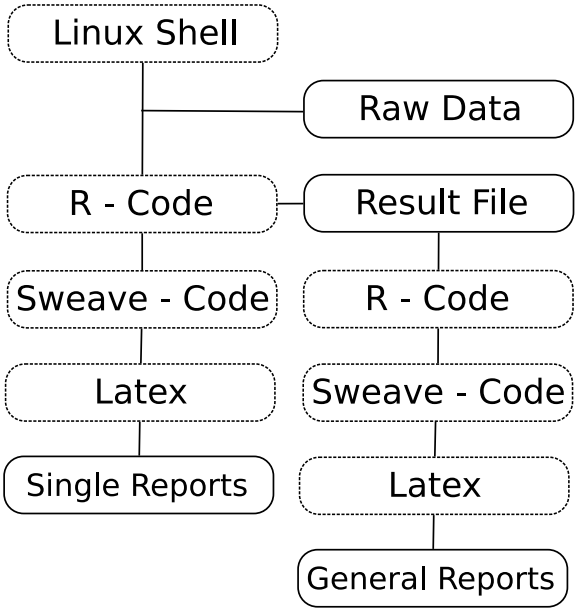

Figure 4.3: Processing workflow of this thesis

5 Results

The results are reported in the following sections. First, I give an overview about constitutive relations for each study area. Second, similarities and differences between the regions are analysed. Two data sets have been analysed. The longer time series (LTS) is presented when there are remarkable differences in contrast to the more comprehensive shorter period (STS, see chapter 3).

5.1 Study areas

5.1.1 British Columbia

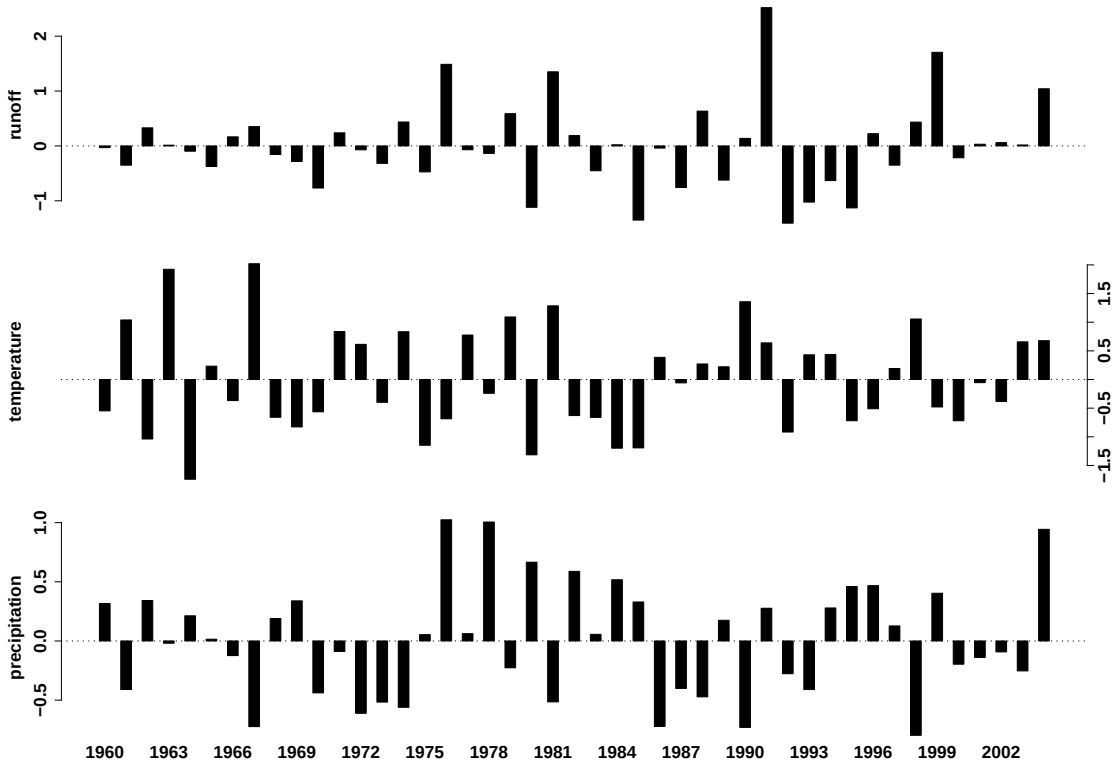

Figure 5.1: Mean anomalies of runoff, air temperature and precipitation in the L3 data set of British Columbia

The mean time series of anomalies in runoff, air temperature and precipitation during the L3 period are presented in figure 5.1. All three variables show a high variation.

The precipitation time series shows a remarkable shift in 1976 when PDO changed from a negative to a positive period (*Moore & Demuth*, 2001). From that point of time the variability in streamflow increased. Negative anomalies in the runoff time series seem to be linked to a combination of negative anomalies in air temperature and positive anomalies in precipitation.

The correlation of runoff with temperature in the BC data set (BCD) is high for the L1 period (see chapter 1.3) and decreases strongly with the change to L2 (figure 5.2) when snowmelt season is completed in the low altitude catchments and the lower parts of the other catchments. During the L3 period the variability is more than double the variability of L1. Values are predominately positive in contrast to the L2 period but the median is almost the same. Some catchments have a more pronounced dependence on temperature again, demonstrating their glacial character. L4 is characterised by a shift toward more negative values. Median values increase slightly. In every period excluding L1, negative correlations of runoff with temperature are present. Median values range between 0.0 and 0.7. The general differences between the L2 and the L3 period show that snowmelt season can be considered to be terminated before L3 begins. Thus this period is chosen as a representative period for glacier runoff in the BCD.

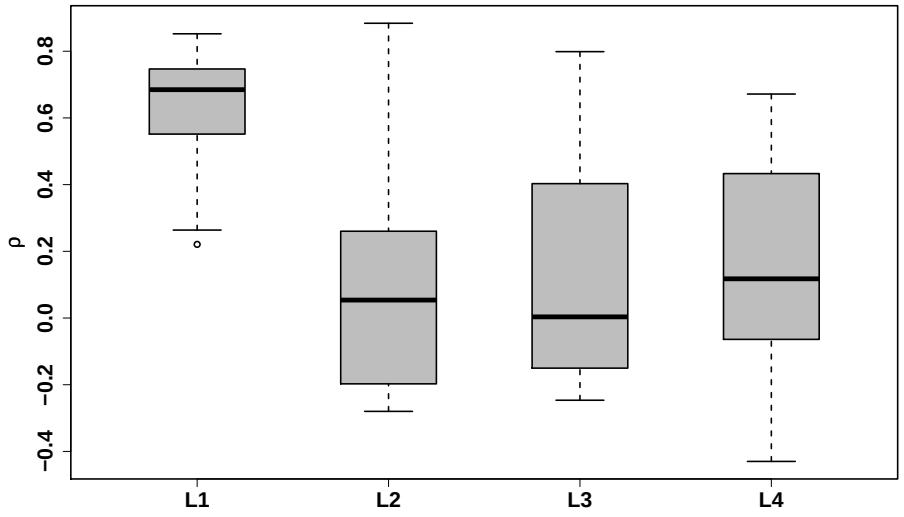

Figure 5.2: Correlation of runoff with air temperature during the ablation period for the British Columbian data set

During the ablation period the correlation of runoff with precipitation rises steadily, what is shown in figure 5.3. The biggest differences occur between L2 and L3 period as well as between L3 and L4 period. The L1 and L2 period are more balanced in terms of positive and negative correlation values, whereas those in L3 and L4 period are predominantly positive. Maxima values of correlation with air temperature have a peak during the L2 period and decrease thereafter. Precipitation instead, becomes

more important during the ablation period because it is no longer stored in the snow. The variation gets bigger, comparable with temperature, when the snow melt season is finished, and geomorphologic characteristics gain in importance in terms of runoff generation.

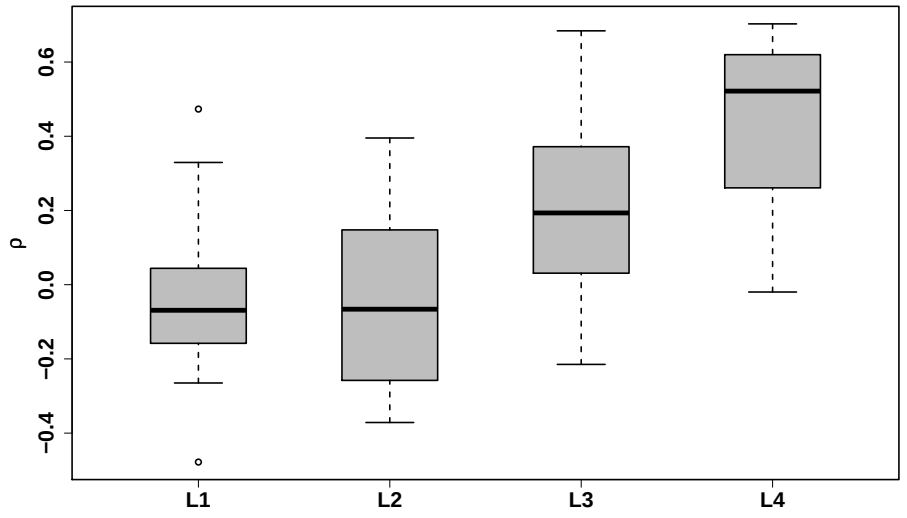

Figure 5.3: Correlation of runoff with precipitation during the ablation period for the British Columbian data set

For the PCA the data set has been separated into geomorphologic parameters and correlation values. The geomorphologic data set (GMD) contains the parameters catchment size, mean altitude, glacier size and fraction, annual precipitation, precipitation during the ablation period as well as the runoff rates for every ablation sub-period. The correlation data set (COD) contains correlation of runoff with air temperature, precipitation, annual precipitation, accumulation period precipitation and autocorrelation of runoff for each ablation sub-period respectively. The GMD shows three major groups in the BCD basins (figure 5.4 *a*). Loading positive on PC1 the basins are marked by high runoff rates. This group is located in the CMR, in contrast to the group loading negative on PC1, where the glaciers of the RM are concentrated. The third group has negative loadings on PC2. All three catchments are located in the NCM. The mean catchment altitude loads negative on PC1. Glacierized fraction and the mean runoff sums (*mrunoff*) in each of the ablation periods have high loadings on PC1. Catchment size, glacier size, average yearly precipitation (*myprec*) and average precipitation during accumulation period (*macyprec*) load high on PC2. The first two components account for 67 % (PC1: 43 %, PC2: 24 %) of total variance in the data set. The first principal component can be interpreted as runoff. Basins with high runoff are mainly located close to the sea (SCM) and can be found at the first quadrant. With growing distance to the coast the mean altitude of the catchments increases and runoff rates decrease. Most of the catchments are located in the southern part of BC. Only three catchments of

the NCM region are included in the data set. The difference in annual precipitation rates and catchment size is responsible for the second component. This leads to the small cluster of C05, C11, and C57. The COD PCA (figure 5.4 *b*) shows also three groups of basins. Loading positive on PC1 and PC2 the highly glacierized catchments cluster of quadrant one (top right sector in figure 5.4) show a strong correlation to air temperature (*cort*). The group is build by four basins located in the NCM and SCM. The second group plots in the second quadrant and is strongly correlated to precipitation during accumulation period (*coracpL1*), to precipitation occuring in spring (*corpL1*), and to the runoff of the previous sub-ablation period (*corLr1*). It is formed predominantly by members of the SCM region. In contrary, basins that can be described as more continentally influenced build the third group. They can be found in the fourth quadrant (top left sector in figure 5.4), showing a higher correlation with precipitation. The first two components account for 58 % (PC1: 36 %, PC2: 22 %) of the total variance in the data set. The general pattern of the two main clusters leads to PC1, and suggest to interpret PC1 as the weather component. In contrary the third group shows a dependence on precipitation during accumulation period and can be characterised as a storage component.

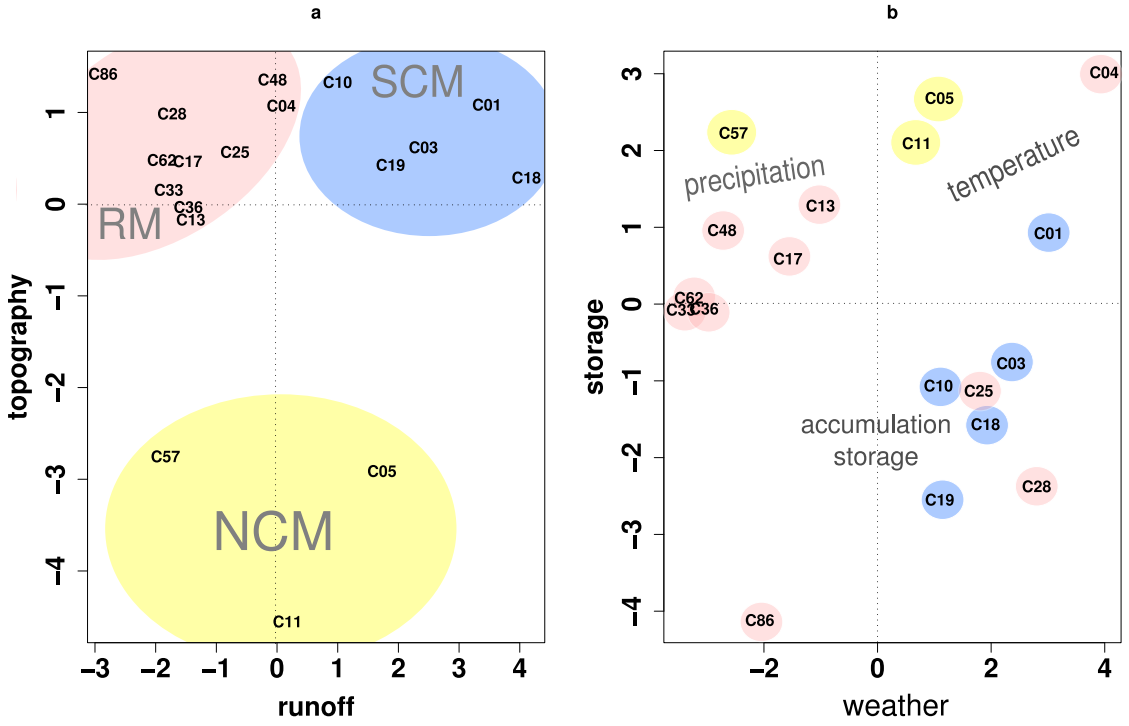

Figure 5.4: interpretation of the PCA of the Canadian data set

5.1.2 Norway

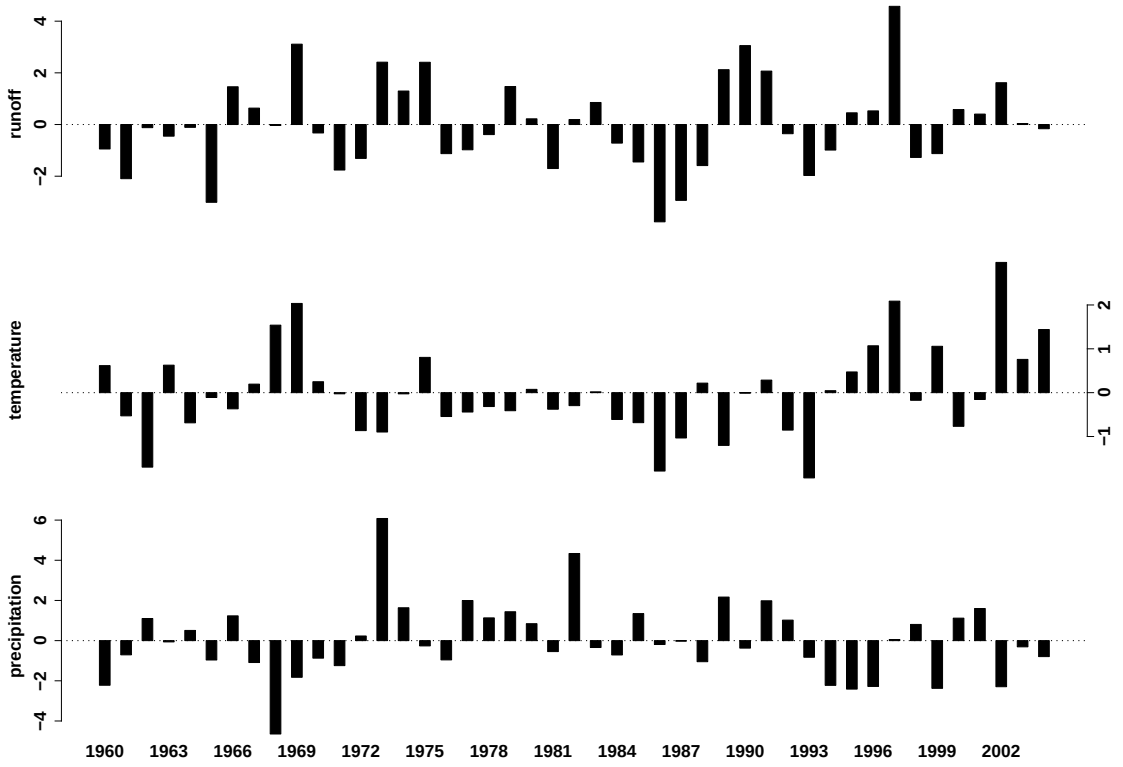

Figure 5.5: Mean anomalies of runoff, air temperature and precipitation in the L3 data set of Norway

For the NOD the mean time series of anomalies in runoff, air temperature and precipitation during the L3 period are presented in figure 5.5. All three variables have high variation. Remarkable is the negative period in temperature anomalies beginning in 1970 and lasting until 1993. In this period the North Atlantic Oscillation (NAO) indexes where predominately negative. The early 1990's are also the point of time when the general behaviour of mass balance in NO changed (see section 2.2.2). Precipitation anomalies behave more or less inverse to this pattern. However, runoff is not following the behaviour of temperature and precipitation. The variability is high over the entire period and changes its sign about every three to five years. This can arise from teleconnections like NAO or the Scandinavian Pattern (SCA). A direct comparison of annual mean values showed no exact accordance. This might be due to the equalising effect of mean values. Precipitation anomalies during the L3 period are above average when NAO is negative. Strong positive anomalies are often followed by positive runoff anomalies. Thus positive runoff anomalies in the negative NAO phase can be caused by rainfall rather than by glacier melt. The correlation of runoff with temperature during the ablation period, shown in figure 5.6, is strong in L1, weakens in L2 and increases again in L3. Negative values can be found especially in L2. The variance is biggest in L2 and L3 period. Median values range between 0.05 and 0.6. Maxima are 0.8 in L1, L2, L3 and 0.6 in L4

minima 0.4 in L1 and about −0.3 in L2, L3, and L4. The remarkable difference can be found in the L3 period, where the range is very high. Correlation between runoff and precipitation shows also its highest variability during the L3 period. The reason for the difference to the Canadian data can be found in the timing of the snow melt period. It is obvious that the L3 period behaves different in L2 and L4. Therefore L3 can be seen as a representative period for glacier runoff in NO. Correlation of runoff with precipitation increases during the summer. Starting with predominantly negative values in L1 the median is slightly positive in L2 and L3. During the L4 period no negative correlation can be observed. The variance is comparable with the temperature correlation.

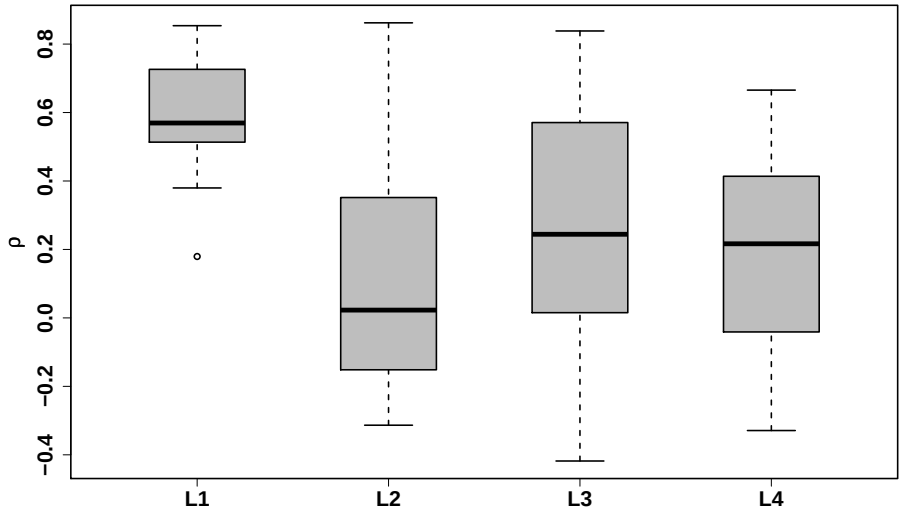

Figure 5.6: Correlation of runoff with air temperature during the ablation period for the Norwegian data set

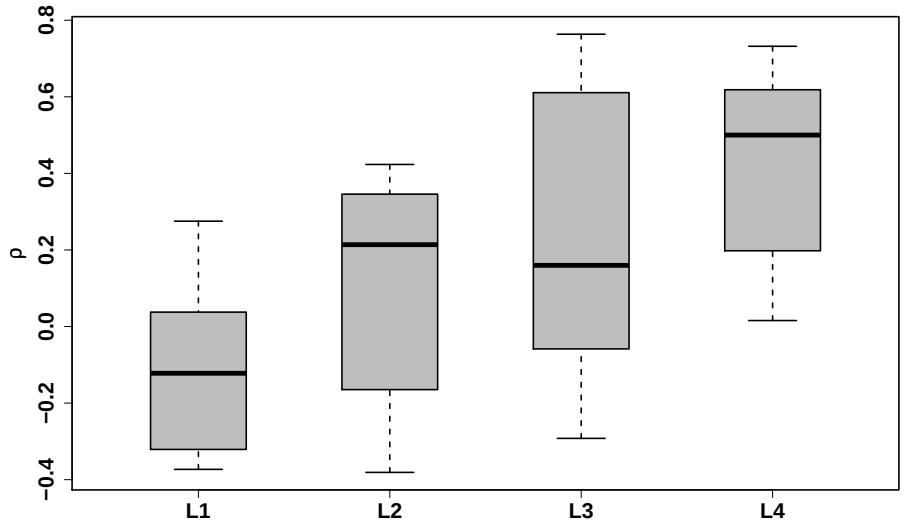

Figure 5.7: Correlation of runoff with precipitation during the ablation period for the Norwegian data set

The PCA of the GMD is presented in figure 5.8 *a*. Beside a big group of basins some outliers can be identified. The first two components account for 70 % (PC1: 45 %, PC2: 25 %) of the total variance in the data set. Positive values in PC1 are close to the loading of the variable *runoff*, *mean precipitation*, and *catchment size*. Positive values in PC2 show correlation with the loadings of *glacier size* and *mean altitude*. High runoff has a negative loading on PC1. All high glacierized catchments have high mean altitudes and a rather small size. They are located at the fourth quadrant. Small runoff rates show a high loading on PC1 in contrary to the PCA of the BCD and EUD, where big runoff rates load high on PC1. PC1 also reflects the continentality of the catchment. N22 and N27 have rather small runoff rates because they are located in the lee of the mountains. The second component can be interpreted as the mean catchment height. The group in the third quadrant is highly affected by snowmelt runoff. The scatter-plot of the COD PCA (figure 5.8 *b*) looks similar to the scatter-plot of the GMD PCA. Once again there appears a big group and some outliers. Three of them can also be identified as outliers in figure 5.8 *a*. This small group has the highest loadings on PC1. The majority of the big group is under-represented in terms of PC1 and PC2. The second component is correlated to precipitation during accumulation period, and to the runoff of the previous sub-ablation period. The first two components account for 64 % (PC1: 42 %, PC2: 22 %) of total variance in the data set. Low altitude catchments show the strongest dependence on precipitation, while the high glacierized catchments are highly correlated to air temperature. High storage dependence are marked by negative numbers in PC2.

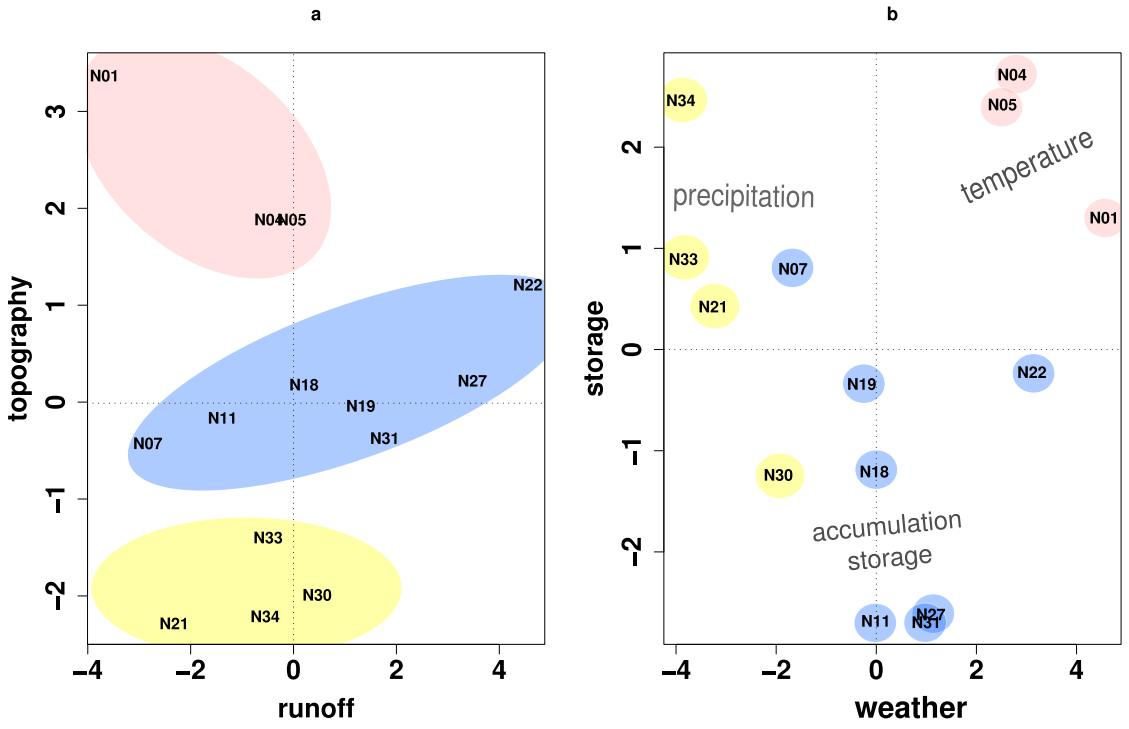

Figure 5.8: Interpretation of the PCA of the Norwegian data set

5.1.3 European Alps

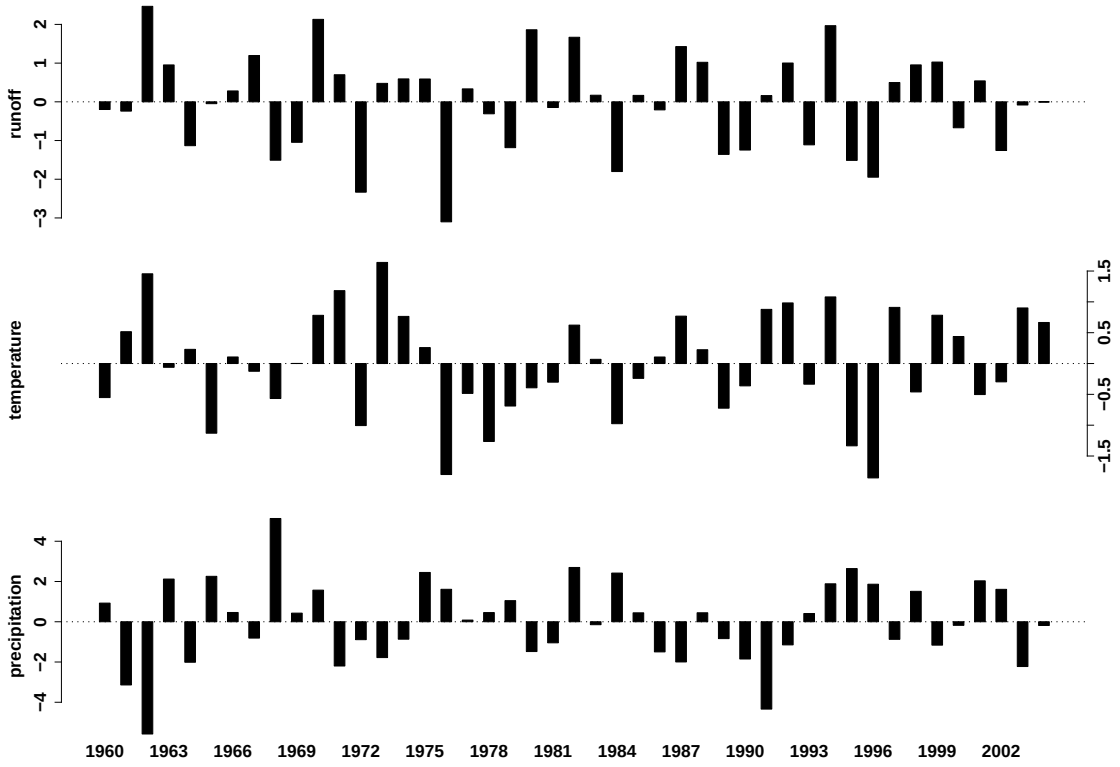

Figure 5.9: Mean anomalies of runoff, air temperature and precipitation in the L3 data set of the European Alps

The mean time series of anomalies in runoff, air temperature and precipitation during the L3 period are presented in figure 5.9. All three variables have high variation and no clear periodicity. Strong negative anomalies in the temperature time series can be found as years with negative anomalies in the runoff anomaly time series. Positive anomalies instead, do not show a consistent effect in the same way, neither does precipitation at all. The influence of NAO has been visually tested. For the most years the summer NAO index (arithmetic mean of June, July, and August) has indeed the same leading sign as the runoff anomaly. For other NAO intervals no such agreement could be verified. Remarkable are some negative years in air temperature anomalies during the 1970's that led to a short term increase in glacier masses apart from the dominating glacier retreat and is present in all time series. However the extreme dry and hot summer of 2003 is not exceptionally visible. The EUD show a strong to medium correlation with air temperature, presented in figure 5.10. While top values slightly decrease from L1 to L4 the minima do not show a constant gradient. Median Values range between 0.2 and 0.7. In the L1 period the basins behave more or less uniform, what results in a low variance. In contrary the following L2 period shows a high variability and even negative correlation for certain catchments. During the L3 period more positive and higher correlation than in L2 can be found. L4 equals L2 in median and variation. The outlier with the lowest

correlation has been identified as the Landquart River in Switzerland, where in spite of a 9 % glacierized catchment area the time series does not show a typical behaviour of a glacier fed river. Instead the correlation with precipitation is unusually high for this catchment, increasing the range mainly in period L2. In the L3 and L4 period the correlation of runoff with precipitation is comparable with the BCD. Correlation with precipitation shows a gradually increasing progress. Again variation is biggest in L2. Later in the ablation period it decreases slightly. Both, figure 5.10 and figure 5.11 show that L3 behaves different to L2 and L4. Therefore L3 can be seen as a representative period for glacier runoff in the EUD.

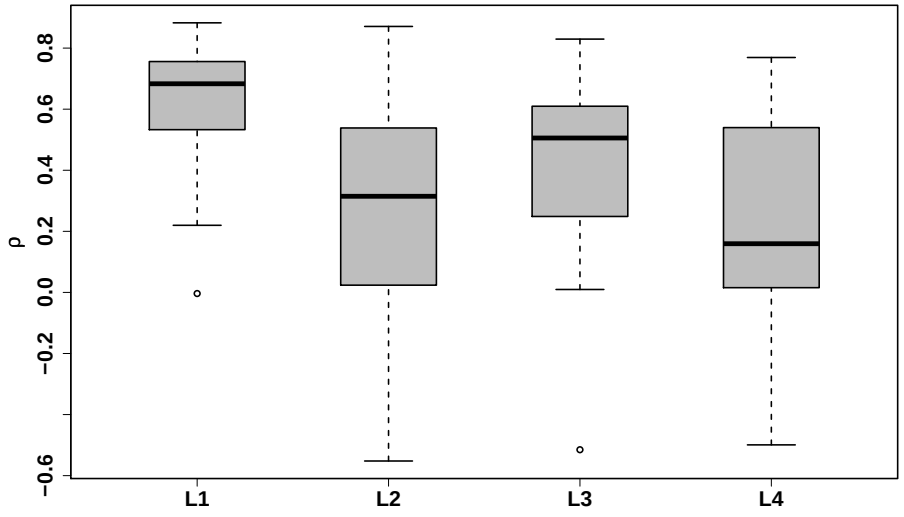

Figure 5.10: Correlation of runoff with air temperature during the ablation period for the European Alps

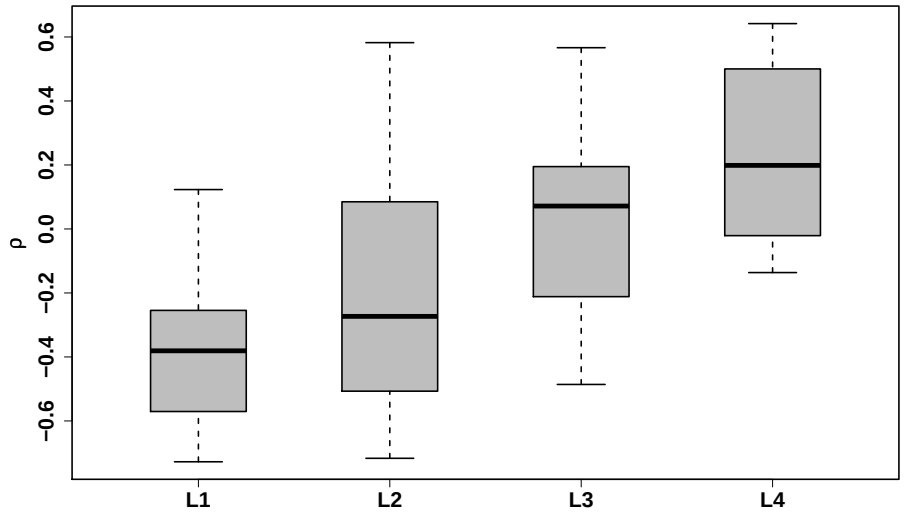

Figure 5.11: Correlation of runoff with precipitation during the ablation period for the European Alps

The GMD PCA of the EU basin data can be partitioned into two bigger groups and some outliers. catchments in the first quadrant have a high summer runoff and a low vertical watershed extension and size. The second quadrant represents basins with a large vertical extension and high summer runoff rates. Most of the basins arrange in the third quadrant because of their rather small summer runoff and large catchment sizes. The fourth quadrant is dominated by medium to small catchments. The first two components account for 63 % (PC1: 41 %, PC2: 22 %) of total variance in the data set. The outliers are identified as Massa catchment and Großtalbach catchment. They are special in terms of the glacierized area that is very high in the Massa catchment (128.7 km^2) and very low in the Großtalbach catchment (3.9 km^2). In the COD PCA the first principal component is strongly linked to high correlation of runoff with temperature and precipitation, whereas the second component has high loadings of correlation of runoff with full year and winter precipitation. The first two components account for 62 % (PC1: 53 %, PC2: 9 %) of the total variance in the data set. The first principal component is again linked to high correlation with actual weather conditions, whereas the second component represents the storage component that derive from winter precipitation. Negative values represent high correlation of runoff with storage. The outliers from figure 5.12 *a* do not show a remarkable characteristic in figure 5.12 *b*. Catchments that are located in quadrant one and two are higher correlated with precipitation, while those located in quadrant three and four depend more on temperature. Storage of precipitation during accumulation plays the biggest role in quadrant two, where the glacierized proportion is low in contrary to quadrant three. E16 is the Averole catchment in France, located at a very high altitude.

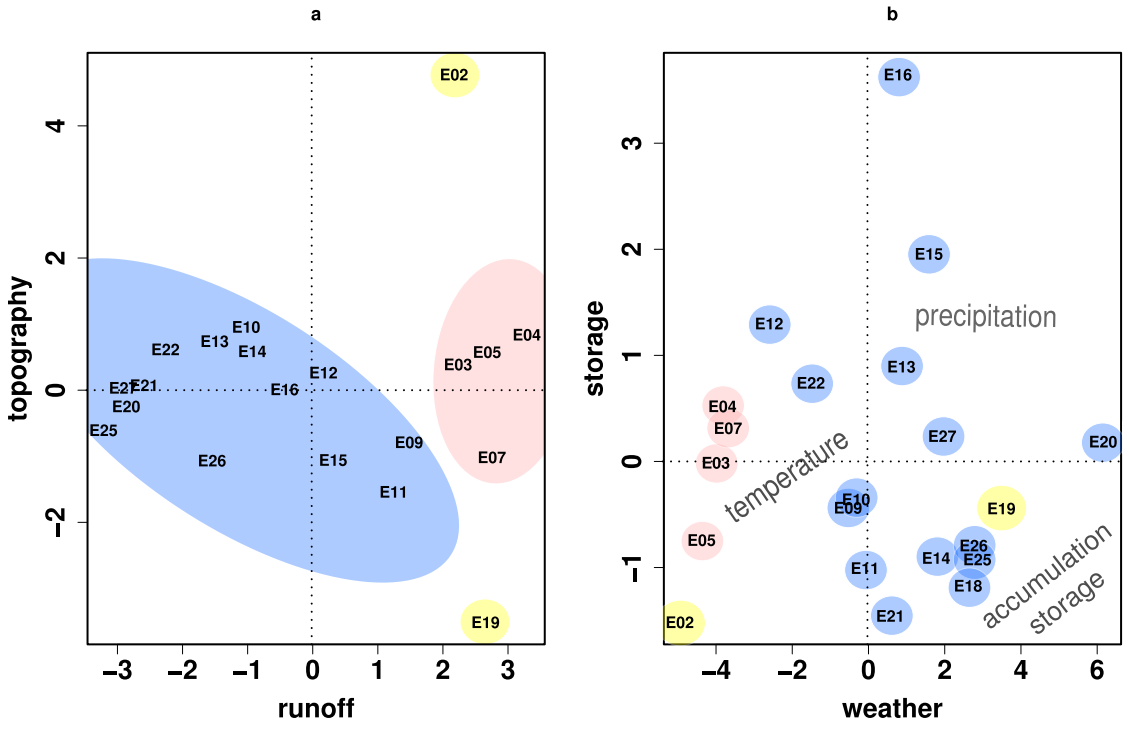

Figure 5.12: Interpretation of the PCA of the European Alps data set

5.2 Comparison of regions

The time series of runoff anomalies are highly variable in each region. During the 1970's all three time series show a shift in either air temperature or precipitation anomalies. Some strong negative temperature anomalies are consistent with strong negative runoff anomalies especially in the EU. The correlation during the ablation period is marked by differences in the correlation of runoff with precipitation. During the L1 period the EU shows a strong negative correlation with precipitation, while the Norwegian and Canadian basins runoff is rather weakly influenced by precipitation. During the L2 period runoff in most of the EU catchments is still negative correlated with precipitation. The Canadian catchments instead show a balanced correlation with slightly positive and slightly negative values. For the Norwegian basins precipitation becomes more important and values are predominantly positive. In the L3 period the mean values of all three regions are slightly positive, the EU subset shows again more negative values than the others. During the L4 period most of the runoff-precipitation correlation values are positive. The shift between the EU and the others persists. The NOD shows by far the highest variability. This is consistent with the correlation of runoff with air temperature in the L3 period, whereas the range of the NOD extends both of the other regions and the majority of the values show a stronger correlation to temperature than in the BCD.

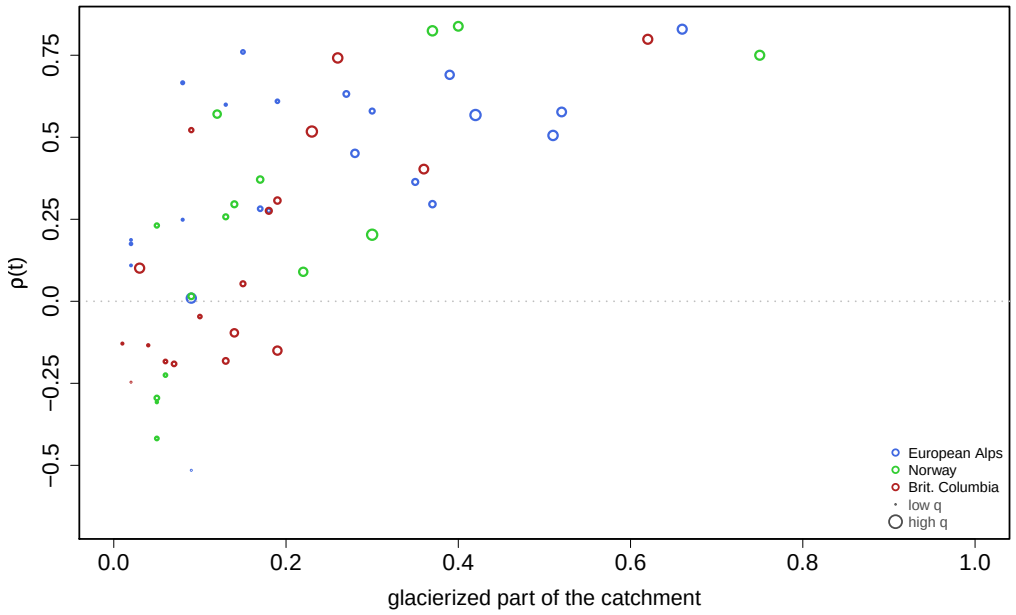

Figure 5.13: Correlation of runoff with temperature in the L3 period depending on the glacierized catchment fraction

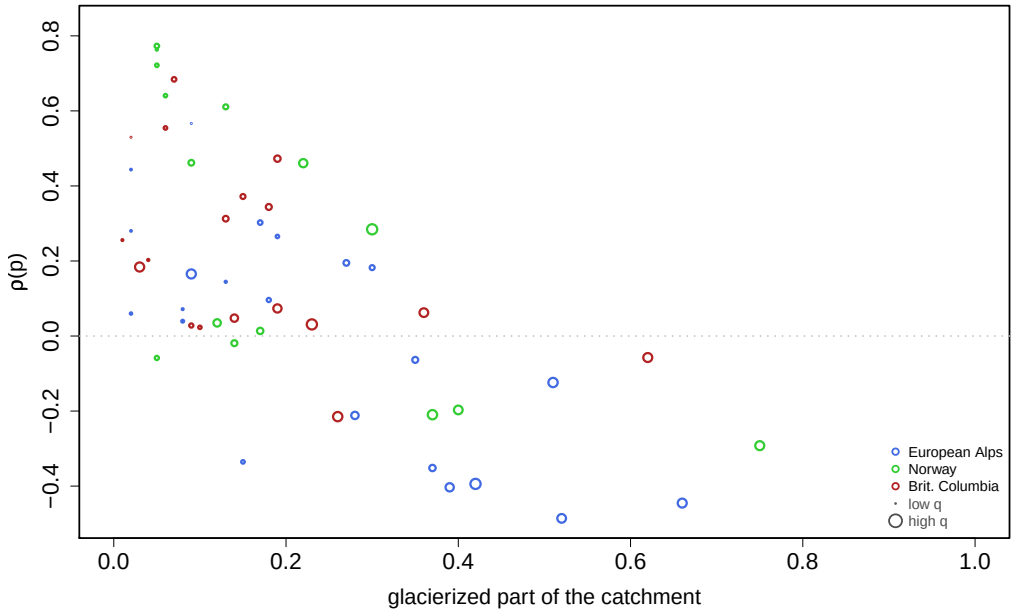

Figure 5.14: Correlation of runoff with precipitation in the L3 period depending on the glacierized catchment fraction

Figure 5.13 shows the correlation of runoff with air temperature during the L3 period in dependency of the glacierized fraction of the catchment. It is highly visible that the correlation gets stronger with increasing glacierized fraction of the catchment. Within the low glacierized catchments negative correlation exists. Basins with a fraction higher than 20 % glacierization are consistently positive in their correlation of runoff with temperature. The variation in the data is high. However, all three regions show a uniform behaviour and no clustering is visible. The correlation of runoff with precipitation in dependency of the glacierized catchment fraction gives a clear result too (figure 5.14). While runoff in low glacierized basins shows a high dependence on precipitation, glacierized basins with a fraction extending 40 % have negative values. Another good comparison for catchments is the river regime after *Pardé* (1947). The mean coefficients of each month where computed for the regions and the results show a good agreement between the Norwegian, and the EU basins. The watersheds of BC have their peak about one month in advance. The increase during the melt season is higher as well as the mean Pardé coefficient at the time of peak.

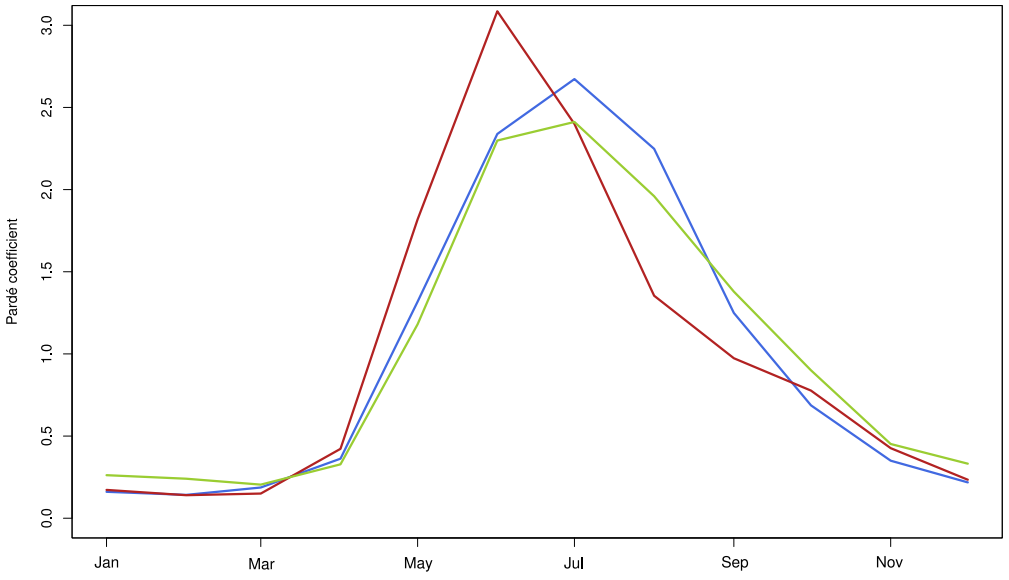

Figure 5.15: Mean Pardé coefficients for Canada, Norway, and the EU

The principal components of the geomorphologic data sets of the EU and NO are very similar. Catchment size and glacier size dominate the variance in the data sets. For BC instead, the geographic location is more widespread and the consequences are highly visible in the scatter-plot (figure 5.4). To get a good comparison for the inter-regional data set cluster analysis have been applied. For the geomorphologic data set the result is presented in figure 5.16. Three main clusters (Cl) can be identified. Cl I and Cl II are formed by European basins. Cl I consists of small catchments. The left side of this Cl is represented by high altitude catchments and

the right side with those located low in terms of mean catchment altitude. The small and high glacierized basins of the EUD dominate this group. Cl II consist of medium size catchments. Once again high mean altitude values are located on the left side whereas low mean altitude catchments are located on the right side of the Cl. The most basins are located in Cl III. It is formed by large catchments and subdivided into three groups. Two of them represent high altitude catchments and the partition in the middle is formed by large catchments with a low mean altitude. The highest glacierized catchments of EUD and BCD are located in this group. However, the Cl II and Cl III have a closer relationship than Cl I and Cl II. It is obvious, that there are differences between the data sets of the several regions. All BCD catchments can be found in Cl III, whereas the NOD and EUD appear in all three clusters. In contrary to the GMD cluster analysis, figure 5.17 proves, that the geomorphologic differences do not imply different behaviour in terms of hydrology. The COD cluster analysis can be divided into three Cl. Each of these Cl is mixed by catchments of all three regions. Cl i is formed by medium sized and big catchments. They are characterised by small runoff rates in any ablation sub-period. The members of this group can be interpreted as continental catchments. They often are located in the lee of a mountain range and build groups in the GMD-PCA as well. These catchments are also members of Cl II and Cl III. Cl ii is formed by very small and by high glacierized catchments. They have high runoff rates in the L2 as well as in the L3 period. Cl iii is formed by all catchments that are marked by high runoff rates during the L2 period and lower runoff rates during the L3 period. This group contains all catchment sizes. The majority of CL II can be found in Cl iii, but there are members in Cl i and Cl ii too. The general distribution of regions and cluster affiliation is pointed out by the colouring of figure 5.16 and figure 5.17.

The trends in dependence of the glacierized fraction of the catchment of the different regions are presented in figure 5.18 . It is easy to see that the regions show a different behaviour. Most of the low glacierized catchments do not show any trend. The reason for positive trends can be found in the high correlation and the change in precipitation rather than in glacio-hydrological reasons. The more glacierized the catchments are, the more likely are positive Sen-slopes. When compared with figure 5.4, figure 5.8, and figure 5.12 it is easy to see that the catchment cluster with a glacierized catchment fraction of smaller 20 % and Sen-Slopes close to zero are build by the precipitation and accumulation storage group members. Positive trends within the same glacierized fraction group are all consistent with accumulation storage group members. Within a subset of catchments that show a higher correlation of runoff with air temperature than 0.3 (HTC) it becomes clearly visible that a galcio-hydrological behaviour of a catchment can be only expected from catchments with a glacierized fraction higher than 10% (see 7 for detailed charts).

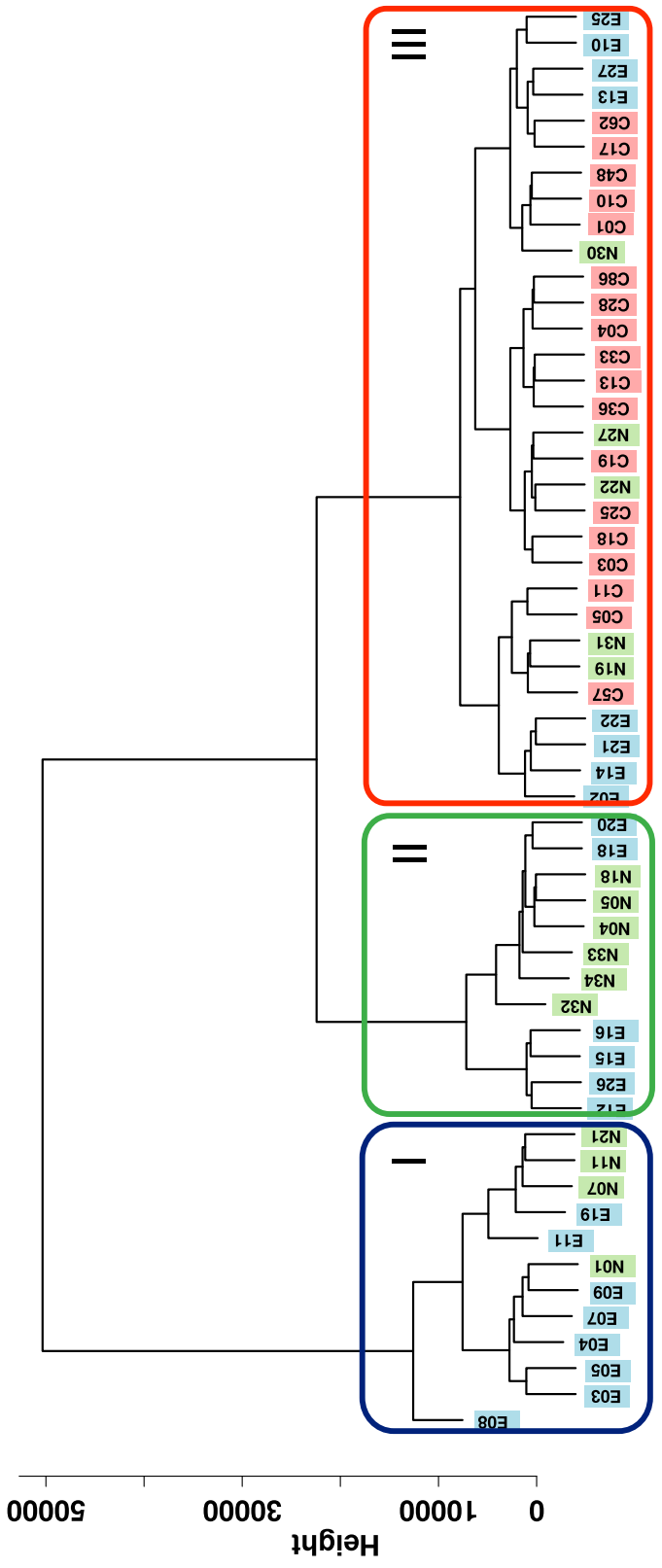

Figure 5.16: Cluster analysis of geomorphologic data set

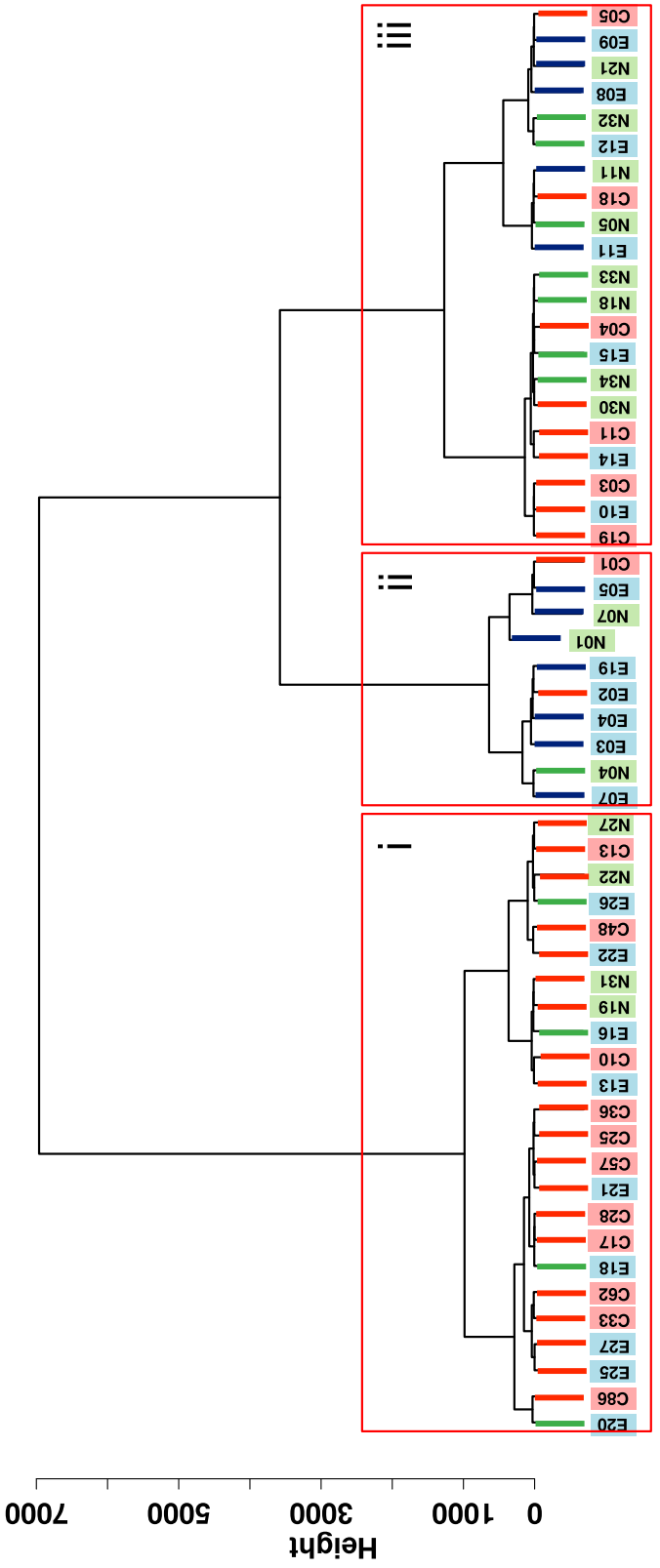

Figure 5.17: Cluster analysis of correlation data set

It is further visible that the EUD and the NOD follow the same linear relationship concerning the gradient, but the EUD linear relationship is shifted towards more glacierized fractions. Trends in NO seem therefore to be stronger than trends in the EU. The data from the BCD just offer a weak possibility in interpretation. Within the HTC there are only six catchments left. Just two of them show a consistent trend. The Canadian river Surprise Creek (C03) has decreasing correlation of runoff with air temperature for daily August data and increasing runoff rates in the L3 period. Precipitation is not replacing temperature as main influence factor, like it can be seen in the Bridge River catchment e.g. Thus it can be assumed that the decreasing trend in correlation of runoff with air temperature derive out of the decreasing glacierized area in the catchment.

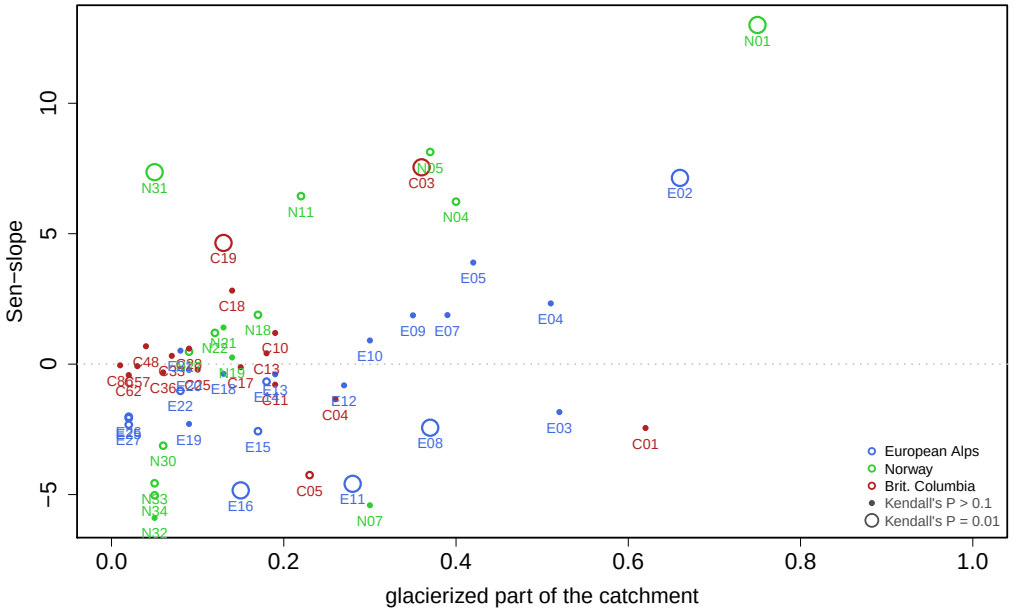

Figure 5.18: Sen-Slope in L3 runoff data, depending on the catchment fraction that is glacierized

Regression analysis gave admissible results, but did not lead to an additional gain in information about the similarity or differences in the streamflow behaviour. The method has also been applied to a moving time frame of five years on a daily data basis. While the influence of temperature is decreasing, the influence of precipitation is increasing for the most BCD basins. The NOD basins instead behave different. In most catchments the correlation of runoff with air temperature shows a positive jump at the end of the 1990's and increase slightly thereafter. Correlation of runoff with precipitation decreases in most of the NOD time series. For the EUD runoff-correlation with precipitation this pattern is also true. However, the influence of air temperature shows increasing, decreasing and constant results for this region.

6 Discussion

The anomalies time series of all three regions showed a high variability in the data, even in standardised mean values. In general streamflow change is not obvious in any of the three data sets. The anomalies of air temperature and precipitation are insufficient to describe the anomaly in runoff data for a whole region, except for negative anomalies of runoff. These are consistent with negative anomalies in air temperature. On the one hand, this indicates that years with low runoff sums are caused by low air temperatures. On the other hand, not all years with low summer air temperature lead to low runoff sums. One possible explanation is the influence of snowfall resulting in a high albedo. *Escher-Vetter & Siebers* (2007) showed that glacier runoff is highly affected by the type of precipitation and the resulting albedo, which affects the ablation area size. Storage effects and the big big order of magnitude in catchment heights and thus in air temperature are further control mechanisms.

The apparent advantage of mean anomaly plots is the possibility to compare climate and runoff time series with large scale atmospheric fluctuations like El Niño Southern Oscillation, PDO and NAO. They are known to have a remarkable influence on climate of the study areas and thus should account for changes in glacier hydrology. In all three regions the anomalies time series show shifts in either precipitation or air temperature. Most of them can be linked to changes in the phases of the oscillation pattern. In all three regions the influence of different large scale atmospheric patterns is visible. The influence of PDO in the BCD and led to a increase in precipitation during the L3 period. From the same point of time the variability of the runoff anomalies time series increased. The EUD do not show to be a strong connection with the value of the NAO. However, the leading sign in L3 periods NAO index corresponds with the leading sign in the L3 runoff anomalies. The NOD runoff anomalies show that negative NAO indexes can influence L3 temperature and thus runoff in the highly glacierized catchments. The air temperature anomalies show a long period of predominately negative values between 1970 and 1990. *Chinn et al.* (2005) showed the negative period in air temperature anomaly to be linked with the negative periods in the NAO. While *Chinn et al.* (2005) explained the positive effect of negative NAO values on precipitation during accumulation period. Figure 5.5 shows that there is also a correlation of NAO with air temperature during the L3 period. Jumps in moving correlation time series may be caused by either large scale climatic fluctuations or can be an evidence for a systematic change in glacier behaviour. Climatic jumps can be found in many time series, e.g. around 1977 and 1988 (*Meier et al.*, 2003).

A general reason for the difference in the EUD and NOD in comparison to the BCD

can be found in the timing of the snow melt period. The glacierized basins in the EUD are located at high altitude leading to a late begin of the snowmelt season. NO instead, has a late snowmelt season due to the geographical location. For BC the location of the glacier catchment has to be considered if the timing of the snowmelt season is of interest. This findings agree with the results of *Déry et al.* (2009). The reason for the shift in the Pardé coefficient might be found in the scales and location of the catchment. The BCD consist of catchment sizes bigger than 100 km^2, the EUD and NOD include much smaller catchments. However, the mean hight of the analysed EUD catchments is much higher than the mean hight of the BCD. Further differences in the correlation of runoff with air temperature and precipitation between BCD, NOD, and EUD can be found, considering the whole ablation period. While NOD is outstanding concerning precipitation during the ablation period, the EUD behaves different comparing to the others in terms of air temperature. Correlation of runoff with temperature shows to be strongly dependent on the fraction of the catchment that is glacierized. As shown in *Maisch et al.* (2000) a loss in glacier size, vertical range and regional degree of glacierization is linked inverse to the glacierized fraction of a basin. Within the dependency on air temperature, presented in figure 5.14, negative correlation only appears in catchments with a glacierized fraction smaller than 20 %. This may be due to evaporation or can be a spurious correlation, reflecting the absence of high air temperatures at days with precipitation. The high variation in the data indicates some other important influences like exposition, glacier height and moisture deficit. The dependency on precipitation has negative values for all catchments with a glacierized fraction bigger than 40 %. The superposition of this two effects leads to a minimum of intra and inter annual variability at glacierized fractions of about 20 % to 40 % (see section 1.2.3). Catchments showing a correlation of runoff with air temperature of more than 0.3 have a glacierized catchment fraction of over 10 %. *Gurtz et al.* (2002) discovered that the glacial influence has to be accounted for a glacierized proportion of bigger than 5 %. The BCD, in contrary to the EUD and NOD, has just a few catchment with a glacierized fraction above 30 %. As a result the mean river regime is snowmelt dominated. Decreasing rates of precipitation may also lead to an earlier exposition of glacier ice and thus to a longer period of glacier runoff. This might result in a higher amount of glacier runoff, as shown by (*Singh & Kumar*, 1997).

The PCAs of the regions show distinct clusters for the BCD. The scatter-plot of the EUD (figure 5.12 *a*) and the NOD (figure 5.8 *a*) is rather uniform. This clarifies that the BCD is not a homogeneous dataset itself. It consist of two or three different behaving unities. The main principal components can be interpreted in the same way for all three regions. Cluster analysis confirms the result of the PCA. While the GMD builds clusters containing only the EU and No catchments, the COD shows that these differences do not account for the general glacio-hydrological behaviour of these catchments. Thus the main separation variable from GMD cluster analysis *catchment size* is expected to be less important in contrary to the *glacierized fraction* of a catchment. *Birsan et al.* (2005) also found altitude and glacier cover to be the main factors controlling streamflow trends in Switzerland.

Differences in trends can be explained by taking the location and the scale of the catchment into account. Highly glacierized catchments are dominated by melt and surface runoff processes. Low glacierized catchments show, due to more developed vegetation and soil, the tendency for subsurface flow soil storage and evapotranspiration. This was also proven by (*Verbunt et al.*, 2003). For the interpretation of trends climate pattern have to be considered as well. Changes in precipitation and accumulated snow are shown to have a big influence in these basins. Their variation is expected to be responsible for the main part of variation of Sen-Slopes in the analysis of this thesis. The combined influence of aspect and altitude may also cause a large degree of scatter observed in the nonglacierized basins, and those with only a small glacierized fraction. This is consistent with the results obtained by *Fountain & Tangborn* (1985). NOD has the strongest trends. This may arise from the high precipitation and thus high rates in mass turnover. Another reason could be the more rapid wastage due to the late change from positive to negative mass balance. The EUD glaciers are reacting in the same way but the lower mass turnover rates make the changes less strong. For the BCD glaciers no general linear relationship was detected. The increase in air temperature might be partially offset by increase in precipitation, what was shown for some catchments by (*Shea et al.*, 2004). It can be assumed that the glaciers of the NCM react like the NOD, whereas the glaciers of the RM react more like the EUD. If the above is a general pattern, one can expand the theory of offset due to mass turnover rate with the general glacier response time that should be visible in the gradient of the regions linear relationship (figure 6.1).

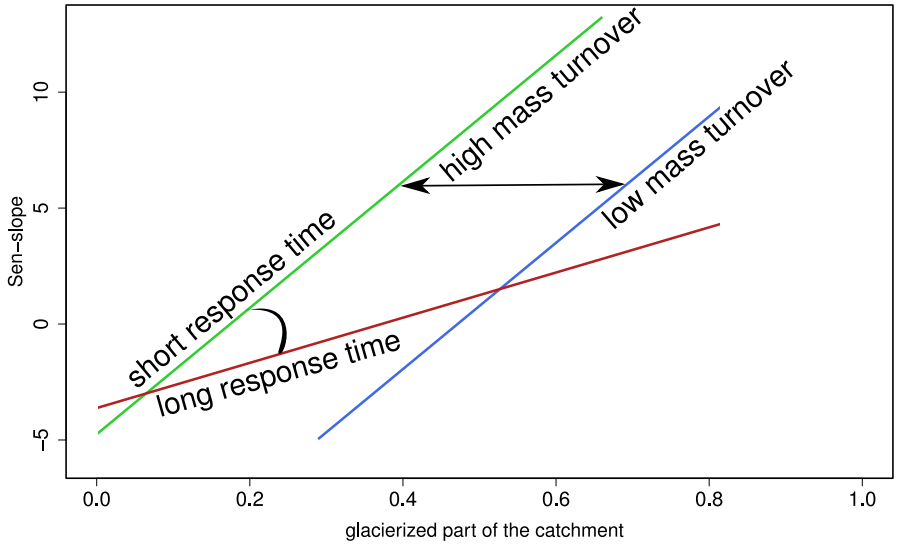

Figure 6.1: Concept of trends in streamflow in dependence of glacierized catchment fraction, mass turnover and response time

7 Conclusion

In BC, NO, and EU the influence of different large scale atmospheric patterns is visible. This dependency implies a difference in the behaviour of stream flow from glacierized basins and puts the method of trend analysis into question if not been taken into account. It is obvious that this influence result in a difference between the study regions. The hydrological behaviour of glacierized catchments is composed by general hydrological processes and the ice covered part with its own special behaviour. The weight of the influence are controlled by the proportions and the climatic input that plays a key roll in activating the particular mechanisms. Thus the glacierized fraction of a catchment is a key parameter in terms of streamflow change. The scales of the catchments in the data set play another important role. Large scale catchments with a big glacierized area are dominated by the non-glacierized parts anyway. The cluster analysis pointed out that catchments of very small sizes in high mountainious areas are more affected by their glacial part than big catchments with the same glacierized fraction. Catchments with a fraction higher than 30% show a distinct glacial behaviour and are the appropriate choice in terms of glacier-fed streamflow analysis. The location of the catchment controls the amount of precipitation. Glaciers can be characterized as continental type or maritime type. The the basins are of different types in each study region. However the timing is controlled by the general weather pattern, what has been shown to be different.

As a result can be said that the general behaviour of glaciers is the same for Canada, Norway, and the European Alps. The driving forces of accumulation storage and precipitation during ablation period as well as the influenceing large scale atmospheric patterns have to be taken into account when the different regions are compared. For a detailed comparison of runoff from the BC glaciers with runoff from glaciers of other regions more time series of medium scale and high glacierized catchments are needed. It would be advisable to compare runoff from SCM with runoff from NCM and RM as a first step. Overall the biggest problems arise of the sparce data availability. By now only about 40 glaciers worldwide have continuous balance measurements with data over the past 20 years (**?**). The impacts of hydropower plants on nature (mainly on habitats and groundwater) are strongly discussed. In terms of science and especially hydrology there should be paid attention on maintaining a sufficiant number of long lasting time series of natural flow within several scales of catchment size, glacierized proportion, and glacier size. Otherwise the prediction of runoff from such catchments will not be possible. Climate data out of reanalysis methods will hopefully get more precise in the future, but measurements need to be continued for validation and to provide consistent time series.

Bibliography

Adalgeirsdóttir, G., Jóhannesson, T., Björnsson, H., Pálsson, F., & Sigurdsson, O. (2006). Response of hofsjoekull and southern vatnajoekull, iceland, to climate change. Journal of Geophysical Research. F. Earth Surface, 111 (F3): F03001.

Aizen, V. B. & Aizen, E. M. (1993). Glacier runoff estimation and simulation of streamflow in the peripheral territory of central asia. IAHS Publication, Seiten 167–179.

Aizen, V. B., Aizen, E. M., Melack, J. M., & Dozier, J. (1997). Climatic and hydrologic changes in the tien shan, central asia. Journal of Climate, 10 (6): 1393–1404.

Andersen, E. O. (2006). Norwegian hydro power and new focus on small hydro power. In Himalayan Small Hydropower Summit, Seite 8.

Arendt, A. A., Echelmeyer, K. A., Harrison, W. D., Lingle, C. S., & Valentine, V. B. (2002). Rapid wastage of alaska glaciers and their contribution to rising sea level. Science, 297 (5580): 382–386.

AtlasOfCanada (2009). Atlas of Canada. 6 Auflage.

Backhaus, K., Erichson, B., Plinke, W., & Weiber, R. (1996). Multivariate Analysenmethoden,. Springer-Verlag, Berlin, Heidelberg, New York, 3rd Auflage.

Barbet, D., Gay, M., Oberlin, G., & Valla, F. (1993). Preliminary hydrological results from sarennes glacier basin, french alps. Acta geológica hispánica, 28 (2-3).

Barnett, T. P., Adam, J. C., & Lettenmaier, D. P. (2005). Potential impacts of a warming climate on water availability in snow-dominated regions. Nature, 438 (7066): 303–309.

Behrens, H., Oerter, H., & Reinwarth, O. (1982). Results of tracer experiments with fluorescent dyes on vernagtferner (oetztal alps, austria) from 1974 to 1982. Zeitschrift für Gletscherkunde und Glazialgeologie, 18 (1): 65–83.

Beniston, M. (2005). Mountain climates and climatic change: An overview of processes focusing on the european alps. Pure and Applied Geophysics, 162 (8): 1587–1606.

Berg, P. & Christensen, J. H. (2008). Poor man's re-analysis over europe. Technischer Bericht, DMI.

Bhutiyani, M. R., Kale, V. S., & Pawar, N. J. (2008). Changing streamflow patterns in the rivers of northwestern himalaya: Implications of global warming in the 20th century. Current Science, 95 (5): 618.

Birsan, M. V., Molnar, P., Burlando, P., & Pfaundler, M. (2005). Streamflow trends in switzerland. Journal of Hydrology, 314 (1-4): 312–329.

Braun, L. N., Escher-Vetter, H., Siebers, M., & Weber, M. (2007). Water balance of the highly glaciated vernagt basin, ötztal alps. alpine space - man & environment, 3: 33–42.

Braun, L. N. & Weber, M. (2001). Wasserspende aus hochalpinen gebieten. In Die Alpen - Ein kostbares Wasserschloss. Bad Reichenhall.

Burn, D. H. & Hag Elnur, M. A. (2002). Detection of hydrologic trends and variability. Journal of Hydrology, 255 (1-4): 107–122.

Chen, J. & Ohmura, A. (1990). On the influence of alpine glaciers on runoff. IAHS, 193: 117–125.

Chinn, T., Winkler, S., Salinger, M. J., & Haakensen, N. (2005). Recent glacier advances in norway and new zealand: a comparison of their glaciological and meteorological causes. Geografiska Annaler, 87 (1): 141–157.

Clarke, G. & Holdsworth, G. (2002). Satellite image atlas of glaciers of the world, Kapitel Glaciers of North America, Seite 55. Corps of Engineers, US Army, Technical Information Analysis Center, Cold Regions Research and Engineering Laboratory, u.s. geological survey professional paper 1386–j–1 Auflage.

Cogley, J. G. (2005). Encyclopedia of hydrological sciences, Band 4, Kapitel Mass and energy balances of glaciers and ice sheets, Seiten 2555–2573. John Wiley & Sons, Ltd.

Collins, D. N. (1982). Water storage in an alpine glacier. Hydrological Aspects of Alpine and High-Mountain Areas IAHS Publication, (138): 113–123.

Collins, D. N. (1987). Climatic fluctuations and runoff from glacierised alpine basins. IAHS-AISH publication, (168): 77–89.

Collins, D. N. (2006). Climatic variation and runoff in mountain basins with differing proportions of glacier cover. Nordic hydrology, 37 (4-5): 315–326.

Déry, S. J., Stahl, K., Moore, R., Whitfield, P., Menounos, B., & Burford, J. (2009). Detection of runoff timing changes in pluvial, nival and glacial rivers of western canada. Water Resources Research.

Déry, S. J. & Wood, E. F. (2005). Decreasing river discharge in northern canada. Geophysical Research Letters, 32 (10).

Dyurgerov, M. & Meier, M. (2005). Glaciers and the changing Earth system: a 2004 snapshot. Institute of Arctic and Alpine Research, University of Colorado, Boulder.

Escher-Vetter, H. & Siebers, M. (2007). Sensitivity of glacier runoff to summer snowfall events. Annals of Glaciology, 46 (1): 309–315.

Evans, I. S. (2006). Glacier distribution in the alps: Statistical modelling of altitude and aspect. Geografiska Annaler: Series A, Physical Geography, 88 (2): 115–133.

Evans, I. S. (2008). A brief report on recent changes in small glaciers in british columbia, canada. Quaternary Newsletter, 118: 28–31.

Ferguson, R. I. (1985). Runoff from glacierized mountains: a model for annual variation and its forecasting. Water Resources Research, 21 (5): 702–708.

Flowers, G. E., Marshall, S. J., Björnsson, H., & Clarke, G. K. C. (2005). Sensitivity of vatnajökull ice cap hydrology and dynamics to climate warming over the next 2 centuries. J. Geophys. Res, 110.

Fountain, A. G. & Tangborn, W. V. (1985). The effect of glaciers on streamflow variations. Water Resources Research, 21 (4): 579–586.

Fountain, A. G. & Walder, J. S. (1998). Water flow through temperate glaciers. Reviews of Geophysics, 36 (3): 299–328.

Fraser, J. (2002). Indicators of climate change for British Columbia, 2002. Ministry of Water, Land and Air Protection, Victoria, BC.

Granato, G. E. (2006). Techniques and Methods of the U.S. Geological Survey, Band 4, Kapitel A7: Kendall-Theil Robust Line (KTRLine—version 1.0)—A visual basic program for calculating and graphing robust nonparametric estimates of linear-regression coefficients between two continuous variables, Seite 31. U.S. Geological Survey.

Gurtz, J., Verbunt, M., Jasper, K., Lang, H., & Zappa, M. (2002). Spatial and temporal variations of hydrological processes in mountainous regions and their modelling. In Proceedings of ICWRER 2002, Band 7, Seite 10. ICWRER.

Haeberli, W., Hoelzle, M., & Bösch, H. (1991). Glacier mass balance bulletin. Bulletin, Seiten 1988–1989.

Hagg, W. (2003). Auswirkungen von Gletscherschwund auf die Wasserspende hochalpiner Gebiete, Vergleich Alpen-Zentralasien. Dissertation, Institute for Geography, University of Munich.

Hamlet, A. F., Huppert, D., & Lettenmaier, D. P. (2002). Economic value of long-lead streamflow forecasts for columbia river hydropower. Journal of Water Resources Planning and Management, 128: 91.

Helsel, D. R. & Hirsch, R. M. (1993). Statistical methods in water resources. Elsevier Science & Technology.

Hirsch, R. M. & Slack, J. R. (1984). Nonparametric trend test for seasonal data with serial dependence. Water Resources Research, 20 (6).

Hisdal, H., Stahl, K., Tallaksen, L. M., & Demuth, S. (2001). Have streamflow droughts in europe become more severe or frequent? International Journal of Climatology, 21 (3).

Hock, R. (2005). Glacier melt: a review of processes and their modelling. Progress in Physical Geography, 29 (3): 362.

Hock, R., Jansson, P., & Braun, L. (2005). Modelling the response of mountain glacier discharge to climate warming. Global Change and Mountain Regions: A State of Knowledge Overview. Advances in Global Change Series. Springer, Dordrecht, Seiten 243–252.

Hooke, R. L. B. (2005). Principles of glacier mechanics. Cambridge University Press.

Huss, M., Farinotti, D., Bauder, A., & Funk, M. (2008). Modelling runoff from highly glacierized alpine drainage basins in a changing climate. Hydrological Processes, 22 (19): 3888–3902.

IPCC (1996). Climate Change 1995: The Science of Climate Change. Cambridge UP. New York. US.

Jansson, P., Hock, R., & Schneider, T. (2003). The concept of glacier storage: a review. Journal of Hydrology, 282 (1-4): 116–129.

Jóhannesson, T., Adalgeirsdóttir, G., Ahlstrøm, A., Andreassen, L. M., Björnsson, H., de Woul, M., Elvehøy, H., Flowers, G. E., Gudmundsson, S., Hock, R., et al. (2006). The impact of climate change on glaciers and glacial runoff in the nordic countries. Seiten 31–34.

Kaser, G. (2006). Mass balance of glaciers and ice caps: Consensus estimates for 1961–2004. Geophysical Research Letters, 33 (19): L19501.

Kaser, G., Juen, I., Georges, C., Gómez, J., & Tamayo, W. (2003). The impact of glaciers on the runoff and the reconstruction of mass balance history from hydrological data in the tropical cordillera blanca, perú. Journal of Hydrology, 282 (1-4): 130–144.

Kendall, M. G. (1938). A new measure of rank correlation. Biometrika, 30 (1-2): 81–93.

Kendall, M. G. (1970). Rank correlation methods. Charles Griffin, London, 4 Auflage.

Kjollmoen, B., Andreassen, L. M., Elvehoy, H., Jackson, M., Tvede, A. M., Laumann, T., & Giesen, R. H. (2007). Glaciological investigations in Norway in 2006. Norwegian Water Resources and Energy Directorate.

Klok, E., Jasper, K., Roelofsma, K., Gurtz, J., & Badoux, A. (2001). Distributed hydrological modelling of a heavily glaciated alpine river basin. Hydrological sciences journal, 46 (4): 553–570.

Koboltschnig, G. R., Schoner, W., Zappa, M., & Holzmann, H. (2007). Contribution of glacier melt to stream runoff: if the climatically extreme summer of 2003 had happened in 1979. ANNALS OF GLACIOLOGY, 46: 303.

Konovalov, V. G. (1994). Snow line and runoff formation in glacial basins. IAHS Publication, 423: 275–283.

Koutsoyiannis, D. & Montanari, A. (2007). Statistical analysis of hydroclimatic time series: Uncertainty and insights. Water resources research, 43 (5).

Kuhn, M. (2005). Gletscher im klimawandel. Bedrohte Alpengletscher. Fachbeiträge des Oesterreichischen Alpenvereins, Serie: Alpine Raumordnung, 27: 35–40.

Kuhn, M. (2007). Omega: Using glaciers as indicators of climatic change. Zeitschrift für Gletscherkunde und Glazialgeologie, 41: 7–28.

Kuhn, M., Markl, G., Kaser, G., Nickus, U., Obleitner, F., & Schneider, H. (1985). Fluctuations of climate and mass balance: different responses of two adjacent glaciers. Z Gletscherk Glazialgeol, 21: 409–416.

Kundzewicz, Z. W. & Robson, A. J. (2004). Change detection in hydrological records—a review of the methodology/revue méthodologique de la détection de changements dans les chroniques hydrologiques. Hydrological Sciences Journal/Journal des Sciences Hydrologiques, 49 (1): 7–19.

Lambrecht, A. & Kuhn, M. (2007). Glacier changes in the austrian alps during the last three decades, derived from the new austrian glacier inventory. Annals of Glaciology, 46 (1): 177–184.

Lang, H. (1973). Variations in the relation between glacier discharge and meteorological elements. IAHS Publication, Seiten 85–94.

Lang, H. (1986). Forecasting meltwater runoff from snow-covered areas and from glacier basins. River Flow Modelling and Forecasting, Seiten 99–127.

Lang, H., Leibundgut, C., & Festel, E. (1979). Results from tracer experiments on the water flow through the aletschgletscher. Zeitschrift für Gletscherkunde und Glazialgeologie, 16 (2): 209–218.

Lemke, P., Ren, J., Alley, R. B., Allison, I., Carrasco, J., Flato, G., Fujii, Y., Kaser, G., Mote, P., Thomas, R. H., et al. (2007). Observations: changes in snow, ice and frozen ground. Titel: Climate change, Seiten 337–383.

Li, W. H., Chen, Y., Hao, X. M., & Huang, X. (2007). Responses of streamflow to climate change in the northern slope of tianshan mountains in xinjiang: A case study of the toutun river basin. Science in China Series D: Earth Sciences, 50: 42–48.

Lin, X., Zhang, Y., Yao, Z., Gong, T., Wang, H., Chu, D., Liu, L., & Zhang, F. (2008). The trend on runoff variations in the lhasa river basin. Journal of Geographical Sciences, 18 (1): 95–106.

Maisch, M., Wipf, A., Denneler, B., Battaglia, J., & Benz, C. (2000). Die Gletscher der Schweizer Alpen: Gletscherhochstand 1850, aktuelle Vergletscherung, Gletscherschwund-Szenarien. Vdf, Hochschulverlag AG an der ETH.

Mann, H. B. (1945). Nonparametric tests against trend. Econometrica: Journal of the Econometric Society, Seiten 245–259.

McCabe, G. J., Fountain, A. G., & Dyurgerov, M. (2000). Variability in winter mass balance of northern hemisphere glaciers and relations with atmospheric circulation. Arctic, Antarctic, and Alpine Research, Seiten 64–72.

McGillivray, B. (2000). Geography of British Columbia: people and landscapes in transition. University of British Columbia Press.

Meier, M. F., Dyurgerov, M. B., & McCabe, G. J. (2003). The health of glaciers: Recent changes in glacier regime. Climatic Change, 59 (1): 123–135.

Moore, R. D. & Demuth, M. N. (2001). Mass balance and streamflow variability at place glacier, canada, in relation to recent climate fluctuations. Hydrological Processes, 15 (18).

Nienow, P. & Hubbard, B. (2006). Encyclopedia of Hydrological Sciences, Band 4, Kapitel Surface and Englacial Drainage of Glaciers and Ice Sheets, Seiten 2575–2586. John Wiley & Sons Hoboken, NJ.

North, N., Kljun, N., Kasser, F., Heldstab, J., Maibach, M., Reutimann, J., & Guyer, M. (2007). Klimaänderung in der schweiz. Indikatoren zu Ursachen, Auswirkungen, Maßnahmen. Umwelt-Zustand.

Oerlemans, J. (1994). Quantifying global warming from the retreat of glaciers. Science, 264 (5156): 243–245.

Oerlemans, J. (2005). Extracting a climate signal from 169 glacier records. Science, 308 (5722): 675–677.

Oerlemans, J. (2008). Minimal Glacier Models. Igitur, Utrecht Publishing & Archiving Services.

Oerlemans, J., Anderson, B., Hubbard, A., Huybrechts, P., Jóhannesson, T., Knap, W. H., Schmeits, M., Stroeven, A. P., van de Wal, R. S. W., Wallinga, J., et al. (1998). Modelling the response of glaciers to climate warming. Climate Dynamics, 14 (4): 267–274.

Oerlemans, J. & Fortuin, J. P. F. (1992). Sensitivity of glaciers and small ice caps to greenhouse warming. Science, 258 (5079): 115–117.

Østrem, G. & Haakensen, N. (1993). Glaciers of europe–glaciers of norway. Satellite image atlas of glaciers of the world. United States Geological Survey Professional Paper.

Pachauri, R. K. & Reisinger, A. (2008). Climate Change 2007: Synthesis Report. IPCC.

Pardé, M. (1947). Fleuves et rivieres, sec. Edn. Colin, Parris.

Paterson, W. S. B. (1998). Physics of glaciers. Butterworth-Heinemann.

Paul, F., Kääb, A., Maisch, M., Kellenberger, T., & Haeberli, W. (2004). Rapid disintegration of alpine glaciers observed with satellite data. Geophysical Research Letters, 31 (21): 33–44.

Pelto, M. S. (2004). Temperature-ablation relationships on glaciers and in alpine areas, north cascades, washington. In EASTERN SNOW CONFERENCE, Seite 135.

Pettitt, A. N. (1979). A non-parametric approach to the change-point problem. Applied Statistics, Seiten 126–135.

Quick, M. C. & Pipes, A. (1977). Ubc watershed model. Hydrol. Sci. Bull, 22 (1): 153–161.

Rees, H. G. & Collins, D. N. (2006). Regional differences in response of flow in glacier-fed himalayan rivers to climatic warming. Hydrological processes, 20 (10).

Reimann, C., Filzmoser, P., Garrett, R., & Dutter, R. (2008). Statistical Data Analysis Explained: Applied Environmental Statistics with R. Wiley, New York.

Röthlisberger, H. (1972). Water pressure in intra-and subglacial channels. Journal of Glaciology, 11 (62): 177–203.

Röthlisberger, H. & Lang, H. (1987). Glacial hydrology. Glacio-fluvial sediment transfer. John Wiley and Sons, Chichester, UK, Seiten 207–284.

Rott, H., Scherler, K., & Reynaud, L. (1993). The glaciers of europe-glaciers of the alps. US Geological Survey Professional Paper, 1386: 52.

Schaefli, B., Hingray, B., & Musy, A. (2007). Climate change and hydropower production in the swiss alps: quantification of potential impacts and related modelling uncertainties. Hydrology and Earth System Sciences, 11 (3): 1191.

Schaefli, B., Hingray, B., Niggli, M., & Musy, A. (2005). A conceptual glacio-hydrological model for high mountainous catchments. Hydrology and Earth System Sciences, 9 (1): 95–109.

Schiefer, B., E. Menounos & Wheate, R. (2008). An inventory and morphometric analysis of british columbia glaciers, canada. Journal of Glaciology, 54 (186): 551–560.

Sen, P. K. (1968). Estimates of the regression coefficient based on kendall's tau. Journal of the American Statistical Association, Seiten 1379–1389.

Shea, J. M., Anslow, F. S., & Marshall, S. J. (2005). Hydrometeorological relationships on haig glacier, alberta, canada. Annals of Glaciology, 40: 52.

Shea, J. M., Marshall, S. J., & Livingston, J. M. (2004). Glacier distributions and climate in the canadian rockies. Arctic, Antarctic, and Alpine Research, 36 (2): 272–279.

Shumway, R. H. & Stoffer, D. S. (2000). Time series analysis and its applications. Springer.

Siegert, M. J. (2005). Encyclopedia of Hydrological Sciences, Kapitel Role of Glaciers and Ice Sheets in Climate and the Global Water Cycle, Seiten 2539–2553. John Wiley & Sons, Ltd.

Singh, P., Arora, M., & Goel, N. K. (2006). Effect of climate change on runoff of a glacierized himalayan basin. Hydrological Processes, 20 (9).

Singh, P. & Bengtsson, L. (2005). Impact of warmer climate on melt and evaporation for the rainfed, snowfed and glacierfed basins in the himalayan region. Journal of Hydrology, 300 (1-4): 140–154.

Singh, P. & Jain, S. K. (2002). Snow and glacier melt in the satluj river at bhakra dam in the western himalayan region. Hydrological Sciences Journal, 47 (1): 93–106.

Singh, P. & Kumar, N. (1997). Impact assessment of climate change on the hydrological response of a snow and glacier melt runoff dominated himalayan river. Journal of Hydrology, 193 (1-4): 316–350.

Singh, P., Ramasastri, K. S., Kumar, N., & Arora, M. (2000). Correlations between discharge and meteorological parameters and runoff forecasting from a highly glacierized himalayan basin. Hydrol Sci J, 45 (5): 637–652.

Stahl, K. & Moore, R. D. (2006). Influence of watershed glacier coverage on summer streamflow in british columbia, canada. Water Resour. Res, 42.

Steiner, D. (2008). Sensitivity of european glaciers to precipitation and temperature – two case studies. Climatic Change, 90 (4): 413.

Theil, H. (1950). A rank-invariant method of linear and polynomial regression analysis (parts 1-3). 53: 386–392.

Tvede, A. M. (1983). Influence of glaciers on the variability of long runoff series. Effect of distribution of snow and ice on streamflow. Report of Norwegian National Committee for Hydrology, 12: 179–189.

Van der Veen, C. J. (1999). Fundamentals of glacier dynamics. Balkema Rotterdam.

Verbunt, M., Gurtz, J., Jasper, K., Lang, H., Warmerdam, P., & Zappa, M. (2003). The hydrological role of snow and glaciers in alpine river basins and their distributed modeling. Journal of Hydrology, 282 (1-4): 36–55.

Weber, M. (2004). Mikrometeorologische Prozesse bei der Ablation eines Alpengletschers. Dissertation, Institut für Meteorologie und Geophysik der Universität Innsbruck.

Willis, I. (2006). Encyclopedia of Hydrological Sciences, Band 4, Kapitel Hydrology of Glacierized Basins, Seiten 2601–2631. John Wiley & Sons Hoboken, NJ.

Zemp, M., Roer, I., Kääb, A., Hoelzle, M., Paul, F., & Haeberli, W. (2009). Global Glacier Changes: facts and figures. WGMS.

Appendix

The following figures and tables contain additional information to chapter 5.

Table .1: Summary of catchmentsizes, glacierized proportion and actual glaciersize in the study area of the European Alps

	catchment size [km^2]	glacierized part	glacier size
Min.:	20.60	0.0200	0.538
1st Qu.:	43.45	0.0900	7.202
Median :	69.50	0.1850	14.360
Mean :	83.76	0.2405	20.313
3rd Qu.:	107.00	0.3650	22.407
Max.:	220.00	0.6600	128.700

Table .2: Summary of catchmentsizes, glacierized proportion and actual glaciersize in the study area of Norway

	catchment size [km^2]	glacierized part	glacier size
Min.:	37.30	0.0500	4.460
1st Qu.:	77.25	0.0550	7.403
Median :	202.00	0.1300	25.350
Mean :	228.01	0.1967	33.890
3rd Qu.:	249.00	0.2600	46.087
Max.:	795.00	0.7500	95.400

Table .3: Summary of catchmentsizes, glacierized proportion and actual glaciersize in the study area of British Columbia

	catchment size [km^2]	glacierized part	glacier size
Min.:	86.5	0.0100	1.844
1st Qu.:	167.8	0.0625	17.655
Median :	387.0	0.1350	52.360
Mean :	501.2	0.1594	77.038
3rd Qu.:	586.8	0.1900	77.058
Max.:	2160.0	0.6200	410.400

Table .4: the catchment characteristic parameteres

	catchment size	glacierized part of the catchment	glaciersize	mean catchment hight	mean runoff L1	mean runoff L2	mean runoff L3	mean runoff L4
E02	195.00	0.66	128.70	2945.00	265.24	826.54	827.26	207.08
E03	38.90	0.52	20.23	2719.00	288.79	867.09	800.94	215.72
E04	78.00	0.51	39.78	2780.00	308.31	853.32	858.11	247.34
E05	55.00	0.42	23.10	3000.00	332.21	1001.83	939.53	201.48
E07	39.30	0.39	15.33	2400.00	454.86	963.34	759.52	177.74
E08	77.80	0.37	28.79	2630.00	337.27	655.24	587.06	168.78
E09	35.70	0.35	12.49	2370.00	327.25	660.57	550.16	156.19
E10	66.50	0.30	19.95	2716.00	214.95	515.16	458.07	118.12
E11	20.60	0.28	5.77	2200.00	514.14	832.83	679.45	204.40
E12	72.50	0.27	19.57	2600.00	289.85	633.94	524.26	124.00
E13	107.00	0.19	20.33	2617.00	328.97	482.23	320.58	112.94
E14	164.00	0.18	29.52	2170.00	350.00	494.12	389.09	122.06
E15	53.70	0.17	9.13	2360.00	459.45	650.48	423.53	198.07
E16	45.00	0.15	6.75	2950.00	262.02	617.71	332.40	99.14
E18	220.00	0.13	28.60		286.50	310.87	197.38	72.06
E19	43.90	0.09	3.95	1820.00	1019.83	1341.89	839.88	299.78
E20	112.00	0.09	10.08	1820.00	127.07	102.99	74.04	35.46
E21	107.00	0.08	8.56	2200.00	190.50	261.17	174.79	57.73
E22	167.40	0.08	13.39	2200.00	213.36	355.43	263.15	80.95
E25	26.90	0.02	0.54	2368.00	275.07	270.94	148.63	71.43
E26	43.30	0.02	0.87	2372.00	321.28	382.56	217.76	95.78
E27	73.30	0.02	1.47	2549.00	215.34	289.74	148.48	77.88
C01	150.00	0.62	93.00	2155.82	303.97	922.26	944.63	273.75
C03	221.00	0.36	79.56	1399.80	559.16	779.45	457.24	196.21
C04	298.00	0.26	77.48	2050.16	267.05	551.76	429.42	108.43

C05	1250.00	0.23	287.50	1614.13	532.59	740.81	551.93	190.76
C06	3940.00	0.23	906.20	1336.25	398.54	548.63	454.57	221.02
C07	5720.00	0.22	1258.40	1774.03	223.54	450.67	395.97	130.12
C09	5780.00	0.20	1156.00	1644.06	251.01	464.16	417.78	150.60
C10	86.50	0.19	16.43	1559.91	498.91	632.18	311.93	170.91
C11	2160.00	0.19	410.40	1678.23	340.88	533.89	401.01	128.68
C13	404.00	0.18	72.72	2002.06	259.43	387.19	230.99	74.29
C17	118.00	0.15	17.70	2285.19	366.97	468.60	194.82	51.40
C18	370.00	0.14	51.80	1014.55	708.61	800.33	646.96	482.57
C19	583.00	0.13	75.79	1299.82	519.23	655.96	448.97	254.39
C25	741.00	0.10	74.10	1432.75	316.02	354.96	164.47	91.31
C28	588.00	0.09	52.92	2083.72	225.95	304.49	194.29	51.15
C33	252.00	0.07	17.64	1918.96	323.97	377.20	131.63	66.62
C36	461.00	0.06	27.66	2133.36	433.16	452.33	165.19	54.78
C48	112.00	0.04	4.48	1755.14	417.70	606.05	283.40	117.54
C57	715.00	0.03	21.45	1607.06	446.12	432.61	173.35	70.60
C62	92.20	0.02	1.84	2080.23	397.23	398.94	119.71	43.15
C86	420.00	0.01	4.20	1861.48	138.07	126.40	44.50	14.90
N01	65.30	0.75	48.98	1546.00	311.69	1140.51	1191.96	318.40
N04	202.00	0.40	80.80	1302.00	294.94	718.50	743.80	266.07
N05	235.00	0.37	86.95	1339.00	298.97	666.09	660.57	232.50
N07	64.60	0.30	19.38	1176.00	728.55	1159.42	967.45	442.72
N11	37.30	0.22	8.21	994.00	378.39	1058.88	653.71	195.70
N18	206.00	0.17	35.02	1371.00	429.52	722.47	419.84	169.29
N19	212.00	0.14	29.68	1397.00	371.69	588.25	349.66	141.10
N21	43.70	0.13	5.68	491.00	738.55	845.92	558.58	306.81
N22	795.00	0.12	95.40	1467.00	229.69	364.58	221.88	75.42
N27	480.00	0.09	43.20	1467.00	239.42	361.52	237.98	108.19
N30	110.00	0.06	6.60	1003.00	628.40	616.26	414.99	271.67

N31	263.00	0.05	13.15	1475.00	359.56	687.72	338.02	124.78
N32	110.00	0.05	5.50	588.00	705.70	525.66	509.17	444.21
N33	507.00	0.05	25.35	841.00	593.44	576.72	423.45	316.74
N34	89.20	0.05	4.46	592.00	515.41	481.09	408.88	297.54

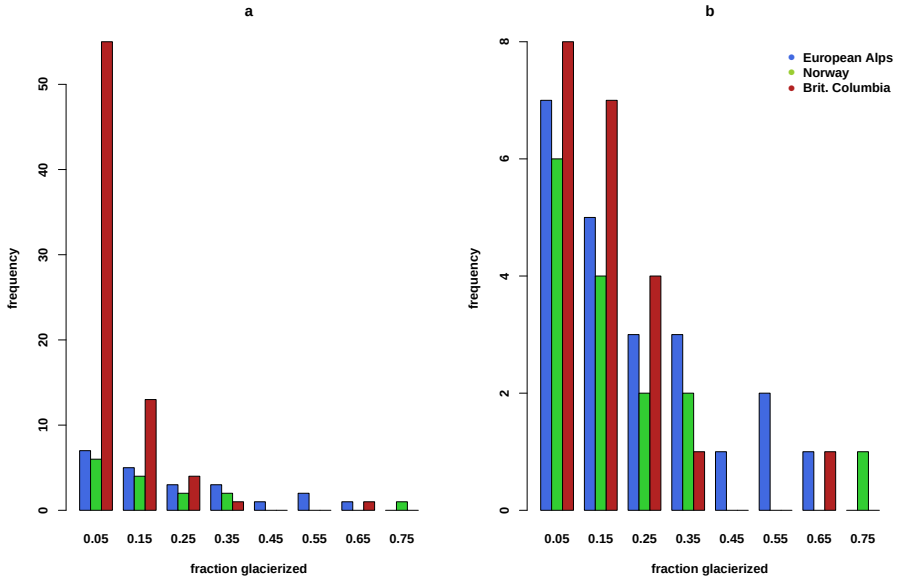

Figure .1: Distribution of glacierization for the study sites in Canada, Norway, and the European Alps. a: original data set. b: fitted Canadian sub set

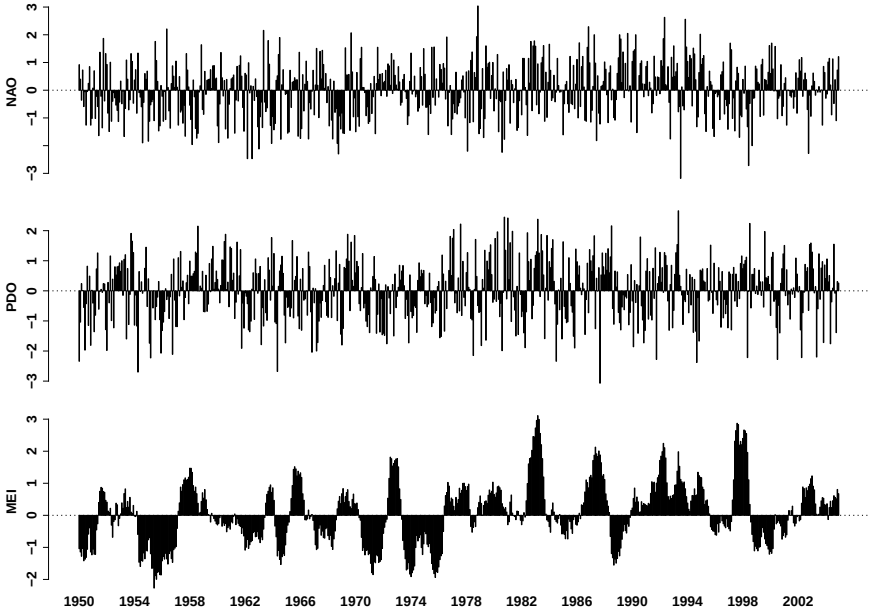

Figure .2: NAO, PDO and multivariate El Niño index

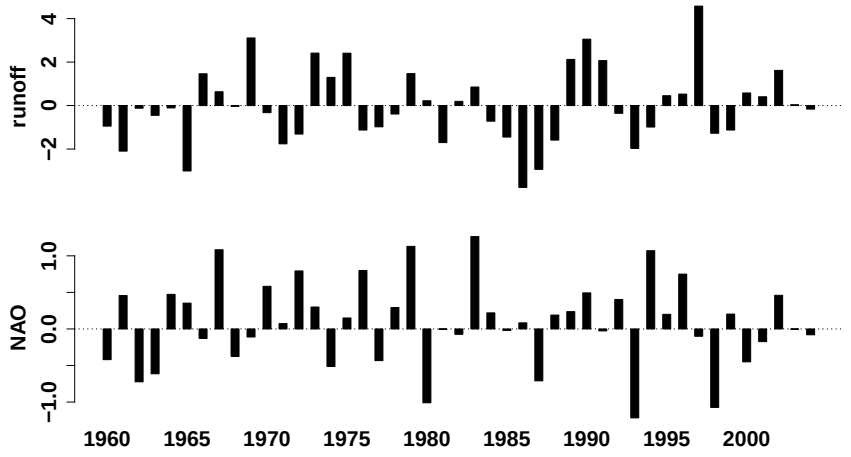

Figure .3: Anomalies in runoff of the European Alps study sites and summer NAO (JJA) values

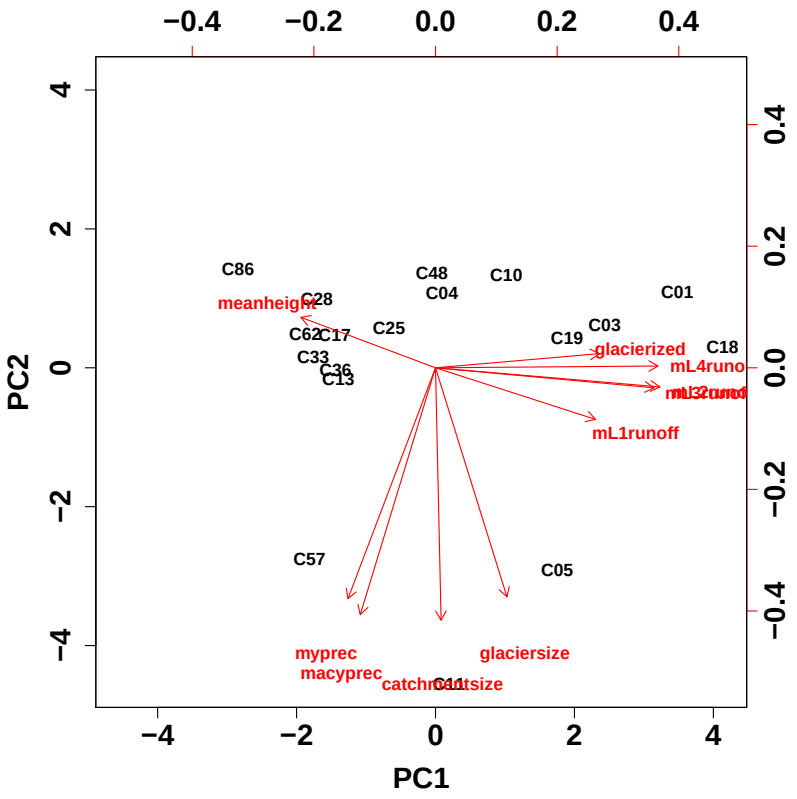

Figure .4: Principal components in the geographical data set of British Columbia

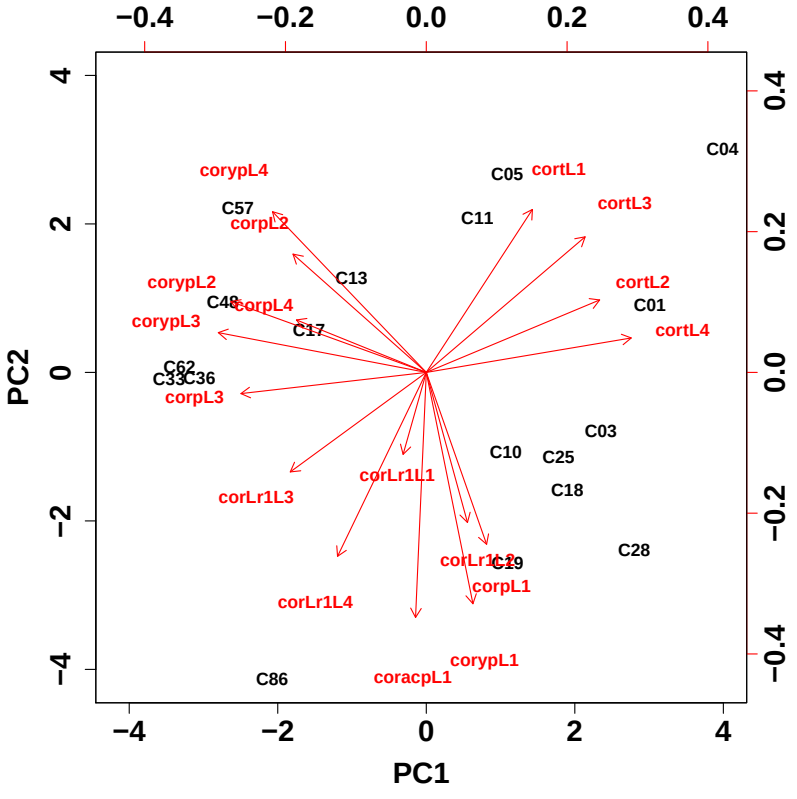

Figure .5: Principal components in the correlation data set of British Columbia

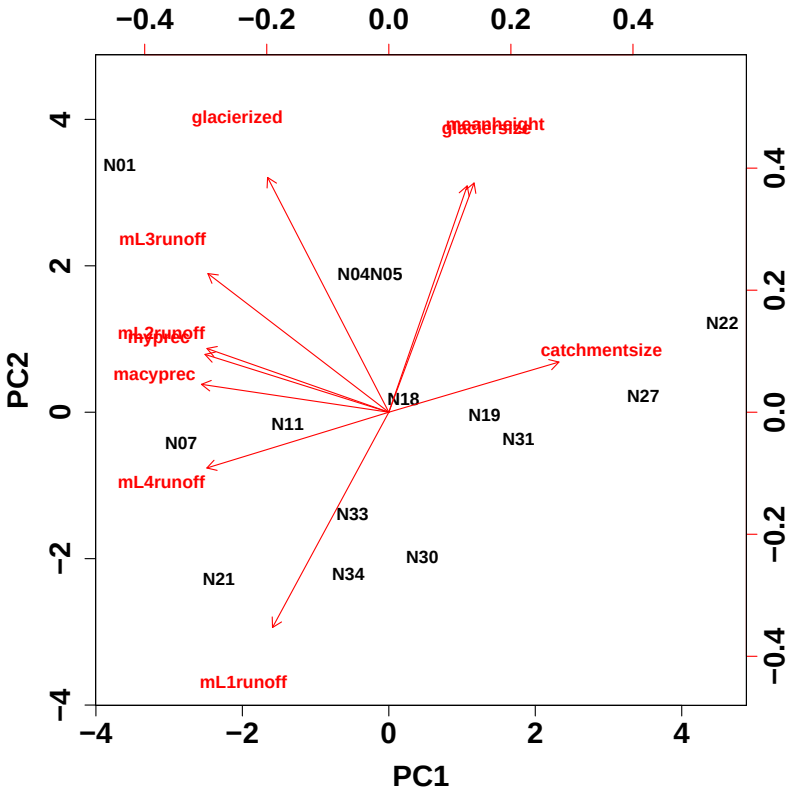

Figure .6: Principal components in the geographical data set of Norway

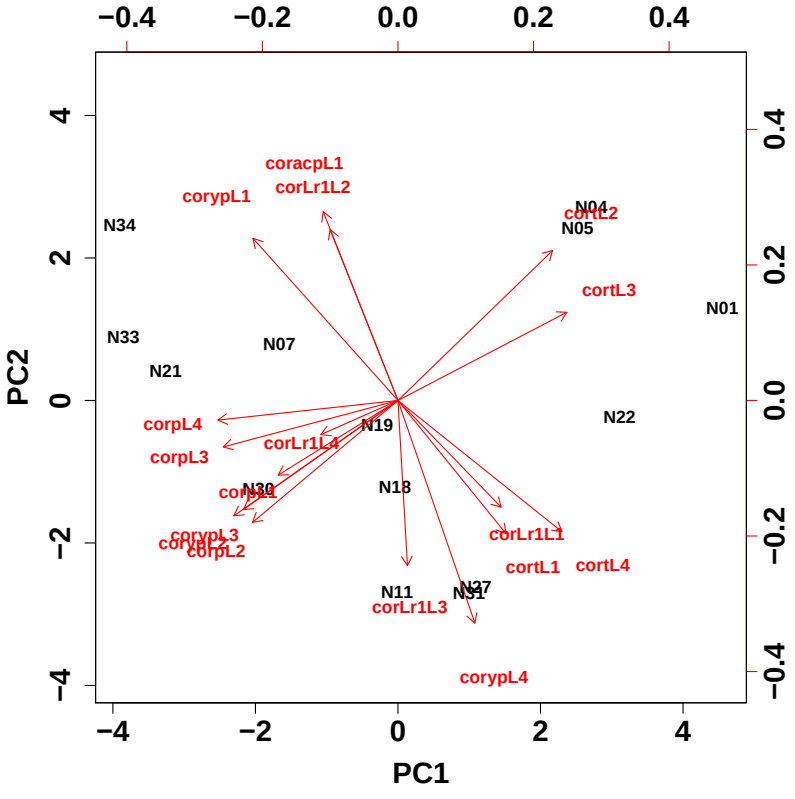

Figure .7: Principal components in the correlation data set of Norway

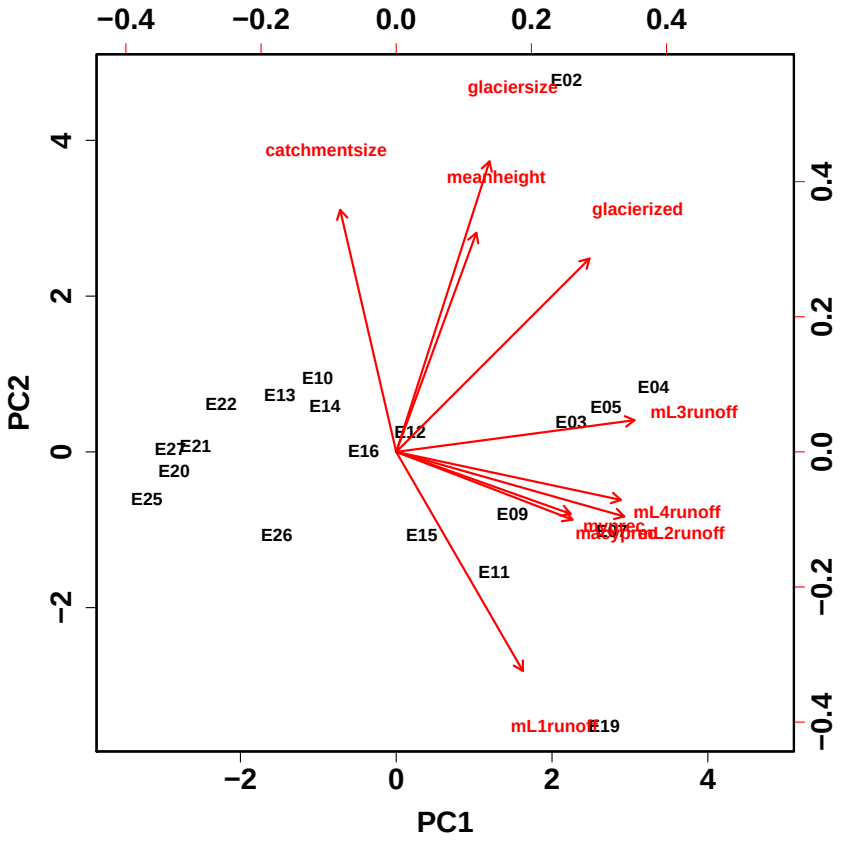

Figure .8: Principal components in the geographical data set of the EU

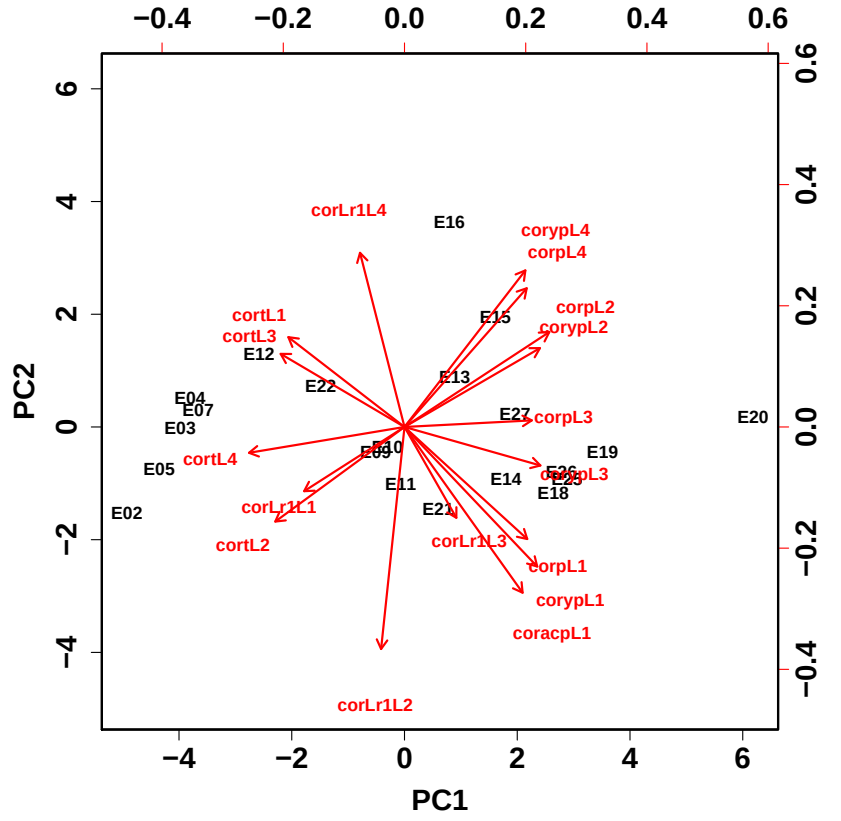

Figure .9: Principal components in the correlation data set of the European Alps

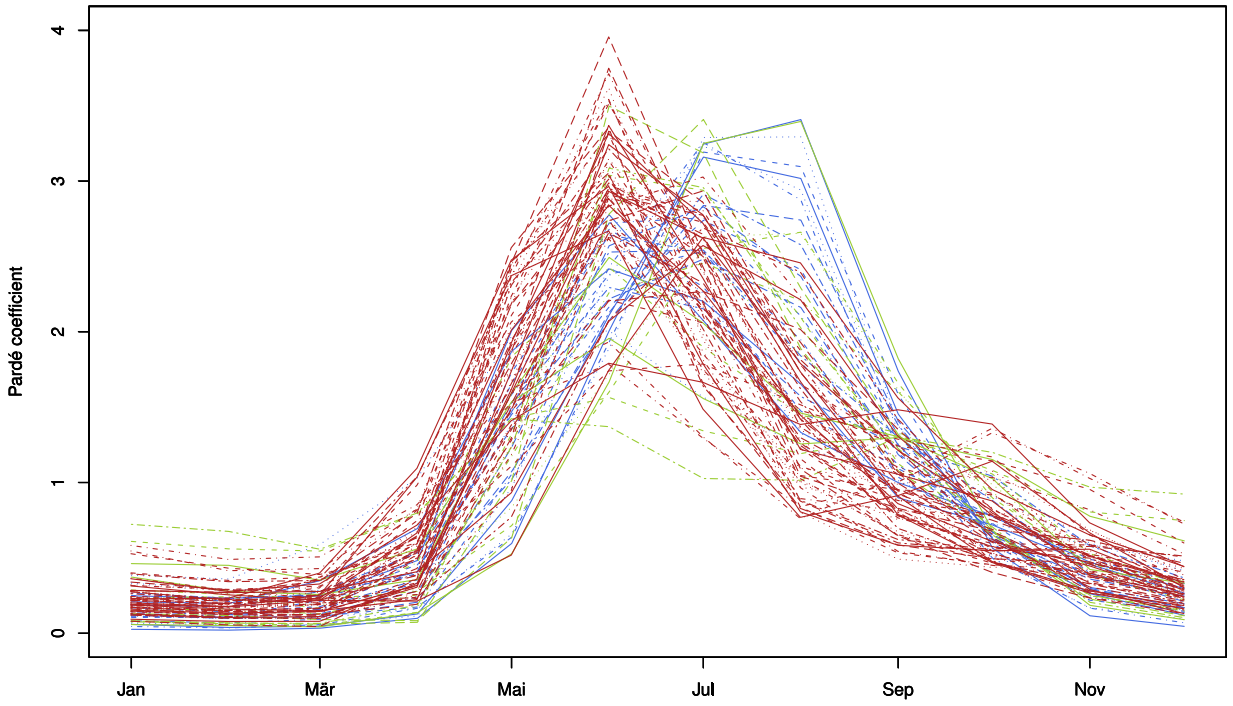

Figure .10: Parde coefficients for the single catchments

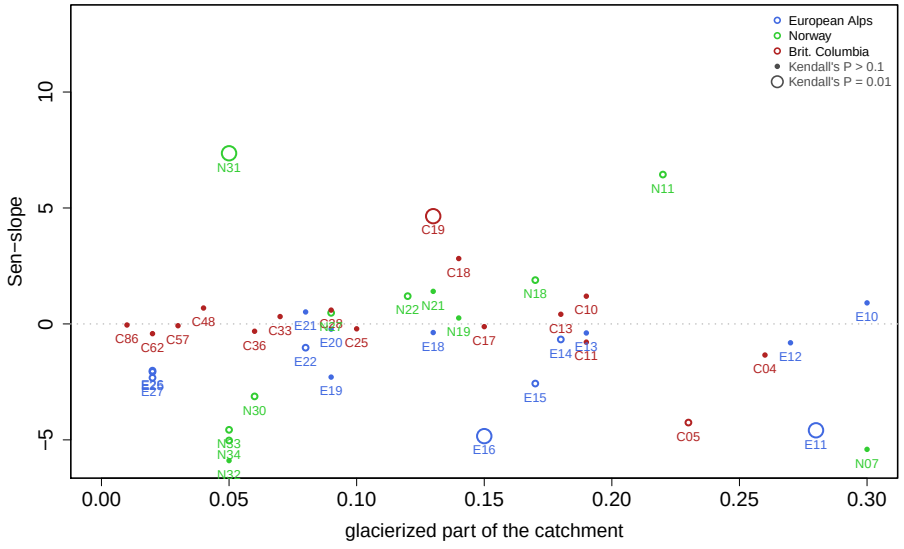

Figure .11: Frame of figure 5.18, expandinng the low glacierized catchments

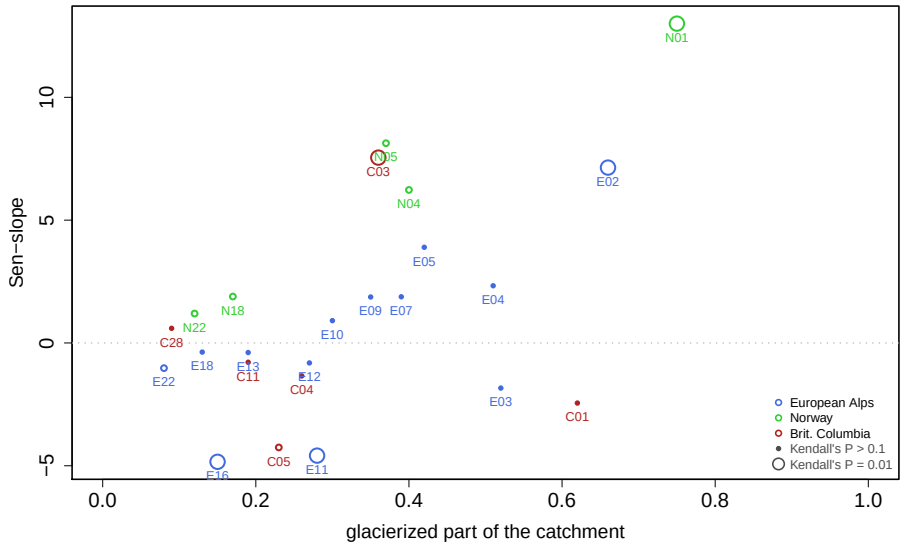

Figure .12: Frame of figure 5.18, excluding catchments with $cort > 0.3$

Ehrenwörtliche Erklärung

Hiermit erkläre ich, dass die Arbeit selbständig und nur unter Verwendung der angegebenen Hilfsmittel angefertigt wurde.

Ort, Datum Unterschrift